

Signals of a Warped SUSY Higgsless Model at the LHC

Diploma thesis by
Laslo Reichert

Supervised by PD Dr. Thorsten Ohl



Institut für Theoretische Physik und Astrophysik,
Universität Würzburg, D-97074 Würzburg, Germany

June 25, 2008

Zusammenfassung

Das Ziel dieser Arbeit war die Berechnung von LHC (Large Hadron Collider) Observablen für ein higgsloses supersymmetrisches Modell mit einer zusätzlichen Raumdimension in gewarptem Hintergrund. Das Modell [1] basiert auf Modellen mit zusätzlichen Raumdimensionen, die in [2] [3] [4] und [5] untersucht wurden. Für die phänomenologische Betrachtung des Modells untersuchen wir die Eigenschaften der ersten Kaluza-Klein Anregung des Gluons und den Kaluza-Klein Grundzustand des Sgluinos, die beide Teil des fünfdimensionalen Eichmultipletts sind.

Die Arbeit ist wie folgt aufgebaut: Zuerst geben wir eine kurze Einführung in extradimensionale Modelle und konstruieren dann eine supersymmetrische fünfdimensionale Theorie. Als nächstes stellen wir das Modell vor, das in dieser Arbeit verwendet wurde. Danach berechnen wir die Massen und Kopplungen des schweren Gluons und des Sgluinos und stellen die Feynmanregeln auf.

Im folgenden Kapitel berechnen wir den partonischen Wirkungsquerschnitt des $2 \rightarrow 4$ Prozesses mit zwei Gluonen im Anfangszustand und einem Top-Antitop und einem Bottom-Antibottom Paar im Endzustand. Für die Berechnung benutzen wir als erstes die Narrow Width Approximation und als zweites eine Monte Carlo Simulation. Um die Narrow Width Approximation zu berechnen, benutzen wir die Programmpakete FeynArts und FormCalc und für die Monte Carlo Simulation implementieren wir das Modell in O'Mega und verwenden dann Whizard zur Erzeugung der Monte Carlo Ereignisse. Da wir bei der Narrow Width Approximation $2 \rightarrow 2$ Prozesse mit festen Endzuständen berechnen, führen wir nur Monte Carlo Simulationen für $2 \rightarrow 4$ Wirkungsquerschnitte durch, die entweder schwere Gluonen oder Sgluinos im Zwischenzustand haben. Das ermöglicht uns im späteren Verlauf, beide Methoden miteinander zu vergleichen. Dabei stellen wir fest, dass die totalen Wirkungsquerschnitte der Narrow Width Approximation und der Monte Carlo Simulation im Fall der schweren Gluonen bis auf 10% und im Fall der Sgluinos bis auf 0.05% miteinander übereinstimmen. Auch die Abhängigkeit des Polarwinkels θ passt nach der Faltung der Narrow Width Approximation mit den Zerfallswahrscheinlichkeit der Quarks im Laborsystem gut mit der Monte Carlo Simulation überein.

Um Vorhersagen für Messungen am LHC machen zu können, berechnen wir im letzten Kapitel den hadronischen $2 \rightarrow 4$ Wirkungsquerschnitt mittels Monte-Carlo-Simulationen. Dazu müssen wir den partonischen $2 \rightarrow 4$ Wirkungsquerschnitt mit den Partonverteilungen der Protonen falten. Im Spektrum der invarianten Masse des Top-Antitop Paares erhalten wir einen Peak, der bei der Masse des schweren Gluons bzw. des Sgluinos liegt. Auch die Polarwinkelverteilung zeigt eine charakteristische Abhängigkeit der neuen Teilchen.

Contents

1	Introduction	1
2	Basics	3
2.1	Flat Extra Dimensions	3
2.1.1	Fermions and Extra Dimensions	3
2.1.2	Gauge Theory and Extra Dimensions	5
2.2	Warped Extra Dimensions	7
3	Supersymmetric Extension in 5D	11
3.1	Supersymmetry in 4D	11
3.1.1	Supersymmetry Algebra	11
3.1.2	Representations of the $N = 1, 2$ Supersymmetry Algebra	12
3.1.3	Superfields	15
3.1.4	Chiral Superfields	16
3.1.5	Vector Superfields	17
3.1.6	Gauge invariant Interactions	18
3.2	Supersymmetry in 5D	19
3.2.1	Supersymmetry in a flat extra dimension	19
3.2.2	Supersymmetry in warped extra dimensions	21
4	The Model	23
4.1	Model Framework	23
4.2	Breaking Scenario	24
5	Feynman Rules	27
5.1	Equations of Motion	27
5.2	Masses	29
5.3	Couplings	33
6	Partonic cross section	39
6.1	Calculation with the Narrow Width Approximation	39
6.1.1	Basics of Narrow Width Approximation	39
6.1.2	Calculation with FeynArts and FormCalc	40
6.2	Monte Carlo Simulation	48
6.2.1	Color Flow	49
6.2.2	Calculation of the $2 \rightarrow 2$ cross sections with O'Mega	55
6.2.3	Results of Monte Carlo simulations	56
6.3	Narrow width vs. Monte Carlo simulation	60
7	Hadronic cross sections and LHC Distributions	64
7.1	Factorization and the Parton Model of QCD	64
7.2	LHC observables	65

8	Conclusions	69
A	Notation and Conventions	70
B	Parameters	72
C	Implementation of the Model in FeynArts	74
D	Implementation of the Model in O'Mega	78

Chapter 1

Introduction

In the near future experiments at the LHC will produce the first data and one of the main tasks will be the measurement of high energy physics, which provides information about the detailed dynamics of electroweak symmetry breaking (EWSB). In the higgsless standard model the scattering of massive W - and Z -Bosons violates unitarity at energies higher than 1.7 GeV. To keep unitarity and to ensure that the theory remains renormalizable the most popular method for breaking the electroweak symmetry is introducing a scalar Higgs field with a vacuum expectation value (VEV). The minimal standard model (SM) including a Higgs accords very well with the electroweak precision data, but until now there is no experimental verification of a scalar Higgs field. Thus the question appears, whether there are other possibilities for EWSB.

Furthermore the minimal SM gives no natural explanation of the huge difference between the TeV scale of the SM and much higher scales like the grand unification and quantum gravity scales. Last but not least the minimal SM cannot describe cold dark matter (CDM), which constitutes 20% of the energy density of the universe [6]. Based on all these facts we can regard the standard model as a well tested effective theory, which is the low energy limit of an extended theory. The most popular extension of the standard model is supersymmetry, but there exist other very interesting approaches like little Higgs or extra dimensions.

The first examinations of extra dimensional theories were done by Theodor Kaluza and Oskar Klein [7][8]. At that time they wanted to unify electromagnetism with gravity through a five dimensional metric field. Shortly after the development of the standard model, there were several approaches how to embed the standard model in extra dimensional theories. In each of these models the extra dimension is compactified and the 5D fields are decomposed with the Kaluza-Klein ansatz. Furthermore the emergence of extra dimensional models gave rise to new approaches to realize EWSB. One finds that extra dimensional models offer the possibility for breaking electroweak symmetry without introducing a Higgs. The EWSB can be rather realized through boundary conditions, which have to be consistent with the variation of the fully gauge invariant action. In this case the unitarity of scattering processes including massive W - and Z -Bosons can be ensured by the exchange of the massive Kaluza-Klein gauge bosons. Furthermore the EWSB via boundary conditions is a soft symmetry breaking and therefore the low energy theory looks like a renormalizable one. Thus such models remain BRST invariant and therefore Ward Identities hold. Since the Higgs mechanism is also necessary for the generation of the fermion masses in a gauge invariant way, one main aspect of constructing extra dimensional models is the mass generation of fermions. For generating fermion masses we follow the approach in [2], where the fermions also propagate in the extra dimension.

In this diploma thesis we examine a warped extra dimensional higgsless supersymmetric model introduced by Alexander Knochel and Thorsten Ohl [1]. The model structure has the following form. The bulk gauge group is $SU(3) \times SU(2)_L \times SU(2)_R \times U(1)_{B-L}$, where B is the baryon and L is the lepton number. The motivation for introducing two $SU(2)$ gauge symmetries in the bulk is the following. The Higgs potential in the minimal SM is invariant under the rotation of all four real components of the scalar field. The rotation corresponds approximately to a global $SO(4) \sim SU(2)_L \times SU(2)_R$ and is reduced

to a custodial $SU(2)_D$ when the Higgs gets a VEV. The remaining custodial gauge symmetry ensures the correct W/Z mass ratio, i.e. $\rho = 1$. To get the same feature in extra dimensional theories we consider an $SU(2)_L \times SU(2)_R$ gauge group in the bulk and break it to a $SU(2)_D$ on the TeV brane. In order to get $U(1)_{EM}$ after integrating out the extra dimension, the $SU(2)_R \times U(1)_{B-L}$ is broken to $U(1)_Y$ on the Planck brane. However in the case of flat extra dimensions the ρ parameter deviates from unity by ten percent, and the lowest Kaluza-Klein excitations of the W and Z are too light. Thus constructing realistic models with flat extra dimensions is not straightforward. In the case of warped extra dimensions we get the correct W/Z mass ratio and the mass gap between the lightest vector bosons and their first Kaluza Klein excitations can be increased to ~ 1 TeV. Moreover warped extra dimensional models have the nice feature to connect the Planck scale with the TeV scale through a warp factor and thus give a natural explanation for the huge scale differences.

Despite these interesting features, models of electroweak symmetry breaking in warped space do not automatically contain stable particles as candidates for CDM. This is because the KK-parity, which is required for stable KK-modes does not hold in warped backgrounds any longer [9] [10]. Thus we have to investigate extensions of warped extra dimensional models. Since SUSY is a well motivated extension of the standard model and it provides natural candidates for cold dark matter, it is reasonable to study SUSY in the background of warped extra dimensions. If the extension is compatible with R-parity, the model provides stable candidates for CDM. An examination of CDM candidates in a supersymmetric extended 5D model was done in [1].

This diploma thesis is organized as follows. In chapter 2 we give a short introduction to flat and warped extra dimensions. Afterwards we explain how to construct supersymmetric theories in extra dimensions, where we exploit the correspondence between 5D $N = 1$ and 4D $N = 2$ SUSY. In chapter 4 we outline the model that we examined in this thesis and in the following part we calculate the Feynman rules, couplings and masses of the heavy gluon, sgluino, gluon and quarks. The gluon, heavy gluon and sgluino are part of the 5D gauge multiplet. In chapter 6 we calculate the partonic $2 \rightarrow 4$ cross section with two gluons in the initial state and a bottom anti-bottom and top anti-top pair in the final state, which are the decay products of the sgluino and heavy gluon of the intermediate state. For the calculation we firstly use the narrow width approximation and secondly we perform a Monte Carlo simulation of the tree level $2 \rightarrow 4$ process. To understand the functionality of the Monte Carlo generator we give a short introduction to the color flow decomposition and at the end of the chapter we compare the narrow width approximation with the Monte Carlo simulation. In chapter 7 we discuss the parton model of hadronic cross sections and make predictions for characteristic measurements of the model at the LHC. In the Appendix we give a short summary of the conventions we used in this thesis, list the couplings which were necessary for the calculation and at the end we explain the implementation of the model in FeynArts and O'Mega.

Chapter 2

Basics

2.1 Flat Extra Dimensions

In this section we will introduce the basic ideas of five dimensional theories with a flat and compact extra dimension with topology $\mathbb{R}^4 \times [0, L]$. Therefore we start with fermions in a 5D theory and explain on the basis of this example the extension from a four to a five dimensional theory, the Kaluza Klein decomposition, the derivation of the 5D equations of motion and thereby how we obtain the mass spectrum of the particles. More details towards this topic can be found in [2] and references therein. In the second part we will examine the characteristics of $SU(N)$ gauge theories in extradimensional models. The notation we use is defined in App. A.

2.1.1 Fermions and Extra Dimensions

In four dimensional theories the Clifford algebra reads

$$\{\gamma^\mu, \gamma^\nu\} = 2g^{\mu\nu} \quad (2.1)$$

and can be extended to a five dimensional Clifford algebra through

$$\{\gamma^M, \gamma^N\} = 2g^{MN} \quad (2.2)$$

with $M = 0, 1, 2, 3, 5$. In 5D the smallest fermionic irreducible representation of the Poincaré group is the Dirac spinor, which contains two two-component spinors from the 4D point of view.

$$\Psi = \begin{pmatrix} \eta_\alpha \\ \bar{\chi}^{\dot{\alpha}} \end{pmatrix} \quad (2.3)$$

In 5D the decomposition of the Dirac spinor in a right- and lefthanded part is meaningless because the 4D-projection operators

$$P^+ = \frac{1}{2}(-i\gamma^5 + 1) \quad P^- = \frac{1}{2}(-i\gamma^5 - 1) \quad (2.4)$$

do not commute with the Lorentz transformations anymore, since γ^5 is already part of the 5D Clifford algebra. The free bulk action for the Dirac spinor Ψ is then given by

$$S_{5,\text{fermion}} = \int d^5x \left(\frac{i}{2} (\bar{\Psi} \gamma^M \partial_M \Psi - \partial_M \bar{\Psi} \gamma^M \Psi) - m_{\text{bulk}} \bar{\Psi} \Psi \right). \quad (2.5)$$

Varying the action with respect to $\bar{\Psi}$ we get the following bulk equation of motion

$$i\gamma^5 \partial_5 \Psi + i\gamma^\mu \partial_\mu \Psi - m_{\text{bulk}} \Psi = 0 \quad (2.6)$$

When we replace the Dirac spinors by expression (2.3) and perform the matrix multiplication with the γ -matrices we can rewrite Eq. (2.6) and get two coupled equations of motion for η and $\bar{\chi}$.

$$\begin{aligned} i\sigma^\mu \partial_\mu \bar{\chi} - \partial_5 \eta - m_{\text{bulk}} \eta &= 0 \\ i\bar{\sigma}^\mu \partial_\mu \eta + \partial_5 \bar{\chi} - m_{\text{bulk}} \bar{\chi} &= 0 \end{aligned} \quad (2.7)$$

However when we vary the action we have to integrate by parts and thus get terms at the boundaries of the fifth dimension.

$$\delta S_{\text{bound}} = \frac{1}{2} \int d^4x [\eta \delta \chi - \chi \delta \eta + \bar{\eta} \delta \bar{\chi} - \bar{\chi} \delta \bar{\eta}]_0^L \quad (2.8)$$

We only regard terms which come from the integration by parts of the fifth dimension because we consider that the fields fall off sufficiently fast at infinity and therefore their value at the 4D-boundaries can be put to zero. Next we have to specify the boundary conditions so that the boundary variation (2.8) vanishes, because we do not want additional dynamics of boundary fields that affect the 5D dynamics. In this part of the work we do not want to go further into the topic of boundary conditions and postpone this issue to Sec. 4.2.

Now we want to discuss how to perform the Kaluza-Klein decomposition of the five dimensional Dirac spinors. In all of the extra dimensional models examined in this work one can get rid of mixing terms between ∂_μ and ∂_5 in the equations of motion. Hence we can always use the factorization ansatz and decompose the 5D field into a part which depends on the extra dimension and a part which depends on the 4D coordinates. Because of the compact extra dimension, η and $\bar{\chi}$ get a discrete spectrum and can then be written as

$$\begin{aligned} \eta(x, y) &= \sum_n \eta_{(n)}(x) f_{\eta, (n)}(y) \\ \bar{\chi}(x, y) &= \sum_n \bar{\chi}_{(n)}(x) f_{\bar{\chi}, (n)}(y), \end{aligned} \quad (2.9)$$

η_n and $\bar{\chi}_n$ are the 4D two-component spinors which form a Dirac spinor of mass m_n and therefore satisfy the 4D equations of motion

$$\begin{aligned} i\bar{\sigma}^\mu \partial_\mu \eta_{(n)} - m_n \bar{\chi}_{(n)} &= 0 \\ i\sigma^\mu \partial_\mu \bar{\chi}_{(n)} - m_n \eta_{(n)} &= 0 \end{aligned} \quad (2.10)$$

Plugging (2.9) into (2.7) we get the following differential equations for g_n and f_n

$$\begin{aligned} f'_{\eta, (n)} + m_{\text{bulk}} f_{\eta, (n)} - m_n f_{\bar{\chi}, (n)} &= 0 \\ f'_{\bar{\chi}, (n)} + m_{\text{bulk}} f_{\bar{\chi}, (n)} - m_n f_{\eta, (n)} &= 0 \end{aligned} \quad (2.11)$$

where f' denotes the derivative of a function f with respect to y . The above first order differential equations are coupled. Hence by combining both we get two decoupled second order equations

$$\begin{aligned} f''_{\eta, (n)} + (m_n^2 - m_{\text{bulk}}^2) f_{\eta, (n)} &= 0 \\ f''_{\bar{\chi}, (n)} + (m_n^2 - m_{\text{bulk}}^2) f_{\bar{\chi}, (n)} &= 0. \end{aligned} \quad (2.12)$$

Depending on the sign of $m_n^2 - m_{\text{bulk}}^2$ we get either $e^{ik_n y}$ and $e^{-ik_n y}$ (for $m_n^2 - m_{\text{bulk}}^2 > 0$) or $e^{k_n y}$ and $e^{-k_n y}$ (for $m_n^2 - m_{\text{bulk}}^2 < 0$) as solutions for $k_n^2 = m_n^2 - m_{\text{bulk}}^2$. Thus we get

$$\begin{aligned} f_{\eta, (n)}(y) &= A_n e^{(i)k_n y} + B_n e^{-(i)k_n y} \\ f_{\bar{\chi}, (n)}(y) &= C_n e^{(i)k_n y} + D_n e^{-(i)k_n y} \end{aligned} \quad (2.13)$$

We find out that for introducing an extra dimension we get a Kaluza-Klein tower for every particle, which means that we have an infinite number of excitations, the so called Kaluza-Klein modes (KK-modes). The ground state with mass m_0 will be identified with the standard model particle. If we want to work with extra dimensional models we have to deal with an infinite particle content when reducing to a 4D theory.

Until now we have only regarded the free bulk action. As in 4D theories we can postulate a gauge invariant Lagrangian to get interaction terms. To construct a 5D gauge invariant interaction we have to introduce a 5D covariant derivative

$$D_M = \partial_M - ig_5 A_M^a T^a, \quad (2.14)$$

where g_5 is the 5D gauge coupling and T^a are the generators of the $SU(N)$ gauge group with $[T^a, T^b] = if^{abc}T^c$. The bulk action then reads

$$S_{5,\text{fermion}} = \int d^5x \left(\frac{i}{2} (\bar{\Psi} \gamma^M D_M \Psi - D_M \bar{\Psi} \gamma^M \Psi) - m_{\text{bulk}} \bar{\Psi} \Psi \right) \quad (2.15)$$

For getting the effective 4D theory we again have to integrate over the fifth dimension.

2.1.2 Gauge Theory and Extra Dimensions

Now we discuss gauge theories in extradimensional models. In 4D the action looks like

$$S_{4,\text{gauge}} = \int d^4x \left(-\frac{1}{4} F_{\mu\nu}^a F^{a,\mu\nu} \right) \quad (2.16)$$

with $F_{\mu\nu}^a = \partial_\mu A_\nu^a - \partial_\nu A_\mu^a - gf^{abc} A_\nu^b A_\mu^c$. The extended 5D action then reads

$$S_{5,\text{gauge}} = \int d^5x \left(-\frac{1}{4} F_{MN}^a F^{a,MN} \right) \quad (2.17)$$

with $F_{MN}^a = \partial_M A_N^a - \partial_N A_M^a - g_5 f^{abc} A_N^b A_M^c$. The 5D action can be separated into the usual 4D term and an additional expression, where the fifth component of the gauge boson appears. This can be done by summing explicitly over the extra dimension. The action can then be written as

$$S_{5,\text{gauge}} = \int d^5x \left(-\frac{1}{4} F_{\mu\nu}^a F^{a,\mu\nu} - \frac{1}{2} F_{\mu 5}^a F^{a,\mu 5} \right) \quad (2.18)$$

We now neglect the 4D term of the gauge action. We denote the reduced action by

$$\begin{aligned} \tilde{S}_{5,\text{gauge}} &= \int d^5x \left(-\frac{1}{2} F_{\mu 5}^a F^{a,\mu 5} \right) \\ &= \frac{1}{2} \int d^5x \left(-\partial_\mu A_5^a \partial^\mu A^{a,5} - \partial_5 A_\mu^a \partial^5 A^{a,\mu} + 2 \partial_5 A_\mu^a \partial^\mu A^{a,5} \right) \end{aligned} \quad (2.19)$$

In the above expression a mixing term proportional to $\partial_5 A_\mu^a \partial^\mu A^{a,5}$ shows up. To avoid this mixing between the fifth component of the vector field and the 4D part, we add the following gauge fixing

$$\begin{aligned} S_{\text{GF}} &= - \int d^5x \frac{1}{2\xi} (\partial_\mu A^{a,\mu} + \xi \partial_5 A^{a,5})^2 \\ &= \int d^5x \left(-\frac{1}{2\xi} (\partial_\mu A^{a,\mu})^2 - \frac{\xi}{2} (\partial_5 A^{a,5})^2 - \partial_\mu A^{a,\mu} \partial_5 A^{a,5} \right) \end{aligned} \quad (2.20)$$

To ensure the cancellation of the mixing terms from (2.19) and (2.20) we have to do an integration by parts. As explained in Sec. 2.1.1 only the integration by parts of the fifth dimension gives a contribution due to the boundaries.

In perturbation theory the fields are treated as free fields and thus the time evolution is defined by the free Hamiltonian. Hence to derive the equations of motion we only have to consider the free 5D gauge action given by

$$S_{5,\text{gauge}}^{\text{free}} = \frac{1}{2} \int d^5x \left(-\partial_\mu A_\nu^a \partial^\mu A^{a,\nu} + \partial_\mu A_\nu^a \partial^\nu A^{a,\mu} - \partial_\mu A_5^a \partial^\mu A^{a,5} \right. \\ \left. - \partial_5 A_\mu^a \partial^5 A^{a,\mu} - \frac{1}{\xi} (\partial_\mu A^{a,\mu})^2 - \xi (\partial_5 A^{a,5})^2 \right) \quad (2.21)$$

Varying the free action with respect to A_ν^a and A_5^a we obtain the following equations of motion

$$-\partial_5^2 A^{a,\nu} + \partial_\mu \partial^\mu A^{a,\nu} - \left(1 - \frac{1}{\xi}\right) \partial^\nu \partial^\mu A_\mu^a = 0 \\ -\partial_\mu \partial^\mu A^{a,5} + \xi \partial_5^2 A^{a,5} = 0 \quad (2.22)$$

After the variation we have to perform an integration by parts again in the extra dimension, which will give an extra term for the variation of the action on the boundaries of the interval. Taking all the boundary terms together we get the following expression

$$\delta S_{\text{bound}} = \int d^4x \left[\partial_5 A_\nu^a \delta A^{a,\nu} - \xi \partial_5 A_5^a \delta A_5^a - A_\nu^a \partial^\nu \delta A^{a,5} - \partial_\nu A^{a,5} \delta A^{a,\nu} \right]_0^L = 0, \quad (2.23)$$

which has to vanish for the same reason as in Sec. 2.1.1. To solve the equations of motion we make the ansatz

$$A_\mu^a(x, y) = \sum_n e^{-ip_n x} \epsilon_\mu^a \lambda_n^a(y) \\ A_5^a(x, y) = \sum_n e^{-ip_n x} \epsilon_5^a \lambda_{5,n}^a(y) \quad (2.24)$$

where ϵ_5^a and ϵ_μ^a are the polarization vectors. Note that there is no summation over the adjoint index of the $SU(N)$ gauge group. Furthermore $p_n^2 = m_n^2$ holds. Plugging the Kaluza-Klein decomposition of A_5^a into the second equation of motion of (2.22) we get

$$p_n^2 \lambda_{5,n}^a(y) + \xi (\lambda_{5,n}^a)''(y) = 0 \quad (2.25)$$

The solution of the above second order differential equation is given by

$$\lambda_{5,n}^a(y) = A_{5,n}^a e^{\frac{i}{\sqrt{\xi}} m_n y} + B_{5,n}^a e^{-\frac{i}{\sqrt{\xi}} m_n y} \quad (2.26)$$

Now we want to solve the first equation of motion of (2.22). Therefore we plug (2.24) in the above equation and assume w.l.o.g. that three of the four polarization vectors ϵ^ν are perpendicular to p_ν and one is parallel to it. In the first case we have $\epsilon^{\nu,a} p_\nu = 0$ and get for $\lambda_n^a(y)$

$$\lambda_n^a(y) = A_n^a e^{im_n y} + B_n^a e^{-im_n y} \quad (2.27)$$

In the second case ($\epsilon^{\nu,a} = p^\nu \bar{\epsilon}^a$) the solution is

$$\lambda_n^a(y) = C_n^a e^{\frac{m_n}{\sqrt{\xi}} y} + D_n^a e^{-\frac{m_n}{\sqrt{\xi}} y} \quad (2.28)$$

We will see later that the non-oscillating solutions are not compatible with the boundary conditions and therefore we can neglect them.

The only type of fields that we have not considered until now are scalar fields, but the extension of the 4D dynamics of scalars to a 5D one is the same as in the case of fermions and vectors shown in the sections before. Therefore we introduce the 5D Lagrangian and the resulting 5D equations of motion with their solutions when we define the model used in this thesis.

2.2 Warped Extra Dimensions

Now we want to extend the flat 5D model to a warped 5D one. Therefore we denote quantities which live in curved spacetime with $\hat{\cdot}$. To understand the dynamics in a warped extra dimensional model better we first introduce the very basics of classical curved spacetimes. General relativity is formulated to be invariant under general coordinate transformations, the so called diffeomorphisms. To get nontrivial dynamics one main aspect of constructing a theory is defining a derivative. In curved spacetime the partial derivative ∂_M is not well defined because $\partial_M A_N$ is no longer a tensor field if A_N is a vector. To obtain a tensor field we define the covariant derivative

$$D_M A_N \equiv \partial_M A_N - \Gamma^P_{MN} A_P, \quad (2.29)$$

where Γ^P_{MN} are the Christoffel symbols. The covariant derivative of A^N is $(\partial_M A^N + \Gamma^N_{MP} A^P)$. To get a geometrical interpretation of the Christoffel symbols we have to go back to the definition of a derivative in general curved spacetime. A tangential space where the vectors A_N are defined exists at every spacetime point. A derivative connects two vectors each living in infinitesimal separated tangent spaces. To get the connection between the two tangential spaces we have to define a map from one tangential space to the other. This map is the so called parallel transport and the Christoffel symbols are the generators of it. After the transformation both vectors are in the same tangential space and the partial derivative can be performed. It makes sense then that in Eq. (2.29) an additional term that comes from the parallel transport appears. From the requirement of metricity

$$D_M \hat{g}_{NP} \equiv \partial_M \hat{g}_{NP} - \Gamma^L_{MN} \hat{g}_{LP} - \Gamma^L_{MP} \hat{g}_{NL} = 0 \quad (2.30)$$

and of the torsionsless condition, $\Gamma^P_{MN} - \Gamma^P_{NM} = 0$, it can be found uniquely that

$$\Gamma^P_{MN} \equiv \frac{1}{2} \hat{g}^{PL} (\partial_M \hat{g}_{NL} + \partial_N \hat{g}_{ML} - \partial_L \hat{g}_{MN}). \quad (2.31)$$

As the spinor representation of the Lorentz group cannot be linearly extended to the general coordinate transformation group of general relativity we have to introduce the Vielbein formalism. Since the spacetime of general relativity is locally Minkowskian, we can set up a local orthogonal coordinate system at each point x^M . The basis vectors $V_M^A(x)$ ($A = 0, 1, 2, 3, 5$) are called the Fünfbein (or tetrad). They are related to the metric tensor $\hat{g}_{MN}(x)$ through

$$\hat{g}_{MN} = g_{AB} V_M^A V_N^B \quad (2.32)$$

where $V_B^M V_M^A = \delta_B^A$ holds true. Extending Eq. (2.29), we require

$$D_M V_N^A \equiv \partial_M V_N^A - \Gamma^P_{MN} V_P^A + w_M^A{}_{\mathcal{B}} V_N^{\mathcal{B}} = 0, \quad (2.33)$$

where $w_M^A{}_{\mathcal{B}}$ denotes the spin connection, which is the connection related to the local gauge transformations, so that the spin connection is nothing else but the gauge field for the Lorentz group. From Eq. (2.33) the spin connection can be expressed as

$$w_M^A{}_{\mathcal{B}} = V^A_N \Gamma^N_{MP} V^P_{\mathcal{B}} - (\partial_M V^A_N) V^N_{\mathcal{B}} \quad (2.34)$$

and is antisymmetric with respect to the Minkowskian indices ($w_M^{AB} = -w_M^{BA}$). The Christoffel symbols then read in terms of the spin connection

$$\Gamma^N_{MP} = V^N_{\mathcal{A}} w_M^{\mathcal{A}}{}_{\mathcal{B}} V^{\mathcal{B}}_P - (\partial_M V^N_{\mathcal{A}}) V^{\mathcal{A}}_P \quad (2.35)$$

Next we want to examine the dynamics of fermions in a warped 5D theory. The action of the fermions is

$$S_{\text{SD,fermion}} = \int d^5x \sqrt{\hat{g}} \left[\frac{i}{2} (\bar{\Psi} \hat{\gamma}^M D_M \Psi - D_M \bar{\Psi} \hat{\gamma}^M \Psi) - m_{\text{bulk}} \bar{\Psi} \Psi \right] \quad (2.36)$$

To rewrite the action in more compact form

$$S_{\text{SD,fermion}} = \int d^5x \sqrt{\hat{g}} (i \bar{\Psi} \hat{\gamma}^M D_M \Psi - m_{\text{bulk}} \bar{\Psi} \Psi) + \text{B.T.} \quad (2.37)$$

we have to perform an integration by parts. Now we have to pose the question whether the integration by parts holds true in curved spacetime. The first approach is to study the covariant derivative and how it acts on $\bar{\Psi} \hat{\gamma}^M \Psi$

$$D_M (\bar{\Psi} \hat{\gamma}^M \Psi) = \bar{\Psi} \hat{\gamma}^M (D_M \Psi) + (D_M \bar{\Psi}) \hat{\gamma}^M \Psi + \bar{\Psi} (D_M \hat{\gamma}^M) \Psi \quad (2.38)$$

To get the integration by parts we know, we have to ensure that the covariant derivative of $\hat{\gamma}^M$ is equal to zero. Moreover it becomes clear that the integration by parts with respect to the partial derivative does not hold any longer because $\partial_M \hat{\gamma}^M$ is not equal to zero in general. To calculate the covariant derivative of $\hat{\gamma}^M$ we must clarify how the spin connection acts on spinors.

Because we are locally in a 5D Minkowsky space, the only transformations that locally exist are the 5D Lorentz ones. Hence the infinitesimal parallel transport of a vector A^A can be written as

$$w_M{}^A{}_B A^B = -\frac{i}{4} w_M{}_{CD} (\Lambda^{CD})^A{}_B A^B \quad (2.39)$$

This can easily be shown when plugging the vector representation of the Lorentz generators

$$(\Lambda^{CD})^A{}_B = i (g^{CA} \delta_B^D - g^{DA} \delta_B^C) \quad (2.40)$$

in Eq. (2.39). Operators transform with the commutator and therefore the infinitesimal parallel transport of γ^A is

$$w_M{}^A{}_B \gamma^B = -\frac{i}{4} [w_M{}_{CD} \Lambda^{CD}, \gamma^A] \quad (2.41)$$

This can be seen after a short calculation by plugging the spinor representation of the Lorentz generators

$$(\Lambda^{CD})^j{}_i = \frac{i}{2} [\gamma^C, \gamma^D]^j{}_i \quad (2.42)$$

in Eq. (2.41) and using the anticommutator relation of the γ -matrices ($\{\gamma^A, \gamma^B\} = 2g^{AB}$). At this point we want to give a short summary how the spin connection acts on vectors and fermions to get a consistent convention. Therefore we require the covariant derivative of the vectors

$$\begin{aligned} D_M A_A &= \partial_M A_A + w_{MA}{}^B A_B = \partial_M A^A - \frac{i}{4} w_M{}_{CD} (\Lambda^{CD})^A{}_B A_B \\ D_M A^A &= \partial_M A^A + w_M{}^A{}_B A^B = \partial_M A^A - \frac{i}{4} w_M{}_{CD} (\Lambda^{CD})^A{}_B A^B \end{aligned} \quad (2.43)$$

and the fermions

$$\begin{aligned} D_M \Psi_i &= \partial_M \Psi_i + w_M{}^j{}_i \Psi_j = \partial_M \Psi_i - \frac{i}{4} w_M{}_{CD} (\Lambda^{CD})^j{}_i \Psi_j \\ D_M \bar{\Psi}_i &= \partial_M \bar{\Psi}_i - w_M{}^j{}_i \bar{\Psi}_j = \partial_M \bar{\Psi}_i + \frac{i}{4} w_M{}_{CD} (\Lambda^{CD})^j{}_i \bar{\Psi}_j \end{aligned} \quad (2.44)$$

Now the only thing to do is to calculate the covariant derivative of $\hat{\gamma}^N$. Thus we regard the covariant derivative of $\bar{\Psi}\hat{\gamma}^N\Psi$ and get

$$\begin{aligned} D_M(\bar{\Psi}\hat{\gamma}^N\Psi) &= (\partial_M\bar{\Psi})\hat{\gamma}^N\Psi + \bar{\Psi}\hat{\gamma}^N(\partial_M\Psi) + \bar{\Psi}(\partial_M\hat{\gamma}^N)\Psi + \bar{\Psi}\Gamma_{MP}^N\hat{\gamma}^P\Psi \\ &= (\partial_M\bar{\Psi})\hat{\gamma}^N\Psi + \bar{\Psi}\hat{\gamma}^N(\partial_M\Psi) - \frac{i}{4}\bar{\Psi}w_M\hat{\gamma}^N\Psi + \frac{i}{4}\bar{\Psi}\hat{\gamma}^Nw_M\Psi + \bar{\Psi}(D_M\hat{\gamma}^N)\Psi \end{aligned} \quad (2.45)$$

With that equality we can write the covariant derivative of $\hat{\gamma}^N$ as follows

$$D_M\hat{\gamma}^N = \partial_M\hat{\gamma}^N + \Gamma_{MP}^N\hat{\gamma}^P - \frac{i}{4}[w_M{}_{CD}\Lambda^{CD}, \hat{\gamma}^N] = 0 \quad (2.46)$$

Plugging Eq. (2.35) and (2.41) in Eq. (2.46) we see that the expression vanishes. Thus an integration by parts exists in curved spacetime

$$\int d^5x \sqrt{g} (\bar{\Psi}\hat{\gamma}^M D_M\Psi) = \int_{\partial S} \sqrt{g} (\bar{\Psi}\hat{\gamma}^M\Psi) - \int d^5x \sqrt{g} (D_M\bar{\Psi}\hat{\gamma}^M\Psi) \quad (2.47)$$

After this short excursion about properties of curved spacetimes we want to come back to warped extra dimensional theories. First we discuss the basic characteristics of the warped 5D model and afterwards explain on the basis of the fermionic action how to obtain the equation of motion and how to solve it. The metric of the warped 5D spacetime is

$$\hat{g}_{MN} = \frac{1}{k^2 z^2} \delta_M^A \delta_N^B g_{AB}, \quad g = \text{diag}(1, -1, -1, -1, -1) \quad (2.48)$$

and from this it follows that the vielbein is

$$V_M{}^A = \frac{1}{kz} \delta_M^A \quad (2.49)$$

To get the correct dynamics for the fermions we have to calculate the spin connection for the warped 5D metric. Therefore we use Eq. (2.34) and (2.31) and obtain

$$\begin{aligned} w_M{}^A{}_B &= -\frac{1}{z} V_B^N V_P^A (\delta_M^5 \delta_N^P + \delta_N^5 \delta_M^P - \hat{g}^{P5} g_{MN}) + \frac{1}{z} V_B^N \delta_M^5 V_N^A \\ &= -\frac{1}{z} V_B^N V_P^A (\delta_M^5 \delta_N^P + \delta_N^5 \delta_M^P - \hat{g}^{P5} g_{MN}) \end{aligned} \quad (2.50)$$

where we used $\partial_M V_N{}^A = -\frac{1}{z} \delta_M^5 V_N{}^A$. Since we want the fermionic spin connection we choose the spin representation of it

$$\begin{aligned} \frac{i}{4} w_M{}_{CD} \Lambda^{CD} &= \frac{1}{8z} V_D^N V_C^P (\delta_N^5 \delta_M^P - \hat{g}^{P5} g_{MN}) [\gamma^C, \gamma^D] \\ &= \frac{1}{8z} (\delta_N^5 \delta_M^P - \hat{g}^{P5} g_{MN}) [\hat{\gamma}^P, \hat{\gamma}^N] \\ &= \frac{1}{4z} (\hat{\gamma}_M \hat{\gamma}^5 - \hat{\gamma}^5 \hat{\gamma}_M) \end{aligned} \quad (2.51)$$

From this we get the following covariant derivative for fermions

$$\begin{aligned} D_\mu &= \partial_\mu - \frac{1}{2z} \hat{\gamma}_\mu \hat{\gamma}^5 \\ D_5 &= \partial_5 \end{aligned} \quad (2.52)$$

Because we have shown that the integration by parts is a valid operation in curved spacetime we can extend the Euler-Lagrange equations to a covariant form

$$\frac{\partial \mathcal{L}}{\partial \Psi} - D_M \frac{\partial \mathcal{L}}{\partial (D_M \Psi)} = 0 \quad (2.53)$$

As a next step we have to clarify what the natural representations of the γ -matrices and the covariant derivative are. Hence the spin representation with Dirac fermions exists only in the local Minkowsky space the natural γ -matrices are the flat ones in opposition to the covariant derivative, which is naturally defined in curved spacetime. Therefore we write the fermionic action as follows

$$\begin{aligned} S_{5D, \text{fermion}} &= \int d^5 x \sqrt{\hat{g}} \left(i V^M_{\mathcal{A}} \bar{\Psi} \gamma^A D_M \Psi - m_{\text{bulk}} \bar{\Psi} \Psi \right) \\ &= \int d^5 x \frac{1}{k^4 z^4} \left(i \delta^M_{\mathcal{A}} \bar{\Psi} \gamma^A D_M \Psi - \frac{c}{z} \bar{\Psi} \Psi \right) \end{aligned} \quad (2.54)$$

where $c = m_{\text{bulk}}/k$ and $\sqrt{\hat{g}} = 1/(k^5 z^5)$. The 4D part of the covariant derivative then reads

$$\begin{aligned} \delta^{\mu}_{\mathcal{A}} \gamma^A D_{\mu} &= \delta^{\mu}_{\mathcal{A}} \gamma^A \left(\partial_{\mu} - \frac{1}{2z} \hat{\gamma}_{\mu} \hat{\gamma}^5 \right) \\ &= \delta^{\mu}_{\mathcal{A}} \gamma^A \partial_{\mu} - \frac{1}{2z} k z \hat{\gamma}^{\mu} \hat{\gamma}_{\mu} \hat{\gamma}^5 \\ &= \gamma^{\alpha} \partial_{\alpha} - \frac{2}{z} \gamma^5 \end{aligned} \quad (2.55)$$

With this information we can derive the equations of motion for η and $\bar{\chi}$

$$\begin{aligned} i \sigma^{\alpha} \partial_{\alpha} \eta + \partial_5 \bar{\chi} - \frac{c+2}{z} \bar{\chi} &= 0 \\ i \sigma^{\alpha} \partial_{\alpha} \bar{\chi} - \partial_5 \eta - \frac{c-2}{z} \eta &= 0 \end{aligned} \quad (2.56)$$

Using the Kaluza-Klein decomposition given in Eq. (2.9) and the 4D equations of motion from (2.10) we get the following equations of motion for the 5D part of the fermionic wave functions

$$\begin{aligned} f'_{\bar{\chi},(n)} + m_n f_{\eta,(n)} - \frac{c+2}{z} f_{\bar{\chi},(n)} &= 0 \\ f'_{\eta,(n)} - m_n f_{\bar{\chi},(n)} + \frac{c-2}{z} f_{\eta,(n)} &= 0 \end{aligned} \quad (2.57)$$

As in the flat case we have two coupled first order differential equations which can be transformed into two second order differential equations

$$\begin{aligned} f''_{\bar{\chi},(n)} - \frac{4}{z} f'_{\bar{\chi},(n)} + \left(m_n^2 - \frac{c^2 - c - 6}{z^2} \right) f_{\bar{\chi},(n)} &= 0 \\ f''_{\eta,(n)} - \frac{4}{z} f'_{\eta,(n)} + \left(m_n^2 - \frac{c^2 + c - 6}{z^2} \right) f_{\eta,(n)} &= 0 \end{aligned} \quad (2.58)$$

whose solutions are linear combinations of Bessel functions

$$\begin{aligned} f_{\bar{\chi},(n)}(z) &= z^{5/2} \left(A_n J_{1/2-c}(m_n z) + B_n Y_{1/2-c}(m_n z) \right) \\ f_{\eta,(n)}(z) &= z^{5/2} \left(C_n J_{1/2+c}(m_n z) + D_n Y_{1/2+c}(m_n z) \right) \end{aligned} \quad (2.59)$$

Using the bulk equations of motion (2.57) we obtain

$$A_n = C_n \quad \text{and} \quad B_n = D_n. \quad (2.60)$$

Chapter 3

Supersymmetric Extension in 5D

Since we want to implement supersymmetry in a warped extra dimensional model we need a five dimensional description of supersymmetry. This means that we first extend the four dimensional supersymmetry algebra to a five dimensional one and in a next step construct the field representations of this algebra. We will see that we can obtain the 5D supersymmetry representations out of 4D representations and thus the 5D action is a sum of the normal 4D supersymmetry action and an additional 5D part. Thus we will first give a short review of 4D supersymmetry. Afterwards we present a formalism for constructing five dimensional supersymmetric theories.

3.1 Supersymmetry in 4D

This section's intention is to give a summary of all main topics of 4D supersymmetry that we need to construct a 5D SUSY. If you want to know more details, [11] offers a well structured introduction in 4D supersymmetric issues. First we start with the algebra of supersymmetry and then we switch over to the representations of this algebra. Next we give a short overview of the superfield formalism and finally construct the most general 4D gauge invariant interaction.

3.1.1 Supersymmetry Algebra

The supersymmetry algebra is the only graded Lie algebra of symmetries of the S-matrix consistent with relativistic quantum field theory. The proof of this statement is based on the Coleman-Mandula theorem, a theorem about the possible symmetries of the S-matrix. The theorem indicates that the most general Lie algebra of symmetries of the S-matrix contains the energy-momentum operator P_μ , the Lorentz generators $M_{\mu\nu}$ and a finite number of operators B_l which transform as scalars under Lorentz transformations and must belong to a Lie algebra of a compact Lie group. For example the gauge transformations contain such operators.

Supersymmetry eludes the restrictions of the Coleman-Mandula theorem by generalizing the notion of a Lie algebra so that the Lie algebra now includes elements whose defining relations involve anticommutators as well as commutators. These new algebras are called superalgebras or graded Lie algebras. They can be written as

$$\{Q, Q'\} = X, \quad [X, X'] = X'', \quad [Q, X] = Q'' \quad (3.1)$$

where Q , Q' and Q'' represent the odd (anticommuting) part of the algebra and X , X' and X'' the even (commuting) part. The operators X are determined by the Coleman-Mandula theorem and therefore either elements of the Poincaré algebra or elements of a Lorentz invariant compact Lie algebra.

The Coleman-Mandula theorem tells us that the anticommutator of the Q 's has to be an element of the Poincaré group. Because the Poincaré algebra only contains spin 1 objects, the Q 's have to be of the form

Q_α^L and $\bar{Q}_{\dot{\alpha}M}$, where \bar{Q} denotes the hermitian conjugate of Q . The Greek indices $(\alpha_1, \dots, \alpha_a, \dot{\alpha}_1, \dots, \dot{\alpha}_b)$ run from one to two and denote two-component Weyl spinors. Moreover the anticommutator of Q_α^L and $\bar{Q}_{\dot{\alpha}M}$ has to close into $P_{\alpha\dot{\alpha}}$

$$\{Q_\alpha^L, \bar{Q}_{\dot{\alpha}M}\} = 2P_{\alpha\dot{\alpha}}\delta_M^L, \quad (3.2)$$

where $P_{\alpha\dot{\alpha}} = \sigma_{\alpha\dot{\alpha}}^\mu P_\mu$ and σ is the intertwiner between the spin and vector representations. The anticommutator of two odd elements, both with undotted indices can be written as

$$\{Q_\alpha^L, Q_\beta^M\} = \epsilon_{\alpha\beta}X^{LM} \quad (3.3)$$

The generators X^{LM} commute with all generators of the Poincaré group and those of a Lorentz invariant compact Lie algebra and for this reason they are called central charges. The supersymmetric algebra then reads

$$\begin{aligned} [P_\mu, Q_\alpha^L] &= [P_\mu, \bar{Q}_{\dot{\alpha}L}] = 0 \\ \{Q_\alpha^L, \bar{Q}_{\dot{\alpha}M}\} &= -2\sigma_{\alpha\dot{\alpha}}^\mu P_\mu \delta_M^L \\ \{Q_\alpha^L, Q_\beta^M\} &= \epsilon_{\alpha\beta}X^{LM} \\ \{\bar{Q}_{\dot{\alpha}L}, \bar{Q}_{\dot{\beta}M}\} &= \epsilon_{\dot{\alpha}\dot{\beta}}X^{LM} \\ [X^{LM}, \bar{Q}_{\dot{\alpha}K}] &= [X^{LM}, \bar{Q}_\alpha^K] = 0 \end{aligned} \quad (3.4)$$

3.1.2 Representations of the $N = 1, 2$ Supersymmetry Algebra

In this part we want to study the 4D $N = 1$ and $N = 2$ representations of supersymmetry on one-particle states since we need these representations later on to understand the decomposition of the 5D superfields in 4D ones. Since the mass operator P^2 is a Casimir operator of the SUSY algebra, the particles in an irreducible representation of the SUSY algebra are of equal mass. Furthermore it can be shown by a short calculation that every representation has the same number of bosonic and fermionic degrees of freedom.

Now we want to construct the representation of the supersymmetry algebra corresponding to massive one-particle states ($P^2 = M^2$). To construct a 4D $N = 2$ SUSY out of $N = 1$ representations we require massive $N = 1$ representations. Thus we show in the following part how to get the massive SUSY $N = 1$ representations very easily. For simplicity we boost the four-vector P_μ to the rest frame $P_\mu = (M, 0, 0, 0)$ and find for the algebra

$$\begin{aligned} \{Q_\alpha^A, \bar{Q}_{\dot{\beta}B}\} &= 2M\delta_{\alpha\dot{\beta}}\delta_B^A \\ \{Q_\alpha^A, Q_\beta^B\} &= \{\bar{Q}_{\dot{\alpha}A}, \bar{Q}_{\dot{\beta}B}\} = 0, \end{aligned} \quad (3.5)$$

where we set the central charges to zero for simplicity. The indices A and B run from one to N . To get a more intuitive access to the supersymmetry algebra we rescale the generators Q so that

$$\begin{aligned} a_\alpha^A &= \frac{1}{\sqrt{2M}} Q_\alpha^A \\ (a_\alpha^A)^\dagger &= \frac{1}{\sqrt{2M}} \bar{Q}_{\dot{\alpha}A} \end{aligned} \quad (3.6)$$

and we recognize the algebra of $2N$ fermionic creation and annihilation operators. The algebra of a_α^A and $(a_\alpha^A)^\dagger$ then reads

$$\begin{aligned} \{a_\alpha^A, (a_\beta^B)^\dagger\} &= \delta_{\alpha\dot{\beta}}\delta_B^A \\ \{a_\alpha^A, a_\beta^B\} &= \{(a_\alpha^A)^\dagger, (a_\beta^B)^\dagger\} = 0 \end{aligned} \quad (3.7)$$

Since the supersymmetry algebra is isomorphic to a $2N$ fermionic oscillator algebra, it can be represented on a Fock space. The Clifford (Fock) vacuum Ω is defined by

$$a_\alpha^A \Omega = 0. \quad (3.8)$$

The states are built by applying the creation operators $(a_\alpha^A)^\dagger$ to the vacuum state Ω

$$\Omega^{(n)}_{A_1 \dots A_n} = \frac{1}{\sqrt{n!}} (a_{\alpha_1}^{A_1})^\dagger \dots (a_{\alpha_n}^{A_n})^\dagger \Omega \quad (3.9)$$

and the dimension of the representation is given by

$$d = 2^{2N} \quad (3.10)$$

Note that we regard only spin 0 vacua in the massive case. The massive $N = 1$ representation of the supersymmetry algebra therefore contains two spin 0 states and one spin $\frac{1}{2}$ state. When we introduce the superfield formalism, we will see that the discussed representation can be identified with a massive chiral superfield.

Next we want to study the supersymmetry representations built from massless one-particle states ($P^2 = 0$). Therefore we use the frame where $P_\mu = (E, 0, 0, -E)$. The algebra then becomes

$$\begin{aligned} \{Q_\alpha^A, \bar{Q}_{\dot{\beta}B}\} &= 2M \begin{pmatrix} 2E & 0 \\ 0 & 0 \end{pmatrix} \delta^A_B \\ \{Q_\alpha^A, Q_\beta^B\} &= \{\bar{Q}_{\dot{\alpha}A}, \bar{Q}_{\dot{\beta}B}\} = 0 \end{aligned} \quad (3.11)$$

Again we rescale the generators Q

$$\begin{aligned} a^A &= \frac{1}{2\sqrt{E}} Q_1^A \\ (a^A)^\dagger &= \frac{1}{2\sqrt{E}} \bar{Q}_{1A} \end{aligned} \quad (3.12)$$

and we find that the algebra consists of N creation and annihilation operators

$$\begin{aligned} \{a^A, (a^B)^\dagger\} &= \delta^A_B \\ \{a^A, a^B\} &= \{(a^A)^\dagger, (a^B)^\dagger\} = 0 \end{aligned} \quad (3.13)$$

Thus we can construct the massless supersymmetry representations by applying the creation operators a^A to a Clifford vacuum with helicity λ . So a^A and $(a^A)^\dagger$ raising and lowering the helicity by $\frac{1}{2}$ and the states can be written as

$$\Omega_{A_1 \dots A_n}^{(n)} = \frac{1}{\sqrt{n!}} (a^{A_1})^\dagger \dots (a^{A_n})^\dagger \Omega_\lambda \quad (3.14)$$

The dimension of the representation is given by 2^N . We regard only the massless representations of vacua with λ equal to 0, $1/2$ and $-1/2$, since these are the representations we need to construct a physical $N = 2$ supersymmetry. To get a CPT invariant theory the states must be doubled, since CPT reverses the sign of the helicity. The CPT-complete representations are shown in Tab. 3.1 and 3.2. Note that the $N = 2$, $\lambda = -1/2$ multiplet is by construction CPT-complete. Moreover the massive 4D $N = 1$ representation is the same as the 4D $N = 1$ CPT-complete massless representation of the spin $-1/2$ and 0 vacua. We will use this identity later to construct the whole theory out of 4D $N = 2$ massless representations.

hel.	$\lambda = -\frac{1}{2}$	$\lambda = 0$	$\lambda = \frac{1}{2}$
1			1
$\frac{1}{2}$	1	1	1
0	1 + 1	1 + 1	
$-\frac{1}{2}$	1	1	1
-1			1

Table 3.1: Massless 4D $N = 1$ representations.

hel.	$\lambda = -\frac{1}{2}$	$\lambda = 0$	$\lambda = \frac{1}{2}$
$\frac{3}{2}$			1
1		1	2
$\frac{1}{2}$	1	2	1
0	2	1 + 1	
$-\frac{1}{2}$	1	2	1
-1		1	2
$-\frac{3}{2}$			1

Table 3.2: Massless 4D $N = 2$ representations.

hel.	1	$-\frac{1}{2}$	0	$\frac{1}{2}$	1
$N = 2$	1	2	1 + 1	2	1
$N = 1$	1	1		1	1
$N = 1$		1	1 + 1	1	

Table 3.3: Decomposition of the 4D $N = 2$ representation ($\lambda = 0$).

hel.	1	$-\frac{1}{2}$	0	$\frac{1}{2}$	1
$N = 2$		1	2	1	
$N = 1$		1	1		
$N = 1$			1	1	

Table 3.4: Decomposition of the 4D $N = 2$ representation ($\lambda = -\frac{1}{2}$).

Each of the $N = 2$ multiplets can now be decomposed in two $N = 1$ representations, as shown in Tab. 3.3 and 3.4 for the case of the spin 0 and spin $-1/2$ vacuum. The $N = 2$, $\lambda = 0$ representation splits into a $N = 1$, $\lambda = 0$ and a $N = 1$, $\lambda = 1/2$ representation. The $N = 2$, $\lambda = -1/2$ representation splits into a $N = 1$, $\lambda = 0$ and a $N = 1$, $\lambda = -1/2$ representation. Massless representations have dimension 2^N and massive representations have dimension 2^{2N} . Thus in the case of $N = 1$ SUSY we have to double the massless $N = 1$ multiplets of Tab. 3.4 to get massive $N = 1$ representations. As we want to have a supersymmetric field theory we have to construct the field representations of the SUSY algebra, which will be explained in the next section. We will see that the doubled $N = 1$ multiplets of Tab. 3.4 can be identified with two massive chiral superfields and the $N = 1$, $\lambda = 1/2$ and $N = 1$, $\lambda = 0$ representations of Tab. 3.3 with a massless vector and a massless chiral superfield, respectively.

3.1.3 Superfields

Now we give a short introduction to the superfield formalism because it provides an elegant and compact description of $N = 1$ supersymmetry field representations. To formulate a supersymmetric field theory we must represent the supersymmetry algebra in terms of fields not restricted by any mass-shell condition first. Therefore we introduce a set of anticommuting parameters $\xi^\alpha, \bar{\xi}_{\dot{\alpha}}$

$$\{\xi^\alpha, \xi^\beta\} = \{\xi^\alpha, Q_\beta\} = \dots = [P_\mu, \xi^\alpha] = 0, \quad (3.15)$$

which allow us to express the supersymmetry algebra in terms of commutators

$$\begin{aligned} [\xi Q, \bar{\xi} \bar{Q}] &= 2 \xi \sigma^\mu \bar{\xi} P_\mu \\ [\xi Q, \xi Q] &= [\bar{\xi} \bar{Q}, \bar{\xi} \bar{Q}] = 0 \\ [P^\mu, \xi Q] &= [P^\mu, \bar{\xi} \bar{Q}] = 0 \end{aligned} \quad (3.16)$$

This leads us to the following definition of the group element of the translation in superspace

$$G(x, \theta, \bar{\theta}) = e^{i(-x_\mu P^\mu + \theta Q + \bar{\theta} \bar{Q})} \quad (3.17)$$

From the left multiplication of two group elements we obtain

$$G(0, \xi, \bar{\xi}) G(x^\mu, \theta, \bar{\theta}) = G(x^\mu + i\theta \sigma^\mu \bar{\theta} - i\xi \sigma^\mu \bar{\theta}, \theta + \xi, \bar{\theta} + \bar{\xi}), \quad (3.18)$$

where the infinitesimal transformation with respect to Q can be written as

$$i(\xi Q + \bar{\xi}\bar{Q}) = \xi^\alpha \left(\frac{\partial}{\partial\theta^\alpha} - i\sigma_{\alpha\dot{\alpha}}{}^\mu \bar{\theta}^{\dot{\alpha}} \partial_\mu \right) + \bar{\xi}_{\dot{\alpha}} \left(\frac{\partial}{\partial\bar{\theta}^{\dot{\alpha}}} - i\theta^\alpha \sigma_{\alpha\dot{\beta}}{}^\mu \epsilon^{\dot{\beta}\dot{\alpha}} \partial_\mu \right) \quad (3.19)$$

Thus we have found a representation of the SUSY generators in the parameter space. Through the right multiplication of two group elements we can define the differential operators D and \bar{D}

$$\begin{aligned} D_\alpha &= \frac{\partial}{\partial\theta^\alpha} + i\sigma_{\alpha\dot{\alpha}}{}^\mu \bar{\theta}^{\dot{\alpha}} \partial_\mu \\ \bar{D}_{\dot{\alpha}} &= -\frac{\partial}{\partial\bar{\theta}^{\dot{\alpha}}} - i\theta^\alpha \sigma_{\alpha\dot{\beta}}{}^\mu \partial_\mu \end{aligned} \quad (3.20)$$

which by their definition satisfy the following anticommutation relations

$$\begin{aligned} \{D_\alpha, \bar{D}_{\dot{\alpha}}\} &= -2i\sigma_{\alpha\dot{\alpha}}{}^\mu \partial_\mu \\ \{D_\alpha, D_\beta\} &= \{\bar{D}_{\dot{\alpha}}, \bar{D}_{\dot{\beta}}\} = 0 \end{aligned} \quad (3.21)$$

and anticommute with Q

$$\{D_\alpha, Q_\beta\} = \{D_\alpha, \bar{Q}_{\dot{\beta}}\} = \{\bar{D}_{\dot{\alpha}}, Q_\beta\} = \{\bar{D}_{\dot{\alpha}}, \bar{Q}_{\dot{\beta}}\} = 0 \quad (3.22)$$

Now we can introduce superfields and superspace. Elements of the superspace are labeled by $s = (x, \theta, \bar{\theta})$ and superfields are functions of the superspace which should be understood in terms of their power series expansion in θ and $\bar{\theta}$

$$\begin{aligned} F(x, \theta, \bar{\theta}) &= f(x) + \theta\Phi(x) + \bar{\theta}\bar{\chi}(x) \\ &+ \theta\theta m(x) + \bar{\theta}\bar{\theta}n(x) + \theta\sigma^\mu\bar{\theta}v_\mu(x) \\ &+ \theta\theta\bar{\theta}\bar{\lambda}(x) + \bar{\theta}\bar{\theta}\theta\Psi(x) + \bar{\theta}\bar{\theta}\theta\bar{\theta}d(x) \end{aligned} \quad (3.23)$$

All higher powers of θ and $\bar{\theta}$ vanish. Linear combinations of superfields are again superfields and similarly products of superfields are again superfields which is based on the fact that Q and \bar{Q} are linear differential operators. Thus the superfields form a linear representation of the supersymmetry algebra. Since the representations are highly reducible we have to demand constraints which reduce the superfields. This conditions lead us to the next two sections where we introduce the chiral and the vector superfield, which enable us to construct a gauge invariant supersymmetric Lagrangian.

3.1.4 Chiral Superfields

Chiral superfields are defined by the condition

$$\bar{D}_{\dot{\alpha}}\Phi = 0 \quad (3.24)$$

Since

$$\bar{D}_{\dot{\alpha}}(x^\mu + i\theta\sigma^\mu\bar{\theta}) = 0 \quad \text{and} \quad \bar{D}_{\dot{\alpha}}\theta = 0, \quad (3.25)$$

the above constraint is easy to solve in terms of

$$y^\mu = x^\mu + i\theta\sigma^\mu\bar{\theta} \quad (3.26)$$

Any function of these variables satisfies (3.24) and can be written as

$$\begin{aligned} \Phi &= A(y) + \sqrt{2}\theta\Psi(y) + \theta\theta F(y) \\ &= A(x) + i\theta\sigma^\mu\bar{\theta}\partial_\mu A(x) - \frac{1}{4}\theta\theta\bar{\theta}\bar{\theta}\square A(x) \end{aligned}$$

$$+ \sqrt{2}\theta\Psi(x) - \frac{i}{\sqrt{2}}\theta\theta\partial_\mu\Psi(x)\sigma^\mu\bar{\theta} + \theta\theta F(x) \quad (3.27)$$

The superfield Φ^\dagger satisfies $D_\alpha\Phi^\dagger = 0$ and is a natural function of $y^{\dagger\mu} = x^\mu - i\theta\sigma^\mu\bar{\theta}$ and $\bar{\theta}$. Its power series is obtained by conjugation of (3.27).

The most general supersymmetric renormalizable Lagrangian involving only chiral superfields reads

$$\mathcal{L} = \Phi_i^\dagger\Phi_j\Big|_{\theta\theta\bar{\theta}\bar{\theta}} + \left[\left(\frac{1}{2}m_{ij}\Phi_i\Phi_j + \frac{1}{3}g_{ijk}\Phi_i\Phi_j\Phi_k + \lambda_i\Phi_i \right) \Big|_{\theta\theta} + \text{h.c.} \right] \quad (3.28)$$

The couplings m_{ij} and g_{ijk} are symmetric in their indices. In terms of the component fields, \mathcal{L} reads

$$\begin{aligned} \mathcal{L} = & i\partial_\mu\bar{\Psi}_i\bar{\sigma}^\mu\Psi_i - A^*\square A_i - \frac{1}{2}m_{ik}\Psi_i\Psi_k - \frac{1}{2}m_{ik}^*\bar{\Psi}_i\bar{\Psi}_k \\ & - g_{ijk}\Psi_i\Psi_j A_k - g_{ijk}^*\bar{\Psi}_i\bar{\Psi}_j A_k^* - \mathcal{V}(A_i, A_j^*), \end{aligned} \quad (3.29)$$

where the the auxiliary fields F_i have been eliminated through their Euler-Lagrange equations. The potential \mathcal{V} has the form $\mathcal{V} = F_k^*F_k$ expressed in fields A_i and A_j^* .

3.1.5 Vector Superfields

Vector superfields satisfy the condition

$$V = V^\dagger \quad (3.30)$$

and therefore can be written as

$$\begin{aligned} V(x, \theta, \bar{\theta}) = & C(x) + i\theta\chi(x) - i\bar{\theta}\bar{\xi}(x) \\ & + \frac{i}{2}\theta\theta[M(x) + iN(x)] - \frac{i}{2}\bar{\theta}\bar{\theta}[M(x) - iN(x)] \\ & - \theta\sigma^\mu\bar{\theta}v_\mu(x) + i\theta\bar{\theta}\bar{\theta}\left[\bar{\lambda}(x) + \frac{i}{2}\bar{\sigma}^\mu\partial_\mu\chi(x)\right] \\ & - \bar{\theta}\bar{\theta}\theta\left[\lambda(x) + \frac{i}{2}\sigma^\mu\partial_\mu\bar{\chi}(x)\right] + \frac{1}{2}\theta\theta\bar{\theta}\bar{\theta}\left[D(x) + \frac{1}{2}\square C(x)\right] \end{aligned} \quad (3.31)$$

The component fields C, D, M, N and v_μ are all real. Now we regard the hermitian field $\Gamma + \Gamma^\dagger$ where Γ and Γ^\dagger are chiral fields

$$\begin{aligned} \Gamma + \Gamma^\dagger = & A + A^* + \sqrt{2}(\theta\Psi\bar{\theta}\bar{\Psi}) + \theta\theta F + \bar{\theta}\bar{\theta}F^* \\ & + i\sigma^\mu\bar{\theta}\partial_\mu(A - A^*) + \frac{i}{\sqrt{2}}\theta\theta\bar{\theta}\bar{\sigma}^\mu\partial_\mu\Psi \\ & + \frac{i}{\sqrt{2}}\bar{\theta}\bar{\theta}\theta\sigma^\mu\partial_\mu\bar{\Psi} - \frac{1}{4}\theta\theta\bar{\theta}\bar{\theta}\square(A + A^*) \end{aligned} \quad (3.32)$$

and we find that in front of the coefficient $\theta\sigma^\mu\bar{\theta}$ stands the gradient $i\partial_\mu(A - A^*)$. This leads us to the following supersymmetric generalization of a gauge transformation

$$V \rightarrow V + \Gamma + \Gamma^\dagger \quad (3.33)$$

Note that the chiral fields Γ and Γ^\dagger have dimension 0 in contrast to a chiral matter-field which has dimension 1. The component fields transform under this gauge transformation as follows

$$\begin{aligned} C & \rightarrow C + A + A^* \\ \chi & \rightarrow \chi - i\sqrt{2}\Psi \end{aligned}$$

$$\begin{aligned}
M + iN &\rightarrow M + iN - 2iF \\
v_\mu &\rightarrow v_\mu - i\partial_\mu(A - A^*) \\
\lambda &\rightarrow \lambda \\
D &\rightarrow D
\end{aligned} \tag{3.34}$$

We find that the choice of the components in (3.31) leaves λ and D gauge invariant. Now we can choose the so called Wess-Zumino (WZ) gauge in which C, χ, M and N are all zero. In spite of the gauge fixing it still remains the usual gauge transformation $v_\mu \rightarrow v_\mu + \partial_\mu \epsilon$. In Wess-Zumino gauge the powers of V looks very simple

$$\begin{aligned}
V &= -\theta\sigma^\mu\bar{\theta}v_\mu(x) + i\theta\theta\bar{\theta}\bar{\lambda}(x) - i\bar{\theta}\bar{\theta}\theta\lambda(x) + \frac{1}{2}\theta\theta\bar{\theta}\bar{\theta}D(x) \\
V^2 &= -\frac{1}{2}\theta\theta\bar{\theta}\bar{\theta}v_\mu v^\mu \\
V^3 &= 0
\end{aligned} \tag{3.35}$$

Next we want to construct the supersymmetric field strength. Therefore we define two chiral fields

$$\begin{aligned}
W'_\alpha &= -\frac{1}{4}\bar{D}\bar{D}D_\alpha V \\
\bar{W}'_{\dot{\alpha}} &= -\frac{1}{4}DD\bar{D}_{\dot{\alpha}} V
\end{aligned} \tag{3.36}$$

and we see that they are gauge invariant

$$W_\alpha = -\frac{1}{4}\bar{D}\bar{D}D_\alpha(V + \Gamma + \Gamma^\dagger) = W_\alpha - \frac{1}{4}\bar{D}\{\bar{D}, D_\alpha\}\Gamma = W_\alpha \tag{3.37}$$

where we used the fact that $\bar{D}\Gamma = D\Gamma^\dagger = 0$. Since W_α and $\bar{W}'_{\dot{\alpha}}$ are chiral fields the $\theta\theta$ and $\bar{\theta}\bar{\theta}$ component respectively of $W^\alpha W_\alpha$ and $\bar{W}'_{\dot{\alpha}}\bar{W}'^{\dot{\alpha}}$ transform into a spacetime derivative. Thus the supersymmetric gauge invariant generalization of the Lagrangian for a free vector field is

$$\mathcal{L} = \frac{1}{4}(W^\alpha W_\alpha|_{\theta\theta} + \bar{W}'_{\dot{\alpha}}\bar{W}'^{\dot{\alpha}}|_{\bar{\theta}\bar{\theta}}) \tag{3.38}$$

which reduces after some integration by parts to

$$\int d^4x \mathcal{L} = \int d^4x \left(\frac{1}{2}D^2 - \frac{1}{4}v^{\mu\nu}v_{\mu\nu} - i\lambda\sigma^\mu\partial_\mu\bar{\lambda} \right) \tag{3.39}$$

3.1.6 Gauge invariant Interactions

In this part we want to present the full $SU(N)$ gauge invariant interaction. We only give a brief review of the extended gauge transformations and the full Lagrangian without going into details of constructing non-abelian gauge theories in supersymmetry. The generalization of gauge transformations on chiral superfields reads

$$\Phi' = e^{-i\Gamma}\Phi, \quad \Phi'^\dagger = \Phi^\dagger e^{i\Gamma^\dagger} \tag{3.40}$$

where the chiral superfields Γ are matrices

$$\Gamma_{ij} = T_{ij}^a \Gamma_a. \tag{3.41}$$

T^a are the generators of the gauge group and get normalized by

$$\text{Tr}[T^a T^b] = \frac{1}{2}\delta^{ab}. \tag{3.42}$$

The Lie algebra reads

$$[T^a, T^b] = if^{abc}T^c, \quad (3.43)$$

where f^{abc} are the structure constants of the gauge group. The supersymmetric field strength W^α can be generalized to

$$W_\alpha = -\frac{1}{4}\bar{D}\bar{D}e^{-V}D_\alpha e^V. \quad (3.44)$$

The vector superfields V are now matrices

$$V_{ij} = T_{ij}^a V_a \quad (3.45)$$

and the non-abelian extension of the gauge transformations reads

$$e^{V'} = e^{-i\Gamma^\dagger} e^V e^{i\Gamma}. \quad (3.46)$$

Now we are ready to write down the most general Lagrangian for the supersymmetric renormalizable interaction of scalar, spinor and vector fields

$$\begin{aligned} \mathcal{L} = & \frac{1}{8g^2} \text{Tr} [W^\alpha W_\alpha|_{\theta\theta} + \bar{W}_{\dot{\alpha}} \bar{W}^{\dot{\alpha}}|_{\bar{\theta}\bar{\theta}}] + \Phi^\dagger e^V \Phi|_{\theta\theta\bar{\theta}\bar{\theta}} \\ & + \left[\left(\frac{1}{2} m_{ij} \Phi_i \Phi_j + \frac{1}{3} g_{ijk} \Phi_i \Phi_j \Phi_k \right) \Big|_{\theta\theta} + \text{h.c.} \right]. \end{aligned} \quad (3.47)$$

3.2 Supersymmetry in 5D

After the brief review of 4D supersymmetry we are now in the position to construct a 5D supersymmetric model. Therefore we first study supersymmetric theories in a flat extra dimension to show the main ideas for constructing such theories and afterwards extend that to a warped extra dimension.

3.2.1 Supersymmetry in a flat extra dimension

In a flat extradimensional model the 4D SUSY algebra given in (3.4) can be generalized straightforwardly to

$$\{Q_i, \bar{Q}_j\} = -2\gamma_{ij}^M P_M, \quad (3.48)$$

where Q_i and \bar{Q}_j are now Dirac spinors and the indices i and j run from 1 to 4. The γ -matrices fulfill the 5D Clifford algebra

$$\{\gamma^M, \gamma^N\} = 2g^{MN} \quad (3.49)$$

as discussed in Sec. 2.1 and the commutator of two infinitesimal SUSY transformations then reads

$$[\delta_\eta, \delta_\xi] = -2(\bar{\eta}\gamma^M \xi - \bar{\xi}\gamma^M \eta) P_M. \quad (3.50)$$

To see the equivalence of 4D $N = 2$ and 5D $N = 1$ SUSY we decompose Q_i and \bar{Q}_j in two two-component spinors Q_1 and Q_2

$$Q = \begin{pmatrix} Q_1 \\ \bar{Q}_2 \end{pmatrix} \quad \text{and} \quad \bar{Q} = \begin{pmatrix} Q_2 \\ \bar{Q}_1 \end{pmatrix}. \quad (3.51)$$

When we now expand the anticommutator of (3.48) in a 4D and 5D part we get

$$\{Q_i, \bar{Q}_j\} = -2\gamma_{ij}^M P_M = -2\gamma_{ij}^\mu P_\mu - 2\gamma_{ij}^5 P_5 \quad (3.52)$$

Using the decomposition of the Dirac SUSY generators in two two-component spinors we can rewrite the above anticommutator to

$$\begin{pmatrix} \{Q_{1,\alpha}, Q_2^\alpha\} & \{Q_{1,\alpha}, \bar{Q}_{1,\dot{\alpha}}\} \\ \{Q_2^\alpha, \bar{Q}_2^{\dot{\alpha}}\} & \{\bar{Q}_2^{\dot{\alpha}}, \bar{Q}_{1,\dot{\alpha}}\} \end{pmatrix} = \begin{pmatrix} -2iP_5 & -2\sigma_{\alpha\dot{\alpha}}^\mu P_\mu \\ -2\bar{\sigma}^{\mu,\dot{\alpha}\alpha} P_\mu & 2iP_5 \end{pmatrix} \quad (3.53)$$

and we find that the 5D SUSY algebra looks like a 4D $N = 2$ one with the central charge iP_5 . Thus we can construct the 5D field representations out of the 4D $N = 1$ one as we have seen in Sec. 3.1.2. Since we can build the required superfields for our theory out of massless representations the central charge has no influence on the representations. Therefore the 5D vector superfield can be composed of a 4D vector superfield V and a massless chiral superfield χ , both in the adjoint representation

$$\begin{aligned} V^a &= -\theta\sigma^\mu\bar{\theta}A_\mu^a - i\bar{\theta}\bar{\theta}\theta\lambda_1^a + \theta\theta\bar{\theta}\bar{\lambda}_1^a + \frac{1}{2}\theta\theta\bar{\theta}\bar{\theta}D^a \\ \chi^a &= \frac{1}{\sqrt{2}}(\Sigma^a + iA_5^a) + \frac{i}{\sqrt{2}}\theta\sigma^\mu\bar{\theta}\partial_\mu(\Sigma^a + iA_5^a) - \frac{1}{4\sqrt{2}}\theta\theta\bar{\theta}\bar{\theta}\square(\Sigma^a + iA_5^a) \\ &\quad + \sqrt{2}\theta\lambda_2^a - \frac{i}{\sqrt{2}}\theta\theta\partial_\mu\lambda_2^a\sigma^\mu\bar{\theta} + \theta\theta C^a \end{aligned} \quad (3.54)$$

The 4D vector superfield is chosen in the Wess-Zumino gauge and a denotes the adjoint $SU(N)$ index. The 5D hypermultiplet consists of one chiral and one antichiral superfield H and H^c

$$\begin{aligned} H &= h + i\theta\sigma^\mu\bar{\theta}\partial_\mu h - \frac{1}{4}\theta\theta\bar{\theta}\bar{\theta}\square h + \sqrt{2}\theta\Psi - \frac{i}{\sqrt{2}}\theta\theta\partial_\mu\Psi\sigma^\mu\bar{\theta} + \theta\theta F \\ H^c &= h^c + i\theta\sigma^\mu\bar{\theta}\partial_\mu h^c - \frac{1}{4}\theta\theta\bar{\theta}\bar{\theta}\square h^c + \sqrt{2}\theta\Psi^c - \frac{i}{\sqrt{2}}\theta\theta\partial_\mu\Psi^c\sigma^\mu\bar{\theta} + \theta\theta F^c \end{aligned} \quad (3.55)$$

In a non supersymmetric theory the extended gauge transformation of a 5D non abelian gauge theory would look like

$$A_M \rightarrow UA_M U^\dagger - \frac{i}{g_5}(\partial_M U)U^\dagger, \quad (3.56)$$

where g_5 is the 5D gauge coupling and $U = e^{ig_5\theta^a(x)T^a}$. It can be split into a 4D and a 5D part

$$\begin{aligned} A_\mu &\rightarrow UA_\mu U^\dagger - \frac{i}{g_5}(\partial_\mu U)U^\dagger \\ A_5 &\rightarrow UA_5 U^\dagger - \frac{i}{g_5}(\partial_5 U)U^\dagger \end{aligned} \quad (3.57)$$

The 4D part of gauge transformation is the usual one and therefore is the same as declared in (3.33). This motivates us to define the gauge transformation of the 5D vector superfield as [3]

$$\begin{aligned} V &\rightarrow e^{-i\Gamma^\dagger} e^V e^{i\Gamma} \\ \chi &\rightarrow e^\Gamma (\chi - \sqrt{2}\partial_5) e^{-\Gamma} \end{aligned} \quad (3.58)$$

since V contains A_μ and χ contains A_5 . The exponentiated 4D vector superfield transforms as $e^V \rightarrow e^\Gamma e^V e^{\Gamma^\dagger}$. Since the gauge transformation for V keeps unchanged to Sec. 3.1.5 we can adopt the gauge invariant action for V given in Eq. 3.38. The dynamics for χ have to be implemented in a 5D gauge invariant way and the full 5D action then reads [3]

$$S_g = \int d^5x \int d^2\theta \frac{1}{4Cg_5^2} \text{Tr}[W^\alpha W_\alpha + \bar{W}_{\dot{\alpha}} \bar{W}^{\dot{\alpha}}]$$

$$+ \int d^5x \int d^4\theta \frac{1}{Cg_5^2} \text{Tr}[(\sqrt{2}\partial_5 + \bar{\chi}) e^{-V} (-\sqrt{2}\partial_5 + \chi) e^V + \partial_5 e^{-V} \partial_5 e^V] \quad (3.59)$$

The chiral and antichiral superfields H and H^c transforms as

$$\begin{aligned} H &\rightarrow e^{-\Gamma} H \\ H^c &\rightarrow e^{\Gamma} H^c \end{aligned} \quad (3.60)$$

and the generalization for the 4D interaction of the chiral superfields to the gauge multiplets from Eq. 3.47 then reads

$$\begin{aligned} S_h &= \int d^5x \int d^4\theta (\bar{H} e^{-V} H + H^c e^V \bar{H}^c) \\ &+ \int d^5x d^2\theta H^c \left[m + \left(\partial_5 - \frac{1}{\sqrt{2}} \chi \right) \right] H + \text{h.c.}, \end{aligned} \quad (3.61)$$

where $\partial_5 - \frac{1}{\sqrt{2}}\chi$ is the covariant derivative associated to ∂_5 . Note that in the case of a flat background the action S_g and S_h are invariant under the full 5D SUSY. We will see in the next section that we cannot keep the the complete 5D SUSY of the action in the case of warped backgrounds.

3.2.2 Supersymmetry in warped extra dimensions

Now we want to examine supersymmetry in warped five dimensional backgrounds. We assume that the backreaction of the matter and gauge fields on the background can be neglected. This saves us from the entire implementation of supergravity. Therefore we only have to take care that the global SUSY transformations are compatible with the isometries of the warped background [1]. In warped extradimensional models the SUSY algebra is easily extended to

$$\{Q_i, \bar{Q}_j\} = 2\hat{\gamma}_{ij}^M P_M = -2\hat{\gamma}_{ij}^\mu P_\mu - 2\hat{\gamma}_{ij}^5 P_5, \quad (3.62)$$

where \hat{g}^{MN} is now the warped metric and $\hat{\gamma}^M$ are the γ -matrices living in warped space time. Since the warped 5D SUSY algebra can be again related to a 4D $N = 2$ SUSY algebra, the superfield representations are the same as in the case of the flat background. We have a 5D vector superfield which is composed of a 4D vector and chiral superfield, V and χ and a 5D hypermultiplet which consists of a chiral and antichiral superfield H and H^c . To understand where the differences between supersymmetry in flat and warped backgrounds are, we study the SUSY transformations δ_ξ and δ_η . The supersymmetry transformation on the coordinates x^M reads

$$x^M \rightarrow x^M + \epsilon^M, \text{ where } -2(\bar{\eta}\gamma^M\xi - \bar{\xi}\gamma^M\eta) P_M \equiv \epsilon^M P_M \quad (3.63)$$

The metric \hat{g}^{MN} changes under this coordinate transformation into

$$\hat{g}_{MN} \rightarrow \hat{g}_{MN} + \epsilon^L \partial_L \hat{g}_{MN} + \hat{g}_{LN} \partial_M \epsilon^L + \hat{g}_{ML} \partial_N \epsilon^L \quad (3.64)$$

Following the paper of Hall, Nomura, Okui and Oliver [4] a global supersymmetry transformation is defined as the the supersymmetry transformation which leaves \hat{g}_{MN} unchanged. Therefore ϵ^M has to satisfy

$$\epsilon^L \partial_L \hat{g}_{MN} + \hat{g}_{LN} \partial_M \epsilon^L + \hat{g}_{ML} \partial_N \epsilon^L = 0 \quad (3.65)$$

where ϵ^M is called a Killing vector and (3.65) is called the Killing vector equation. When we express the Killing vectors through the SUSY parameters ξ and η we find that the Killing vector equation is fulfilled if ξ (and η) satisfy the following condition [1]

$$\xi(x, y) = e^{-2Rky/2} (\xi_\alpha^0, 0)^T. \quad (3.66)$$

ξ is now called a Killing spinor. Note that the presence of the Killing vector equation reduces the 5D SUSY to a 4D one.

The supersymmetric gauge action in a 5D warped spacetime then reads [4] [5]

$$\begin{aligned}
S_g = & \int d^5x \int d^2\theta \frac{R}{4Cg_5^2} \text{Tr}[W^\alpha W_\alpha + \bar{W}_{\dot{\alpha}} \bar{W}^{\dot{\alpha}}] \\
& + \int d^5x \int d^4\theta \frac{e^{-2Rky}}{RCg_5^2} \text{Tr}[(\sqrt{2}\partial_5 + \bar{\chi}) e^{-V} (-\sqrt{2}\partial_5 + \chi) e^V + \partial_5 e^{-V} \partial_5 e^V] \quad (3.67)
\end{aligned}$$

and the bulk action of the hypermultiplet coupled to the gauge fields is given by

$$\begin{aligned}
S_h = & \int d^5x \int d^4\theta \text{Re}^{-2Rky} (\bar{H} e^{-V} H + H^c e^V \bar{H}^c) \\
& + \int d^5x d^2\theta e^{-3Rky} H^c \left[\partial_5 - \frac{1}{\sqrt{2}} \chi - \left(\frac{3}{2} - c \right) Rk \right] H + \text{h.c.} \quad (3.68)
\end{aligned}$$

The warped character of the fields appear in their redefinitions we have to make. We will see this in Chap. 5.

Chapter 4

The Model

In this chapter we want to give a brief description of the higgsless model [1] we used in this thesis. The superfield representations and the appropriate action in an extra dimensional warped background was discussed in chapters 2 and 3. The task of this chapter is first to introduce the particle content of the model and second to discuss the main ideas of higgsless symmetry breaking without going into detail. We will illustrate the mechanism in some more detail in the next section, where we explicitly show, for the example of the quarks and the component fields of the 5D $SU(3)$ gauge multiplet, how masses come up. Therefore we specify the symmetries in the volume of the extra dimension and on the boundaries and how the symmetry breaking is encoded in the boundary conditions first.

4.1 Model Framework

The warped spacetime in which the model lives is a slice of AdS5. The AdS5 space was made famous by Lisa Randall and Raman Sundrum [12] and is a solution to Einsteins's equations in a setup with two branes and appropriate cosmological terms. The AdS5 space in the proper distance coordinates is defined by the following metric (see also App. A)

$$ds^2 = e^{-2Rky} g_{\mu\nu} dx^\mu dx^\nu - R^2 dy^2 \quad (4.1)$$

where $y \in [0, \pi]$, R is the radius of the extra dimension and k is the curvature. k is a scale of order the Planck scale. The fixed points at $y = 0, \pi$ will be taken as the boundaries of two branes, extending in the x^μ directions, so that they are the boundaries of the five dimensional spacetime. The volume between the two branes is called bulk. Since in AdS5 the metric scaling causes a scaling of the parameters of the fields in particular of the massless graviton field we denote the brane at $y = 0$ Planck or UV brane and the brane at $y = \pi$ IR brane. The entire 5D spacetime setup is illustrated in Fig. 4.1.

The symmetry in the bulk is a left-right symmetric gauge group

$$G = SU(3)_C \times SU(2)_L \times SU(2)_R \times U(1)_X, \quad (4.2)$$

where X is the $(B - L)/2$ quantum number. B denotes the baryon number and L is the lepton number. Thus X is $1/6$ for quarks and $-1/2$ for leptons. The coupling constants are denoted by g_{5C} , $g_L = g_R = g_5$ and \tilde{g}_5 . For each gauge group in the bulk we get a 5D gauge multiplet (3.54). The component fields for all 5D gauge multiplets are listed in Tab. 4.1 and 4.2. We neglect the auxiliary fields since they are no physical degrees of freedom. We denote the fifth components of the gauge multiplet as would-be Goldstones, since in the unitary gauge they will be *eaten* by the massive gauge bosons. Following [1] each standard model fermion is implemented by two doublets transforming under $SU(2)_L$ and $SU(2)_R$, respectively

$$\begin{aligned} \Psi_L &= (\Psi_L^u, \bar{\Psi}_L^{u^c}, \Psi_L^d, \bar{\Psi}_L^{d^c})^T \\ \Psi_R &= (\Psi_R^u, \bar{\Psi}_R^{u^c}, \Psi_R^d, \bar{\Psi}_R^{d^c})^T \end{aligned} \quad (4.3)$$

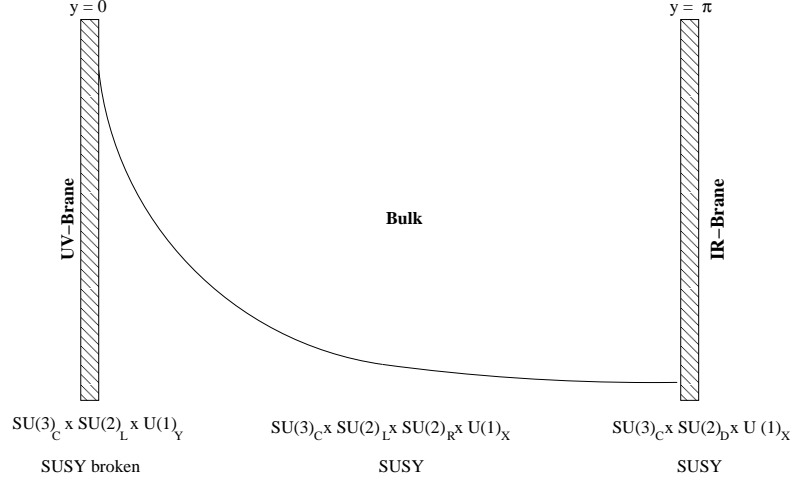


Figure 4.1: Outline of the model framework. The curved line implies the curvature of the five dimensional background.

Each of the doublets gets a 5D Dirac mass, which is denoted by c_L and c_R . They are defined as in Sec. 2.2. The particle content of the $SU(2)_L$ and $SU(2)_R$ transforming 5D hypermultiplets is shown in Tab. 4.3. As in the case of the 5D gauge multiplets the auxiliary fields do not contribute any physical degrees of freedom.

At last we have to define the gauge fixing action S_{gf}

$$S_{\text{gf}} = - \int d^5x \frac{R}{2\xi} \left[\partial_\mu A^{\mu,a} - \xi \frac{e^{-2Rky}}{R} (\partial_5 - 2Rk) A_5^a \right]^2. \quad (4.4)$$

The choice was made to eliminate the mixing of the fifth component and the 4D part of the vector.

4.2 Breaking Scenario

The symmetry breaking via boundary conditions is implemented so that

$$G \rightarrow \begin{cases} SU(3)_C \times SU(2)_L \times U(1)_Y & \text{on the UV brane} \\ SU(3)_C \times SU(2)_D \times U(1)_X & \text{on the IR brane} \end{cases} \quad (4.5)$$

holds on the boundaries. On the UV brane the $SU(2)_R$ and $U(1)_X$ are broken down to the $U(1)_Y$ hypercharge. On the IR brane the $SU(2)_L$ and $SU(2)_R$ are broken to a $SU(2)_D$ custodial symmetry which is generated by $T_D^a = T_L^a + T_R^a$. The maximal subgroup contained in both breaking scenarios is $SU(3)_C \times U(1)_{EM}$. Thus this is the only remaining symmetry group after the integration over the extra dimension. The boundary conditions have to be implemented in a way that they respect the breaking scenario and ensure that the variation of the boundary action vanishes. Furthermore the supersymmetry is only broken on the UV brane to get a particle spectrum that is compatible with experimental data [1]. The particle content after the symmetry breaking is shown in Tab. 4.1, 4.2 and 4.3.

We are now ready to write down the supersymmetric boundary conditions. The BCs for the 5D vector multiplet on the IR brane reads

$$\begin{bmatrix} 1 & -1 \\ \partial_y & \partial_y \end{bmatrix} \begin{bmatrix} V^L \\ V^R \end{bmatrix} \Big|_{y=\pi} = 0$$

$SU(2)_L \times SU(2)_R \times U(1)_X$	after EWSB	name
$A_L^{1,2}, A_R^{1,2}$	$W_{(n)}^\pm$	KK W -Boson
A_L^3, A_R^3, B	$\gamma_{(n)}, Z_{(n)}$	KK photon, KK Z -Boson
$A_{5,L}^{1,2}, A_{5,R}^{1,2}$	$A_{5,(n)}^\pm$	would-be KK Goldstone
$A_{5,L}^3, A_{5,R}^3, B_5$	$A_{5,(n)}^0$	would-be KK Goldstone
$\lambda_{1,L}^{1,2}, \lambda_{1,R}^{1,2}, \lambda_{2,L}^{1,2}, \lambda_{2,R}^{1,2}$	$\lambda_{(n)}^\pm$	KK chargino
$\lambda_{1,L}^3, \lambda_{1,R}^3, \lambda_{2,L}^3, \lambda_{2,R}^3, \lambda_{1,X}, \lambda_{2,X}$	$\lambda_{1,(n)}^0, \lambda_{2,(n)}^0$	KK neutralino
$\Sigma_L^{1,2}, \Sigma_R^{1,2}$	$\Sigma_{(n)}^\pm$	KK schargino
$\Sigma_L^3, \Sigma_R^3, \Sigma_X$	$\Sigma_{(n)}^0$	KK sneutralino

Table 4.1: The left column lists the component fields of the $SU(2)_L$, $SU(2)_R$ and $U(1)_X$ 5D gauge multiplet. The fermionic fields in the left column are Weyl spinors and the upper index denotes the $SU(2)$ gauge index. The middle column shows the particle content after the EWSB and integration over the extra dimension. In the notation chosen here $\lambda_{(n)}^\pm$ is a Dirac spinor and $\lambda_{1,(n)}^0$ and $\lambda_{2,(n)}^0$ are Majorana spinors.

$SU(3)_C$	after EWSB	name
A^a	$A_{(n)}^a$	KK gluon
A_5^a	$A_{5,(n)}^a$	would-be KK Goldstone
λ_1^a, λ_2^a	$\lambda_{(n)}^a$	KK gluino
Σ^a	$\Sigma_{(n)}^a$	KK sgluino

Table 4.2: The left column lists the component fields of the $SU(3)_C$ 5D gauge multiplet. The fermionic fields in the left column are all Weyl spinors and the upper index denotes the $SU(3)$ gauge index. The middle column shows the particle content after the EWSB and integration over the extra dimension. In the notation chosen here $\lambda_{(n)}^a$ is a Dirac spinor.

$SU(3)_C \times SU(2)_L \times SU(2)_R \times U(1)_X$	after EWSB
$\Psi_L^u, \bar{\Psi}_L^{u^c}, \Psi_R^u, \bar{\Psi}_R^{u^c}$	$u_{(n)}, c_{(n)}, t_{(n)}, \nu_{e,(n)}, \nu_{\mu,(n)}, \nu_{\tau,(n)}$
$\Psi_L^d, \bar{\Psi}_L^{d^c}, \Psi_R^d, \bar{\Psi}_R^{d^c}$	$d_{(n)}, s_{(n)}, b_{(n)}, e_{(n)}, \mu_{(n)}, \tau_{(n)}$
$h_L^u, h_L^{u^c}, h_R^u, h_R^{u^c}$	$\tilde{u}_{i,(n)}, \tilde{c}_{i,(n)}, \tilde{t}_{i,(n)}, \tilde{\nu}_{e_{i,(n)}}, \tilde{\nu}_{\mu_{i,(n)}}, \tilde{\nu}_{\tau_{i,(n)}}$
$h_L^d, h_L^{d^c}, h_R^d, h_R^{d^c}$	$\tilde{d}_{i,(n)}, \tilde{s}_{i,(n)}, \tilde{b}_{i,(n)}, \tilde{e}_{i,(n)}, \tilde{\mu}_{i,(n)}, \tilde{\tau}_{i,(n)}$

Table 4.3: The left column lists the component fields of the $SU(2)_L$ and $SU(2)_R$ transforming 5D hypermultiplet. The fermionic fields in the left column are all Weyl spinors. The right column shows the particle content after EWSB and the integration over the extra dimension. The quarks are represented as Dirac spinors and the neutrinos as Majorana spinors. The index i of the sfermions runs from 1 to 2.

$$\begin{aligned}
& \left[\begin{array}{cc} \partial_y & -\partial_y \\ 1 & 1 \end{array} \right] e^{-2Rky} \left[\begin{array}{c} \chi^L \\ \chi^R \end{array} \right] \Big|_{y=\pi} = 0 \\
& \partial_y V^X(\pi) = 0, \quad \chi^X(\pi) = 0 \\
& \partial_y V^C(\pi) = 0, \quad \chi^C(\pi) = 0
\end{aligned} \tag{4.6}$$

and on the UV brane they have the form

$$\begin{aligned}
& \left[\begin{array}{cc} g_{5x} \partial_y & g_5 \partial_y \\ -g_5 & g_{5x} \end{array} \right] \left[\begin{array}{c} V^{R,3} \\ V^X \end{array} \right] \Big|_{y=0} = 0 \\
& \left[\begin{array}{cc} g_{5x} & g_5 \\ -g_5 \partial_y & g_{5x} \partial_y \end{array} \right] e^{-2Rky} \left[\begin{array}{c} \chi^{R,3} \\ \chi^X \end{array} \right] \Big|_{y=0} = 0 \\
& \partial_y V^L(0) = 0, \quad \chi^L(0) = 0 \\
& V^{R,12}(0) = 0, \quad \partial_y e^{-2Rky} \chi^{R,12} = 0 \\
& \partial_y V^C(0) = 0, \quad \chi^C(0) = 0
\end{aligned} \tag{4.7}$$

The boundary conditions for the quarks on IR and UV brane, respectively are

$$\begin{aligned}
\Psi_R - m_f \rho^2 \Psi_R^c \Big|_{y=0} &= 0 \\
\Psi_L^c \Big|_{y=0} &= 0 \\
\Psi_R - \mu \Psi_L \Big|_{y=\pi} &= 0 \\
\Psi_L^c + \mu \Psi_R^c \Big|_{y=\pi} &= 0
\end{aligned} \tag{4.8}$$

We will see in the next section how the 5D Dirac masses c_L and c_R and the parameters μ and ρ affect the quark masses. Moreover we will discuss the origin of μ and ρ . Following [1] we remove all scalars from the UV brane by setting them to zero at the UV brane

$$\begin{aligned}
\Sigma^L(0) = \Sigma^R(0) = \Sigma^X(0) = \Sigma^C(0) &= 0 \\
h_L^i(0) = h_R^{c,i}(0) &= 0
\end{aligned} \tag{4.9}$$

This pushes the $SU(3)_C$ and $U(1)_X$ gauge scalars up to a mass of $\simeq 1.2$ TeV.

Chapter 5

Feynman Rules

In this thesis we want to study the characteristics of the lightest KK-mode of the KK sgluino (sgluino) and the first KK-mode of the gluon (heavy gluon) and examine whether we can measure these two particles at the LHC. To make theoretical predictions for LHC observables we need the effective 4D couplings and vertex structures of the interactions of the sgluino and heavy gluon to the standard model particles. This includes the self-interactions of the KK-gluon, the coupling of the sgluino to the gluon and the interaction of the sgluino and KK-gluon to the quarks. To get the couplings we have to solve the equations of motion for the fifth component of the 5D wave functions. This allows us to integrate out the extra dimension and to get the effective 4D theory. From the remaining effective 4D Lagrangian we can read off the Lorentz and $SU(3)$ gauge structure of the couplings and determine the Feynman rules.

5.1 Equations of Motion

First we study the 5D part of the gauge action given in (3.67) for the special case of $SU(3)_C$. Therefore we replace g_5 by g_{5C} and set $C = 1/2 (\text{Tr}[T^a T^b] = C\delta^{ab})$. To get the correct equations of motion for the sgluino and the heavy gluon we need the part of the 5D gauge action which contains Σ^a , A_μ^a and A_5^a . Σ^a and A_5^a are part of χ^a and A_μ^a occurs in V^a , both defined in (3.54). To get the action in terms of the component fields we have to calculate e^V and e^{-V} , which is easily done since all orders higher than V^2 vanish

$$\begin{aligned}
 e^V &= 1 + V + \frac{V^2}{2} = 1 - \theta\sigma^\mu\bar{\theta}A_\mu - i\bar{\theta}\bar{\theta}\theta\lambda_1 + i\theta\theta\bar{\theta}\bar{\lambda}_1 + \frac{1}{2}\theta\theta\bar{\theta}\bar{\theta}D \\
 &\quad + \frac{1}{2}(\theta\sigma^\mu\bar{\theta}A_\mu)(\theta\sigma^\nu\bar{\theta}A_\nu) \\
 e^{-V} &= 1 - V + \frac{V^2}{2} = 1 + \theta\sigma^\mu\bar{\theta}A_\mu + i\bar{\theta}\bar{\theta}\theta\lambda_1 - i\theta\theta\bar{\theta}\bar{\lambda}_1 - \frac{1}{2}\theta\theta\bar{\theta}\bar{\theta}D \\
 &\quad + \frac{1}{2}(\theta\sigma^\mu\bar{\theta}A_\mu)(\theta\sigma^\nu\bar{\theta}A_\nu)
 \end{aligned} \tag{5.1}$$

Moreover we plug the superfield χ^a in terms of its component fields in the 5D gauge action. After the full expansion and the integration over the superspace coordinates θ and $\bar{\theta}$ we obtain

$$\begin{aligned}
 S_{\text{g,5D}}[A_\mu^a, A_5^a, \Sigma^a] &= \int d^5x \frac{e^{-2Rky}}{Rg_{5C}^2} \left[-\frac{1}{2}\partial_\mu\Sigma^a\partial^\mu\Sigma^a - \frac{1}{2}\partial_\mu A_5^a\partial^\mu A_5^a \right. \\
 &\quad + \frac{1}{2}\partial_5 A_\mu^a\partial_5 A^{a,\mu} - (\partial_5 A_\mu^a)(\partial^\mu A_5^a) - (\partial_5 D^a)\Sigma^a \\
 &\quad - \frac{1}{8}f^{ade}f^{bce}\Sigma^a\Sigma^b A_\mu^c A^{d,\mu} - \frac{1}{8}f^{ade}f^{bce}A_5^a A_5^b A_\mu^c A^{d,\mu} \\
 &\quad \left. - \frac{1}{2}f^{abc}A_5^a\Sigma^b D^c - \frac{1}{2}f^{abc}(\partial_5 A_\mu^a)A^{b,\mu}A_5^c + \frac{1}{2}f^{abc}\Sigma^a(\partial_\mu\Sigma^b)A^{c,\mu} \right].
 \end{aligned} \tag{5.2}$$

For the expansion we make use of the identities given in the Appendix of [11] and we employ the $SU(3)$ algebra ($[T^a, T^b] = i f^{abc} T^c$ and $\text{Tr}[T^a T^b] = C \delta^{ab}$). Note that we neglect all components of the 5D gauge action which do not contain A_μ^a , A_5^a or Σ^a and that we only study the $\theta\theta\bar{\theta}$ part. As we can see the auxiliary fields D^a appear in the action. To get rid of them we have to use the equations of motion of D^a . Therefore we must examine the 4D part of the gauge action

$$S_{g,4D} = \int d^5x \int d^2\theta \frac{R}{4Cg_{5C}^2} \text{Tr}[W^\alpha W_\alpha] + \text{h.c} \quad (5.3)$$

and thus we have to derive the explicit form of the supersymmetric field strength W_α defined in (3.36)

$$\begin{aligned} W_\alpha &= -i\lambda_{1,\alpha} + \left[\delta_\alpha^\beta D - \frac{i}{2} (\sigma^\mu \bar{\sigma}^\nu)_\alpha^\beta (\partial_\mu A_\nu - \partial_\nu A_\mu) \right] \theta_\beta + \theta\theta \sigma_{\alpha\dot{\alpha}}^\mu \partial_\mu \bar{\lambda}_1^{\dot{\alpha}} \\ \bar{W}_{\dot{\alpha}} &= i\bar{\lambda}_{\dot{\alpha}} + \left[\epsilon_{\dot{\alpha}\beta} D + \frac{i}{2} \epsilon_{\dot{\alpha}\gamma} (\bar{\sigma}\sigma)^\gamma_{\dot{\beta}} (\partial_\mu A_\nu - \partial_\nu A_\mu) \right] \bar{\theta}^{\dot{\beta}} - \epsilon_{\dot{\alpha}\beta} \bar{\theta}^{\dot{\beta}} \bar{\sigma}^{\mu,\dot{\beta}\alpha} \partial_\mu \lambda_\alpha. \end{aligned} \quad (5.4)$$

The supersymmetric field strength is taken from [11]. After the integration over $d^2\theta$ and some integration by parts the 4D part of the gauge action reads

$$S_{g,4D} = \int d^5x \frac{R}{g_{5C}^2} \left[\frac{1}{2} D^a D^a - \frac{1}{4} F_{\mu\nu}^a F^{a,\mu\nu} - i\lambda_1^a \sigma^\mu \partial_\mu \bar{\lambda}_1^a \right], \quad (5.5)$$

which can be easily calculated by using (5.4) and the identities of the spinor algebra discussed in the Appendix of [11]. Now we can assemble the equations of motion for D^a and the auxiliary field may then be written as

$$D^a = -\frac{e^{-2Rky}}{R^2} (\partial_5 \Sigma^a - 2Rk \Sigma^a) \quad (5.6)$$

Plugging (5.6) in the expanded gauge action $S_{g,4D} + S_{g,5D} [A_\mu^a, A_5^a, \Sigma^a]$ we obtain the following equations of motion for Σ^a

$$\frac{e^{-2Rky}}{R^2} (\partial_5 \partial_5 \Sigma^a - 4Rk \partial_5 \Sigma^a + 4R^2 k^2 \Sigma^a) - \partial_\mu \partial^\mu \Sigma^a = 0. \quad (5.7)$$

Using the Kaluza-Klein Ansatz $\Sigma^a = \sum f_{\Sigma,(n)}^a(y) \Sigma_{(n)}^a(x)$ and the 4D equation of motion $\square \Sigma^a + m^2 \Sigma^a = 0$ we can write down the differential equation for $f_{\Sigma,(n)}^a$

$$\frac{e^{-2Rky}}{R^2} \left(f_{\Sigma,(n)}^{a''} - 4Rk f_{\Sigma,(n)}^{a'} + 4R^2 k^2 f_{\Sigma,(n)}^a \right) + m_n^2 f_{\Sigma,(n)}^a = 0 \quad (5.8)$$

whose solution are linear combinations of Bessel functions

$$f_{\Sigma,(n)}^a = e^{2Rky} \left(A_{(n)}^a J_0 \left(\frac{m_n e^{Rky}}{k} \right) + B_{(n)}^a Y_0 \left(\frac{m_n e^{Rky}}{k} \right) \right) \quad (5.9)$$

Next we want to derive the equations of motion for the gluon $A_\mu^a(x, y)$. To get the correct equations of motion we have to consider the gauge fixing given in (4.4) and obtain after the variation

$$\square A_\mu^a - \left(1 - \frac{1}{\xi} \right) \partial_\mu \partial_\nu A^{a,\nu} - \frac{e^{-2Rky}}{R^2} (\partial_5 - 2Rk) \partial_5 A_\mu^a = 0 \quad (5.10)$$

We make again the Kaluza-Klein decomposition for the 5D gluon field $A_\mu^a(x, y) = \sum f_{g,(n)}^a(y) A_{\mu,(n)}^a(x)$. Since $A_{\mu,(n)}^a$ satisfies the 4D equation of motion

$$\square A_{\mu,(n)}^a - \left(1 - \frac{1}{\xi} \right) \partial_\mu \partial_\nu A_{(n)}^{a,\nu} = -m_n^2 A_{\mu,(n)}^a \quad (5.11)$$

we can write down the differential equation for $f_{g,(n)}^a(y)$

$$\frac{e^{-2Rky}}{R^2} \left(f_{g,(n)}^{a''} - 2Rk f_{g,(n)}^{a'} \right) + m_n^2 f_{g,(n)}^a = 0. \quad (5.12)$$

The solutions are again combinations of Bessel functions

$$f_{g,(n)}^a(y) = e^{-Rky} \left(A_{(n)}^a J_1 \left(\frac{m_n e^{Rky}}{k} \right) + B_{(n)}^a Y_1 \left(\frac{m_n e^{Rky}}{k} \right) \right) \quad (5.13)$$

Since the equation of motion for the fermions is the same as in Sec. 2.2 we adopt the result derived in (2.59). There remains nothing else to do than to rewrite the solutions in proper distance coordinates

$$\begin{aligned} f_{\Psi,(n)}(y) &= \left(\frac{e^{Rky}}{k} \right)^{5/2} \left(C_n J_{1/2+c} \left(m_n \frac{e^{Rky}}{k} \right) + D_n Y_{1/2+c} \left(m_n \frac{e^{Rky}}{k} \right) \right) \\ f_{\bar{\Psi}^c,(n)}(y) &= \left(\frac{e^{Rky}}{k} \right)^{5/2} \left(A_n J_{1/2-c} \left(m_n \frac{e^{Rky}}{k} \right) + B_n Y_{1/2-c} \left(m_n \frac{e^{Rky}}{k} \right) \right) \end{aligned} \quad (5.14)$$

A more interesting issue are the couplings of the fermions to the sgluino. To get them we study the 5D part of the hypermultiplet action (3.68)

$$S_{\text{h,5D}} = \int d^5x \int d^2\theta e^{-3Rky} H^c \left[\partial_5 - \frac{1}{\sqrt{2}} \chi - \left(\frac{3}{2} - c \right) Rk \right] H + \text{h.c.} \quad (5.15)$$

Since we are interested in the interaction part of the 5D hypermultiplet action, it is sufficient to expand the term $H^c \chi H$ and $\bar{H} \bar{\chi} \bar{H}^c$. After the expansion and the integration over the superspace coordinates θ and $\bar{\theta}$ we obtain

$$\begin{aligned} S_{\text{h,5D}}|_{\text{int}} &= - \int d^5x \frac{e^{-3Rky}}{\sqrt{2}} \left[C^a h^c T^a h + C^{a\dagger} h^\dagger T^a h^{c\dagger} \right. \\ &\quad + \frac{1}{\sqrt{2}} (\Sigma^a + iA_5^a) h^c T^a F + \frac{1}{\sqrt{2}} (\Sigma^a - iA_5^a) F^\dagger T^a h^{c\dagger} \\ &\quad + \frac{1}{\sqrt{2}} (\Sigma^a + iA_5^a) F^c T^a h + \frac{1}{\sqrt{2}} (\Sigma^a - iA_5^a) h^\dagger T^a F^{c\dagger} \\ &\quad - \frac{1}{\sqrt{2}} (\Sigma^a + iA_5^a) \Psi^c T^a \Psi - \frac{1}{\sqrt{2}} (\Sigma^a - iA_5^a) \bar{\Psi} T^a \bar{\Psi}^c \\ &\quad \left. - \lambda_2^a \Psi^c T^a h - \bar{\lambda}_2^a h^\dagger T^a \bar{\Psi}^c - \lambda_2^a h^c T^a \Psi - \bar{\lambda}_2^a \bar{\Psi} T^a h^{c\dagger} \right] \end{aligned} \quad (5.16)$$

Finally, we want to determine the coupling term of the gluon to the fermions. To achieve this we have to expand the 4D part of the hypermultiplet action (3.68). After the integration over $d^4\theta$ we get the following interaction term for the gluon and the fermions

$$S_{\text{h,4D}}|_{\text{int}} = - \int d^5x \text{Re} e^{-2Rky} \frac{1}{2} \left[A_\mu^a \bar{\Psi} \bar{\sigma}^\mu T^a \Psi + \Psi^c T^a \sigma^\mu \bar{\Psi}^c A_\mu^a \right] \quad (5.17)$$

5.2 Masses

In this section we want to show how to get the standard model fermion masses out of the 5D parameters first and then how the masses of the KK sgluinos $\Sigma_{(n)}^a$ and the KK gluons $A_{\mu,(n)}^a$ can be calculated. To understand how the fermion masses come out of the boundary conditions of the hypermultiplets H and H^c (see Sec. 4.2) we need a better understanding of where the boundary conditions come from. The fermion

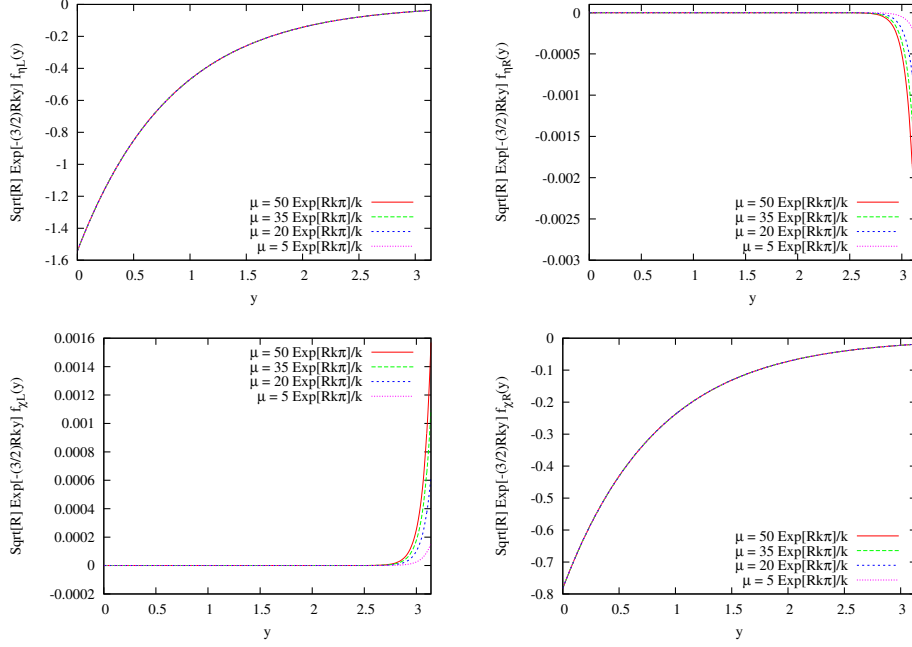


Figure 5.1: $f_{\Psi_L}(y)$, $f_{\Psi_R}(y)$, $f_{\Psi_L^c}(y)$ and $f_{\Psi_R^c}(y)$ for different values of μ . ($\rho = 3.8 \times \sqrt{1/k}$, $c_L = -60/100$, $c_R = 60/100$)

boundary conditions on the IR brane (4.8) have their origin in a brane localized mass term, which mixes $SU(2)_L$ and $SU(2)_R$ fermions [2]

$$S_{\text{IR}} = \int d^4x e^{-3Rky} \mu (\Psi_R \Psi_L^c + \bar{\Psi}_L^c \bar{\Psi}_R + \Psi_L \Psi_R^c + \bar{\Psi}_R^c \bar{\Psi}_L) \Big|_{y=\pi} \quad (5.18)$$

The additional brane term and thus the mass correction is proportional to μ and the values of the fermion wave functions on the IR brane. The μ dependence of the 5D fermion wave functions $f_{\Psi_L}(y)$, $f_{\Psi_R}(y)$, $f_{\Psi^c_L}(y)$ and $f_{\Psi^c_R}(y)$ is shown in Fig. 5.1.

The fermion boundary condition on the Planck brane comes from the mixing term [2]

$$S_{\text{Planck}} = \int d^4x \left(-i\bar{\xi}\bar{\sigma}^\mu \partial_\mu \xi - i\eta\sigma^\mu \partial_\mu \bar{\eta} + f(\eta\xi + \bar{\xi}\bar{\eta}) + M\sqrt{k^{-1}}(\Psi_R^c \xi + \bar{\xi} \bar{\Psi}_R^c) \right) \Big|_{y=0}, \quad (5.19)$$

where ξ and η are brane localized fermions, which together form a Dirac spinor with a Dirac mass f on the brane. ρ is in this context defined as $\rho = M^2/f^2k$. We see in the next section that the parameter ρ appears in the normalization of the fermion wave functions and because of that the masses decrease with growing ρ . This dependence can also be seen in Fig. 5.2, since the fermion wave functions become flatter with growing ρ and thus the 5D overlap integral in front of the bulk mass term in (2.36) becomes smaller.

Finally we examine how the 5D fermionic wave functions depend on the bulk parameters c_L and c_R . We choose c_L and c_R antisymmetric, because we will later use such parameter sets to get the physical fermion masses. As we can see in Fig. 5.3 the 5D fermionic wave functions become more localized to the IR brane for lower absolute values of c_L and c_R . The larger values of the 5D fermionic wave functions on the IR brane lead to a higher contribution of the μ boundary term (5.18) and thus to higher masses of the fermions.

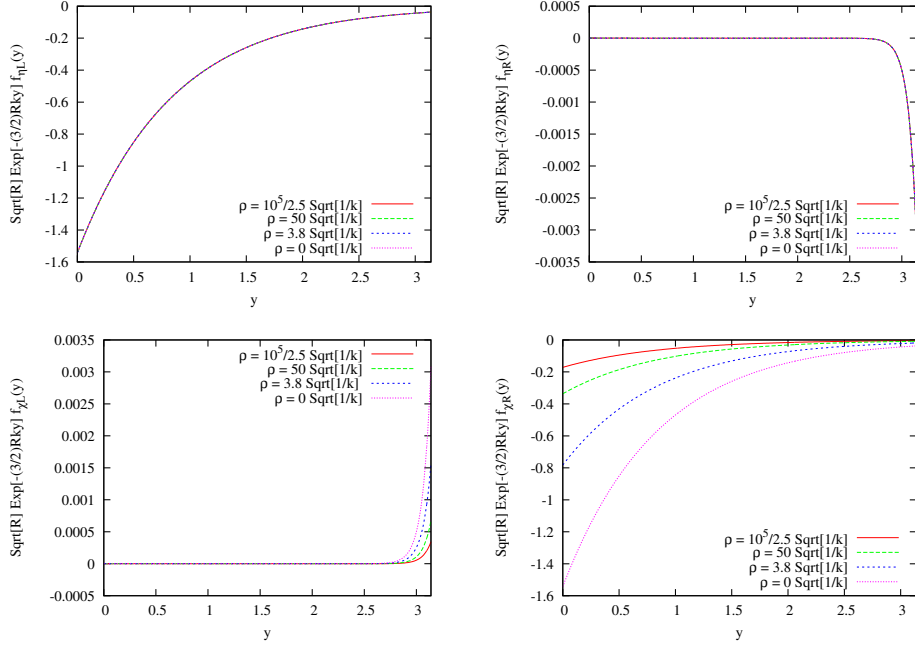


Figure 5.2: $f_{\Psi_L}(y)$, $f_{\Psi_R}(y)$, $f_{\Psi_L^c}(y)$ and $f_{\Psi_R^c}(y)$ for different values of ρ . ($\mu = 50 \times e^{Rk\pi}/k$, $c_L = -60/100$, $c_R = 60/100$)

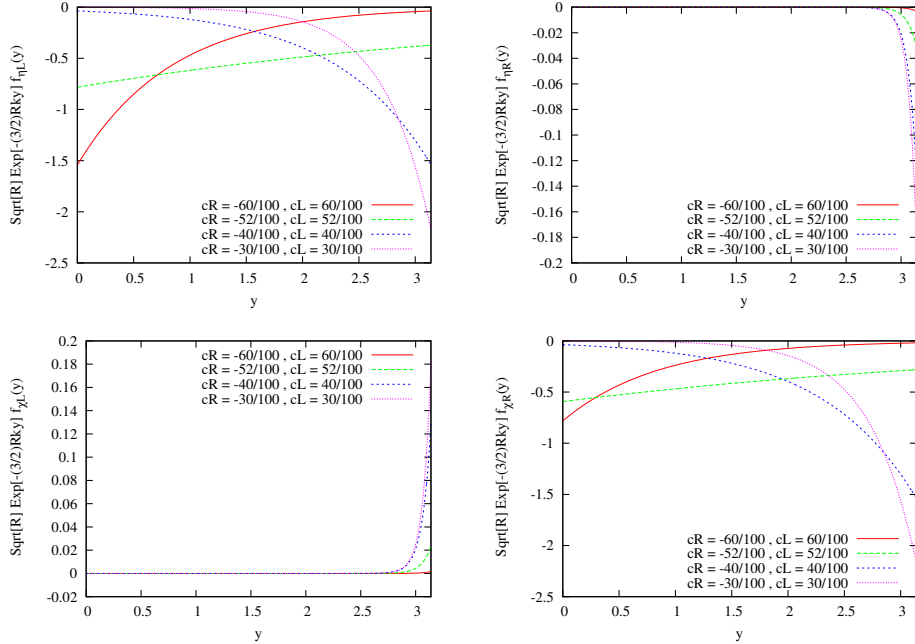


Figure 5.3: $f_{\Psi_L}(y)$, $f_{\Psi_R}(y)$, $f_{\Psi_L^c}(y)$ and $f_{\Psi_R^c}(y)$ for different values of c_L and c_R . ($\mu = 50 \times e^{Rk\pi}/k$, $\rho = 3.8 \times \sqrt{1/k}$)

R	$1.19 \times 10^{-18} \text{ GeV}^{-1}$
k	10^{19} GeV

Table 5.1: Warped 5D model parameters.

	$\mu / (e^{Rk\pi}/k)$	$\rho/\sqrt{1/k}$	c_R	c_L	m/GeV
u	54.59	3.87	-60/100	60/100	0.00309
d	54.59	0	-60/100	60/100	0.00618
c	113.39	0	-52/100	52/100	1.31017
s	113.39	51.92	-52/100	52/100	0.11077
t	785.85	0	-1/3	40/100	171.106
b	785.85	41750	-1/3	40/100	3.87311

Table 5.2: Warped 5D model parameters for the fermions.

Now we are ready to determine the fermion masses. For this we have to calculate the radius R of the extra dimension. Since we want to have a realistic model we must satisfy the experimental constraints. The mass of the W -Boson is measured at 80.4 GeV. Therewith and with a curvature $k = 10^{19} \text{ GeV}$ we can calculate R from the following condition

$$m_W^2 = \frac{k e^{-2Rk\pi}}{(1 - \kappa)R\pi} \quad (5.20)$$

The factor $(1 - \kappa)$ in the denominator comes from a brane term [1] that we have to introduce to get a sufficiently large tree level mass of the lightest chargino λ^\pm , which escapes the current detection bounds. The tree level chargino mass is approximately given by [1]

$$m_{\lambda^\pm} \simeq \sqrt{1 + \kappa} m_W. \quad (5.21)$$

To get a chargino mass which is not excluded by existing experiments, we set $\kappa = 0.4$. The calculated value for R is listed in Tab. 5.1.

The rest of the parameters and the resulting masses of the quarks are given in Tab. 5.2.

At last we have to determine the masses of the heavy gluon and the sgluino. Therefore we use the boundary conditions given in (4.6) and (4.7) and get the masses shown in in Tab. 5.3. It is interesting, that both particles have the same mass. This is based on the fact that the heavy gluon and the sgluino have the same boundary conditions. But we would expect the masses to change when we calculate the mass corrections. At tree level the masses stay equal for higher KK-modes of the gluons and the scalars, as illustrated in Fig. 5.4. The intersections of the plotted function with the x -axes indicate the masses of the particles since the boundary conditions are satisfied at these points.

$m_{g(1)}$	1420.85 GeV
$m_{\Sigma(0)}$	1420.85 GeV

Table 5.3: Mass of the heavy gluon and the sgluino.

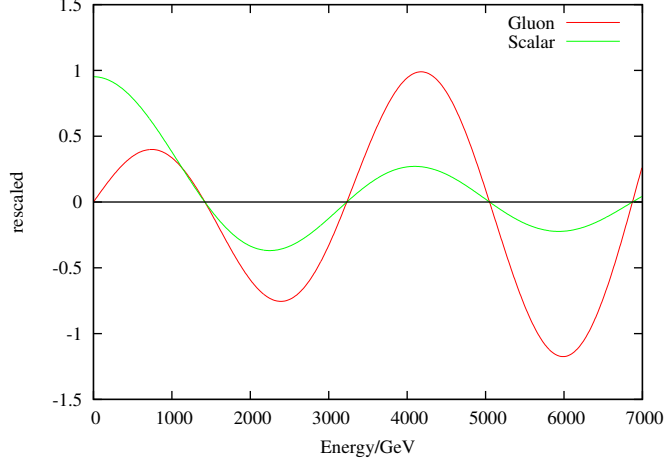


Figure 5.4: The roots of the plotted functions indicate the masses of the KK-gluon $A_{\mu,(n)}^a$ and of the sgluino, respectively.

5.3 Couplings

In this section we calculate the couplings required for the tree level cross sections we want to study in this thesis. To obtain the correct normalizations, Dirac structure and coupling constants we have to do some redefinitions

$$\begin{aligned}
\Psi &\rightarrow e^{-\frac{1}{2}Rky} \Psi \\
A_\mu &\rightarrow g_{5C} A_\mu \\
A_5 &\rightarrow g_{5C} R A_5 \\
\lambda_1 &\rightarrow g_{5C} e^{-\frac{3}{2}Rky} \lambda_1 \\
\lambda_2 &\rightarrow -i g_{5C} R e^{-\frac{1}{2}Rky} \lambda_2 \\
\Sigma &\rightarrow g_{5C} R \Sigma \\
\sigma^\alpha &= V_\mu^\alpha \sigma^\mu \\
g^{\alpha\beta} &= V_\mu^\alpha V_\nu^\beta \hat{g}^{\mu\nu} \\
\sqrt{g} &= R e^{-4Rky}
\end{aligned} \tag{5.22}$$

After the redefinitions we have to derive the normalization of the wave functions and the couplings to get the correct 4D effective action. To obtain the standard 4D action for scalars and gluons

$$\begin{aligned}
S_{4D,\text{scalar}} &= \int d^4x \left(-\frac{1}{2} \partial_\alpha \Sigma^a \partial^\alpha \Sigma^a \right) \\
S_{4D,\text{gluon}} &= \int d^4x \left(-\frac{1}{4} F^{a,\alpha\beta} F_{\alpha\beta}^a \right)
\end{aligned} \tag{5.23}$$

we require the following normalizations

$$\begin{aligned}
\int dy R e^{-2Rky} f_{\Sigma,(n)} f_{\Sigma,(m)} &= \delta_{nm} \\
\int dy R f_{g,(n)} f_{g,(m)} &= \delta_{nm}.
\end{aligned} \tag{5.24}$$

The 5D wave functions are by construction orthonormal and thus we can neglect mixing terms between different KK-modes. The normalization of the fermions is a bit more complicated but the derivation goes

through as before. The normalization of the fermion reads

$$\int dy \operatorname{Re}^{-3Rky} \left(f_{\Psi_L,(n)} f_{\Psi_L,(m)}^* + f_{\Psi_R,(n)} f_{\Psi_R,(m)}^* \right) + \rho^2 f_{\Psi_R,(n)} f_{\Psi_R,(m)} \Big|_{y=0} = \delta_{nm} \quad (5.25)$$

Last we have to derive how the 5D gauge coupling g_{5C} is related to the 4D gauge coupling g_{4C} . The relation

$$g_{5C} = 2\sqrt{R\pi}g_{4C} \quad (5.26)$$

stems from the fact that we want to have a the standard vertex structure in 4D. Now we are ready to calculate the couplings. We start with the coupling of the fermions to the sgluino. The interaction term reads (see Eq. (5.16))

$$\int d^5x \left[-Rg_{5C} \frac{e^{-4Rky}}{2} \left(\Sigma^a \Psi_L^c T^a \Psi_L + \Sigma^a \bar{\Psi}_L T^a \bar{\Psi}_L^c + \Sigma^a \Psi_R^c T^a \Psi_R + \Sigma^a \bar{\Psi}_R T^a \bar{\Psi}_R^c \right) \right] \quad (5.27)$$

Note that we have performed the redefinitions declared in (5.22). Plugging the KK decomposition in the above expression we obtain

$$\begin{aligned} \sum_l \sum_n \sum_m \left[\int d^4x \Sigma_{(l)}^a \Psi_{L,(n)}^c T^a \Psi_{L,(m)} \int dy \frac{g_{5C}}{2} \operatorname{Re}^{-4Rky} f_{\Sigma,(l)} f_{\Psi_L,(n)} f_{\Psi_L,(m)} \right. \\ + \int d^4x \Sigma_{(l)}^a \bar{\Psi}_{L,(n)} T^a \bar{\Psi}_{L,(m)}^c \int dy \frac{g_{5C}}{2} \operatorname{Re}^{-4Rky} f_{\Sigma,(l)} f_{\bar{\Psi}_L,(n)} f_{\bar{\Psi}_L,(m)} \\ + \int d^4x \Sigma_{(l)}^a \Psi_{R,(n)}^c T^a \Psi_{R,(m)} \int dy \frac{g_{5C}}{2} e^{-4Rky} f_{\Sigma,(l)} f_{\Psi_R,(n)} f_{\Psi_R,(m)} \\ \left. + \int d^4x \Sigma_{(l)}^a \bar{\Psi}_{R,(n)} T^a \bar{\Psi}_{R,(m)}^c \int dy \frac{g_{5C}}{2} \operatorname{Re}^{-4Rky} f_{\Sigma,(l)} f_{\bar{\Psi}_R,(n)} f_{\bar{\Psi}_R,(m)} \right] \quad (5.28) \end{aligned}$$

Since the 5D wave functions f_Ψ , $f_{\bar{\Psi}}$, f_{Ψ^c} and $f_{\bar{\Psi}^c}$ are real we can assume that

$$f_\Psi = f_{\bar{\Psi}} \quad \text{and} \quad f_{\Psi^c} = f_{\bar{\Psi}^c}. \quad (5.29)$$

As a consequence of the boundary condition on the IR brane we can use that

$$\Psi_{L,(n)} = \Psi_{R,(n)} \quad \Psi_{L,(n)}^c = \Psi_{R,(n)}^c \quad \bar{\Psi}_{L,(n)} = \bar{\Psi}_{R,(n)} \quad \bar{\Psi}_{L,(n)}^c = \bar{\Psi}_{R,(n)}^c, \quad (5.30)$$

if the μ parameter is not equal to zero, as in our case. Using (5.29) and (5.30) we can rewrite (5.28) as follows

$$\begin{aligned} \sum_{l,n,m} \left[- \int d^4x \left(\Sigma_{(l)}^a \Psi_{(n)}^c T^a \Psi_{(m)} + \Sigma_{(l)}^a \bar{\Psi}_{(n)} T^a \bar{\Psi}_{(m)} \right) \right. \\ \left. \times \int dy \frac{g_{5C}}{2} \operatorname{Re}^{-4Rky} \left(f_{\Sigma,(l)} f_{\Psi_L,(n)} f_{\Psi_L,(m)} + f_{\Sigma,(l)} f_{\Psi_R,(n)} f_{\Psi_R,(m)} \right) \right] \quad (5.31) \end{aligned}$$

and thus get for the effective 4D coupling

$$g_{\Sigma f \bar{f},(nlm)} = \int dy \frac{g_{5C}}{2} \operatorname{Re}^{-4Rky} \left(f_{\Sigma,(l)} f_{\Psi_L,(n)} f_{\Psi_L,(m)} + f_{\Sigma,(l)} f_{\Psi_R,(n)} f_{\Psi_R,(m)} \right) \quad (5.32)$$

The numerical results for the couplings of the quarks to the sgluino are shown in Tab. 5.4. For the calculation we used the parameters given in Tab. 5.1 and 5.2 and an effective 4D strong coupling constant equal to $g_{4C} = 1.216$. The couplings of the d - and c -quark are zero, because in that case the sum of $f_{\Sigma,(l)} f_{\Psi_L,(n)} f_{\Psi_L,(m)}$ and $f_{\Sigma,(l)} f_{\Psi_R,(n)} f_{\Psi_R,(m)}$ is zero up to numerical fluctuations.

$g_{\Sigma u\bar{u},(000)}$	1.79×10^{-9}
$g_{\Sigma d\bar{d},(000)}$	0
$g_{\Sigma s\bar{s},(000)}$	7.93×10^{-6}
$g_{\Sigma c\bar{c},(000)}$	0
$g_{\Sigma b\bar{b},(000)}$	0.0068
$g_{\Sigma t\bar{t},(000)}$	-0.152

Table 5.4: Couplings of the quarks to the sgluino.

$g_{gu_L\bar{u}_L,(100)}$	-0.227	$g_{gu_R\bar{u}_R,(100)}$	-0.057
$g_{gd_L\bar{d}_L,(100)}$	-0.227	$g_{gd_R\bar{d}_R,(100)}$	-0.227
$g_{gc_L\bar{c}_L,(100)}$	-0.125	$g_{gc_R\bar{c}_R,(100)}$	-0.00081
$g_{gs_L\bar{s}_L,(100)}$	-0.125	$g_{gs_R\bar{s}_R,(100)}$	-0.00089
$g_{gb_L\bar{b}_L,(100)}$	2.253	$g_{gb_R\bar{b}_R,(100)}$	0.0014
$g_{gt_L\bar{t}_L,(100)}$	1.666	$g_{gt_R\bar{t}_R,(100)}$	2.931

Table 5.5: Couplings of the quarks to the heavy gluon.

To get the coupling of the fermions to the gluons we have to do the same procedure as in the case of the sgluino, where we now use the action given in (5.17). After the redefinition and the insertion of the KK decomposition we obtain

$$\sum_{l,n,m} \left[- \int d^4x A_{\mu,(n)}^a \bar{\Psi}_{(n)} \bar{\sigma}^\mu T^a \Psi_{(m)} \int dy \frac{g_{5C}}{2} \text{Re} e^{-3Rky} (f_{g,(l)} f_{\Psi_L,(n)} f_{\Psi_L,(m)} + f_{g,(l)} f_{\Psi_R,(n)} f_{\Psi_R,(m)}) \right. \\ \left. - \int d^4x A_{\mu,(n)}^a \Psi_{(n)}^c \sigma^\mu T^a \bar{\Psi}_{(m)}^c \int dy \frac{g_{5C}}{2} \text{Re} e^{-3Rky} (f_{g,(l)} f_{\Psi_L^c,(n)} f_{\Psi_L^c,(m)} + f_{g,(l)} f_{\Psi_R^c,(n)} f_{\Psi_R^c,(m)}) \right], \quad (5.33)$$

where again we used (5.29) and (5.30) and get for the 4D couplings

$$g_{g\Psi\bar{\Psi},(lnm)} = \int dy \frac{g_{5C}}{2} \text{Re} e^{-3Rky} (f_{g,(l)} f_{\Psi_L,(n)} f_{\Psi_L,(m)} + f_{g,(l)} f_{\Psi_R,(n)} f_{\Psi_R,(m)}) \\ g_{g\Psi^c\bar{\Psi}^c,(lnm)} = \int dy \frac{g_{5C}}{2} \text{Re} e^{-3Rky} (f_{g,(l)} f_{\Psi_L^c,(n)} f_{\Psi_L^c,(m)} + f_{g,(l)} f_{\Psi_R^c,(n)} f_{\Psi_R^c,(m)}) \quad (5.34)$$

The numerical values of the couplings of the quarks to the heavy gluon are listed in Tab. 5.5. We used the parameters from Tab. 5.1 and 5.2 again and an effective 4D strong coupling constant $g_{4C} = 1.216$. The coupling constant of the quarks to the massless gluon is g_{4C} . The couplings of the quarks to the heavy gluon increase with respect to larger quark masses and change sign in the case of the bottom and top quarks. This stems from the fact that the quark-quark-heavy gluon coupling grows for a decreasing absolute value of c_L and c_R and changes sign at $c_L, c_R = 1/2$.

Since it is always the same mechanism to get the 4D effective couplings we only state the results.

Investigating (5.2), we get the interaction terms between the gluons and the sgluinos

$$\begin{aligned} & \sum_{l,n,m} \int d^4x f^{abc} \Sigma_{(l)}^a \left(\partial_\mu \Sigma_{(n)}^b \right) A_{(m)}^{c,\mu} \int dy R \frac{g_{5c}^2}{2} e^{-2Rky} f_{\Sigma,(l)} f_{\Sigma,(n)} f_{g,(m)} \\ & - \frac{1}{2} \sum_{l,n,m,r} \int d^4x f^{ade} f^{bce} \Sigma_{(l)}^a \Sigma_{(n)}^b A_{\mu,(m)}^c A_{(r)}^{d,\mu} \int dy R \frac{g_{5c}^2}{4} e^{-2Rky} f_{\Sigma,(l)} f_{\Sigma,(n)} f_{g,(m)} f_{g,(r)} \end{aligned} \quad (5.35)$$

and the 4D effective couplings then read

$$\begin{aligned} g_{g\Sigma\Sigma,(lnm)} &= \int dy R \frac{g_{5c}^2}{2} e^{-2Rky} f_{\Sigma,(l)} f_{\Sigma,(n)} f_{g,(m)} \\ g_{gg\Sigma\Sigma,(lnmr)}^2 &= \int dy R \frac{g_{5c}^2}{4} e^{-2Rky} f_{\Sigma,(l)} f_{\Sigma,(n)} f_{g,(m)} f_{g,(r)} \end{aligned} \quad (5.36)$$

Expanding the term $\frac{1}{4} F_{\mu\nu}^a F^{a,\mu\nu}$ of (5.5) we get the 4D couplings of the three and four gluon vertex

$$\begin{aligned} g_{ggg,(lnm)} &= \int dy R \frac{g_{5c}^2}{2} f_{g,(l)} f_{g,(n)} f_{g,(m)} \\ g_{gggg,(lnmr)}^2 &= \int dy R \frac{g_{5c}^2}{4} f_{g,(l)} f_{g,(n)} f_{g,(m)} f_{g,(r)}. \end{aligned} \quad (5.37)$$

The Lorentz and $SU(3)$ structure of the remaining 4D part of the three and four gluon vertex looks like the structure in standard $SU(N)$ gauge theories. The only difference are the KK indices of the 4D wave function. The numerical results of the KK gluon self-interactions and the coupling of the KK gluon to the sgluino are shown in Tab. 5.6 and 5.7. $g_{ggg,(001)}$ and $g_{gggg,(0001)}$ are equal to zero because of orthogonality. This is obvious since the 5D wave function of the massless gluon is a constant.

Now we are ready to construct the Feynman rules for our theory. To get the Feynman rules out of the Lagrangian we have to do the following steps [13]

- Multiplication of every vertex by an i
- Replacing every partial derivative ∂_μ by $-ip_\mu$
- Symmetrization of identical fields

Since the fields have an additional KK index the symmetrization is reduced to the one without the KK decomposition. But the summation over the KK index cancels the effect of that lack of symmetrization and we end up with the vertices we know from standard $SU(N)$ gauge theories [14]. The results are presented in Fig. 5.5.

$g_{\text{ggg},(000)}$	g_{4_C}
$g_{\text{ggg},(001)}$	0
$g_{\text{ggg},(011)}$	g_{4_C}
$g_{\text{ggg},(111)}$	7.901
$g_{\text{gggg},(0000)}^2$	$g_{4_C}^2$
$g_{\text{gggg},(0001)}^2$	0
$g_{\text{gggg},(0011)}^2$	$g_{4_C}^2$
$g_{\text{gggg},(0111)}^2$	9.604
$g_{\text{gggg},(1111)}^2$	69.833

Table 5.6: Couplings of the gluons ($g_{4_C} = 1.216$).

$g_{\text{g}\Sigma\Sigma,(000)}$	g_{4_C}
$g_{\text{g}\Sigma\Sigma,(100)}$	3.950
$g_{\text{gg}\Sigma\Sigma,(0000)}^2$	$g_{4_C}^2$
$g_{\text{gg}\Sigma\Sigma,(0100)}^2$	4.802
$g_{\text{gg}\Sigma\Sigma,(1100)}^2$	23.278

Table 5.7: Couplings of the gluons to the sgluinos ($g_{4_C} = 1.216$).

$$= ig_{\underline{g}f\bar{f},(lnm)} \gamma^{\mu_1} T^a$$

$$= g_{\underline{g}\underline{g}\underline{g},(lnm)} f^{abc} [g^{\mu_1\mu_2} (p_1 - p_2)^{\mu_3} + g^{\mu_2\mu_3} (p_2 - p_3)^{\mu_1} + g^{\mu_1\mu_3} (p_3 - p_1)^{\mu_2}]$$

$$- ig_{\underline{g}\underline{g}\underline{g}\underline{g},(lnmr)}^2 [f^{abe} f^{cde} (g^{\mu_1\mu_4} g^{\mu_2\mu_3} - g^{\mu_1\mu_3} g^{\mu_2\mu_4})$$

$$= + f^{ace} f^{bde} (g^{\mu_1\mu_2} g^{\mu_3\mu_4} - g^{\mu_1\mu_3} g^{\mu_2\mu_4})$$

$$+ f^{ade} f^{bce} (g^{\mu_1\mu_2} g^{\mu_3\mu_4} - g^{\mu_1\mu_4} g^{\mu_2\mu_3})]$$

$$= ig_{\Sigma f\bar{f},(lnm)} T^a$$

$$= g_{\underline{g}\Sigma\Sigma,(lnm)} f^{abc} (p_3^{\mu_1} - p_2^{\mu_1})$$

$$= - ig_{\underline{g}\underline{g}\Sigma\Sigma,(lnmr)}^2 g^{\mu_1\mu_2} (f^{abe} f^{cde} + f^{bde} f^{ace})$$

Figure 5.5: Vertices of the couplings among fermions, gluons and the sgluinos.

Chapter 6

Partonic cross section

As we want to make predictions for detecting non-standard model particles, we must think about cross sections, which deliver signals that can be clearly assigned to characteristic particles predicted by our model. The first idea is to generate the particles we want to measure on-shell in a $2 \rightarrow 2$ cross section and in a second step to let them decay into standard model particles we can detect at the LHC. We hope to see a characteristic peak in the invariant mass spectrum of the decaying particles at the production threshold and characteristic angular distributions of the decay products. In this thesis we want to study cross sections where the first Kaluza-Klein excitation of the gluon and the sgluino contribute. By means of observables, which depend on the character of the sgluino and heavy gluon, we may distinguish our model from the standard model including a Higgs boson and in particular from other extensions of the standard model, like for example SUSY in 4D.

Since at LHC energies the colliding protons have a high gluon density, we study cross sections with two gluons in the initial state. Furthermore the massive particles produced in the intermediate should decay into two quark-antiquark pairs. Therefore we have to calculate $2 \rightarrow 4$ cross sections. For the calculation we first use the narrow width approximation and second, we perform a Monte Carlo simulation of the complete tree level $2 \rightarrow 4$ process. For all calculations we use the unitary gauge for the massive gauge bosons. Thus we can neglect all contributions of the fifth component of the KK gluon.

6.1 Calculation with the Narrow Width Approximation

6.1.1 Basics of Narrow Width Approximation

In this section we want to calculate the $2 \rightarrow 4$ cross section using the narrow width approximation (NWA). Therefore we have to calculate the $2 \rightarrow 2$ scattering of two gluons into heavy gluon and sgluino pairs and afterwards multiply the cross section with the decay probability of the produced particles. The $2 \rightarrow 2$ amplitudes we want to study are shown in Fig. 6.1 and 6.2. When comparing the NWA with the full $2 \rightarrow 4$ tree level calculation we have to account for symmetry factors of the phase space. Thus we want to discuss briefly how both approaches are connected. The $2 \rightarrow 4$ cross section can be written as

$$\begin{aligned} d\sigma(gg \rightarrow q_i \bar{q}_i q_j \bar{q}_j) &= \frac{1}{n_4} |\mathcal{M}(gg \rightarrow q_i \bar{q}_i q_j \bar{q}_j)|^2 d\Phi^{(4)} \\ &\approx \frac{1}{n_4} \left(|\mathcal{M}(gg \rightarrow P_1 P_2)|^2 d\Phi^{(2)} \right) \text{BR}(P_1 \rightarrow q_i \bar{q}_i) \text{BR}(P_2 \rightarrow q_j \bar{q}_j) \\ &= \frac{n_2}{n_4} \left(\frac{1}{n_2} |\mathcal{M}(gg \rightarrow P_1 P_2)|^2 d\Phi^{(2)} \right) \text{BR}(P_1 \rightarrow q_i \bar{q}_i) \text{BR}(P_2 \rightarrow q_j \bar{q}_j) \\ &= \frac{n_2}{n_4} d\sigma(gg \rightarrow P_1 P_2) \text{BR}(P_1 \rightarrow q_i \bar{q}_i) \text{BR}(P_2 \rightarrow q_j \bar{q}_j) \end{aligned} \quad (6.1)$$

where $d\Phi^{(2)}$ and $d\Phi^{(4)}$ are the phase space measures for a $2 \rightarrow 2$ and $2 \rightarrow 4$ process, respectively. The relation (6.1) holds exactly in the case of vanishing interference terms. P_1 and P_2 denote the intermediate state particles which decay into quarks q_i and q_j . i and j run from 1 to 3 and indicate the generation. $\text{BR}(P_1 \rightarrow q_i \bar{q}_i)$ and $\text{BR}(P_2 \rightarrow q_j \bar{q}_j)$ are the branching ratios of particle P_1 and P_2 . The branching ratio is the decay probability and can be calculated from the decay rates Γ

$$\text{BR}(P_k \rightarrow q_i \bar{q}_i) = \frac{\Gamma(P_k \rightarrow q_i \bar{q}_i)}{\sum_{s,t} \Gamma(P_k \rightarrow f_s f_t)}, \quad (6.2)$$

where f_s and f_t are all the possible decay products of P_k . The sum over all possible decay rates is defined as the width of the particle. n_2 and n_4 are symmetry factors of the phase space $d\Phi^{(2)}$ and $d\Phi^{(4)}$. They will be important in the case of identical particles in the final states, since the phase space then has to be reduced by $1/n!$, where n is the number of the identical particles. For instance $n_4 = 2!2! = 4$ for two identical quark anti-quark pairs in the final state and $n_4 = 1$ for two different ones. n_2 equals $2!$ in the case of two identical particles in the intermediate state, otherwise $n_2 = 1$.

To make use of the NWA the width of the particle has to be significantly smaller than its mass. We will see later that this requirement is satisfied.

We will assume that the decay of the particles is isotropic in their rest frame. To make the approximation that the angular distribution of the $2 \rightarrow 2$ cross section remains the same after the decay, we have to ensure that the on-shell produced particles are sufficiently boosted. To become clear about this issue we make a short estimate. Since the decaying particles are of equal mass the absolute value of the three momentum is given by

$$\|\vec{p}\| = p = \sqrt{\frac{S}{4} - m^2}, \quad (6.3)$$

where \sqrt{S} is the the center of mass energy. When we assume that $\sqrt{S} = 4000$ GeV and the mass of the outgoing particle is equal to $m = 1420.85$ GeV, which is the mass of the predicted heavy gluon and sgluino, we get

$$p \approx m. \quad (6.4)$$

Now we have to calculate the Lorentz factor $\beta = v/c$, which is needed to boost a particle from the rest frame to momentum p . For simplicity we choose the boost in z-direction. After the boost, p can be expressed as follows

$$p = \beta\gamma m, \quad (6.5)$$

where $\gamma = 1/\sqrt{1 - \beta^2}$. After solving (6.5) for β we obtain $\beta \approx 0.7$. In chapter 6.3 we will discuss whether the value of β is sufficiently large to legitimate the assumption that the decay products move in the same direction as the outgoing particle of the $2 \rightarrow 2$ process.

To calculate the $2 \rightarrow 2$ cross sections and decay rates we use FeynArts and FormCalc. Therefore we implemented the model into FeynArts, which is discussed in App. C.

6.1.2 Calculation with FeynArts and FormCalc

In this section we want to calculate the $2 \rightarrow 2$ cross sections shown in Fig. 6.1 and 6.2 and the following decays in terms of the NWA by FeynArts and FormCalc. To get there, we need the phase space of two-body final states.

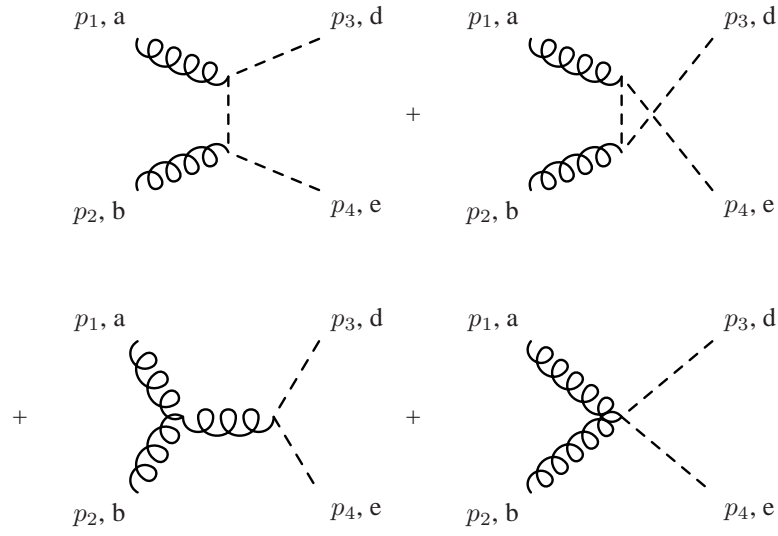


Figure 6.1: Amplitude for the process $gg \rightarrow \Sigma\Sigma$.

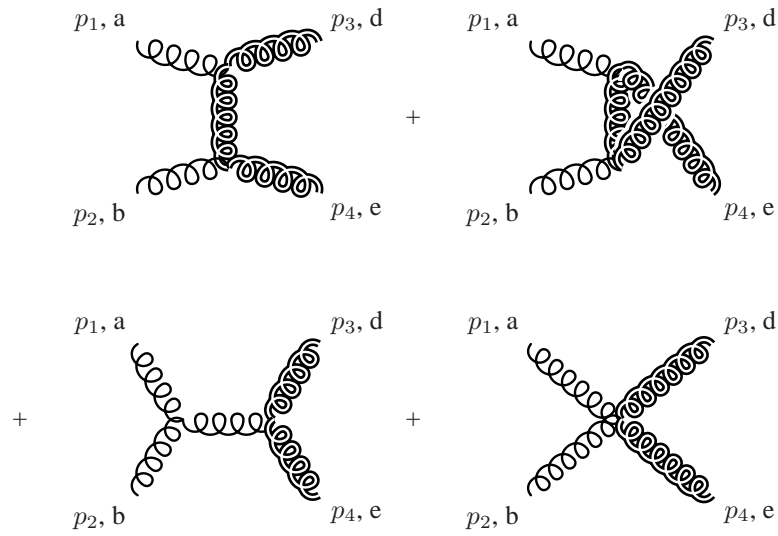


Figure 6.2: Amplitude for the process $gg \rightarrow g_1 g_1$.

Since the phase space is Lorentz invariant we choose the rest frame for the decay and the center of mass system for the $2 \rightarrow 2$ cross section. The differential cross section of the decay of a massive particle with mass M in two particles with equal mass m reads [13]

$$d\sigma = \frac{1}{32\pi^2 M} |\mathcal{M}|^2 \sqrt{1 - \frac{4m^2}{M^2}} d\Omega, \quad (6.6)$$

where \mathcal{M} is the scattering amplitude and $d\Omega = d\phi d\text{Cos}(\theta)$. The differential cross section of a $2 \rightarrow 2$ scattering process is given by [13]

$$d\sigma = \frac{1}{64\pi^2 S} |\mathcal{M}|^2 \sqrt{1 - \frac{4m^2}{S}} d\Omega, \quad (6.7)$$

where m is the mass of the outgoing particles. Note that we have used the Mandelstam variables S , T and U defined by

$$\begin{aligned} S &= (p_1 + p_2)^2 \\ T &= (p_1 - p_3)^2 \\ U &= (p_1 - p_4)^2. \end{aligned} \quad (6.8)$$

p_1 and p_2 are the momenta of the incoming particles and p_3 and p_4 are the momenta of the outgoing ones. We use FormCalc to calculate the square of the absolute value of the scattering amplitude \mathcal{M} . Since FormCalc provides results depending on the Mandelstam variables, we want to rewrite the Mandelstam variables T and U with respect to S to get a more compact expression. Therefore we need the momenta p_1 , p_2 , p_3 and p_4 in terms of S and the scattering angle θ . In the center of mass frame the momenta of two massless particles in the initial state and two massive particles with mass m in the final state read

$$\begin{aligned} p_1 &= (\sqrt{S}/2, 0, 0, \sqrt{S}/2) \\ p_2 &= (\sqrt{S}/2, 0, 0, -\sqrt{S}/2) \\ p_3 &= (\sqrt{S}/2, 0, \text{Sin}(\theta)\sqrt{S/4 - m^2}, \text{Cos}(\theta)\sqrt{S/4 - m^2}) \\ p_4 &= (\sqrt{S}/2, 0, -\text{Sin}(\theta)\sqrt{S/4 - m^2}, -\text{Cos}(\theta)\sqrt{S/4 - m^2}), \end{aligned} \quad (6.9)$$

where for simplicity we have chosen the momenta of the incoming particles in z -direction. T is derived by $T = (p_1 - p_3)^2$ and U can be easily calculated by using the identity $S + T + U = \sum_{i=1}^4 m_i^2$. T and U then read

$$\begin{aligned} T &= -\frac{S}{2} \left(1 - \frac{2m^2}{S} - \sqrt{1 - \frac{4m^2}{S}} \text{Cos}(\theta) \right) \\ U &= -S - T + 2m^2 \end{aligned} \quad (6.10)$$

The transition probability $|\mathcal{M}|^2$ for the $2 \rightarrow 2$ cross section in the center of mass frame with two heavy gluons in the final state then reads

$$\begin{aligned} |\mathcal{M}_{\text{gg} \rightarrow \text{g}(1)\text{g}(1)}|^2 &= \frac{9g_{4c}^2}{16S \left(S + (4m_{g(1)}^2 - S)\text{Cos}(\theta)^2 \right)^2} \left(3S + (-4m_{g(1)}^2 + S)\text{Cos}(\theta)^2 \right) \\ &\times \left(48m_{g(1)}^4 (2 - 2\text{Cos}(\theta)^2 + \text{Cos}(\theta)^4) - 8m_{g(1)}^2 S (3 + 2\text{Cos}(\theta)^2 + 3\text{Cos}(\theta)^4) \right. \\ &\left. + S^2 (19 - 10\text{Cos}(\theta)^2 + 3\text{Cos}(\theta)^4) \right) \end{aligned} \quad (6.11)$$

Note that we summed over the polarizations and the adjoint $SU(3)$ index in the final state and averaged the initial state with respect to the polarizations and the adjoint $SU(3)$ index. Plugging (6.11) in (6.7)

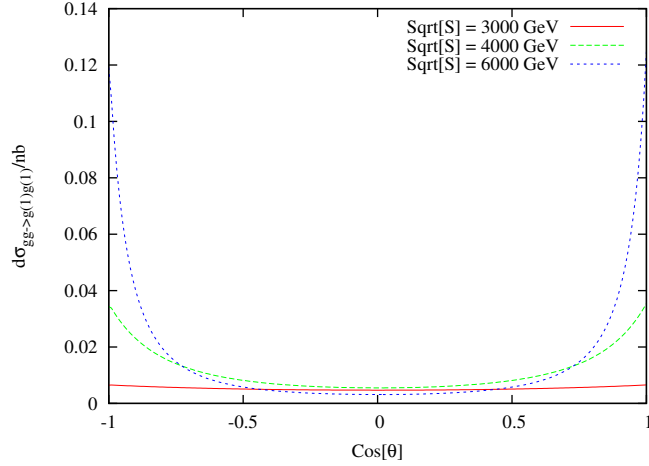


Figure 6.3: Differential cross section of two gluons in the initial state and two heavy gluons in the final state depending on $\text{Cos}(\theta)$ for different values of \sqrt{S} .

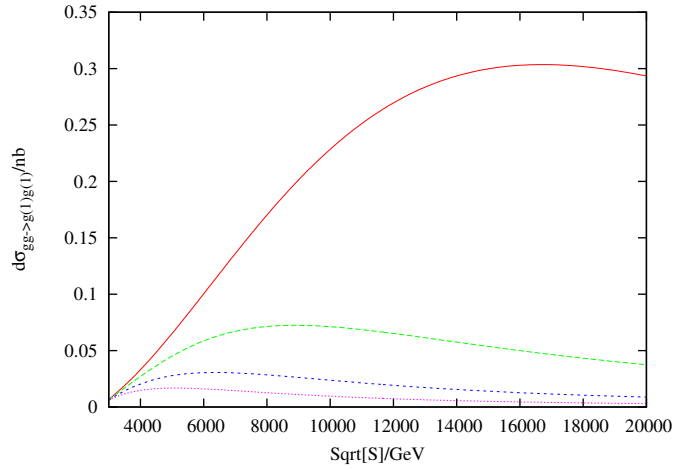


Figure 6.4: Differential cross section of two gluons in the initial state and two heavy gluons in the final state depending on \sqrt{S} for different values of θ .

we get the differential cross section. Since \mathcal{M} is independent on the azimuthal angle φ we perform the integration over φ which gives us a factor 2π and the solid angle reduces to $d\text{Cos}(\theta)$. The dimension of $d\sigma$ is $1/\text{GeV}^2$. To rewrite $d\sigma$ in units of nb where $1 \text{ nb} = 10^{-28} \text{ m}^2$ we have to multiply $d\sigma$ by a factor $10^{37} \hbar^2 c^2 \approx 0.389 \times 10^6 \text{ nb GeV}^2$. The dependence of the differential cross section $d\sigma$ on $\text{Cos}(\theta)$ and \sqrt{S} is plotted in Fig. 6.3 and 6.4. We see that the cross section is tree level unitary, because $d\sigma$ decreases for sufficiently high energies as $1/S$. Moreover, at higher energies the forward and backward scattering is enhanced. This stems from the fact that we can assume the outgoing particles to be massless in the limit of very high energies. In this limit the differential cross section will diverge for forward and backward scattering since the intermediate state particle of the T and U channel of the scattering amplitude become on-shell. This effect can also be seen in Fig. 6.5, where the S channel, the $T + U$ channel and the contact vertex are plotted over $\text{Cos}(\theta)$ for different energies. All contributions increases for ninety degree scattering with respect to higher energies. Thus the decrease of the full cross section for $\pi/2$ scattering is an effect of destructive interference.

Calculating the transition probability of the $2 \rightarrow 2$ scattering amplitude with two sgluinos in the final

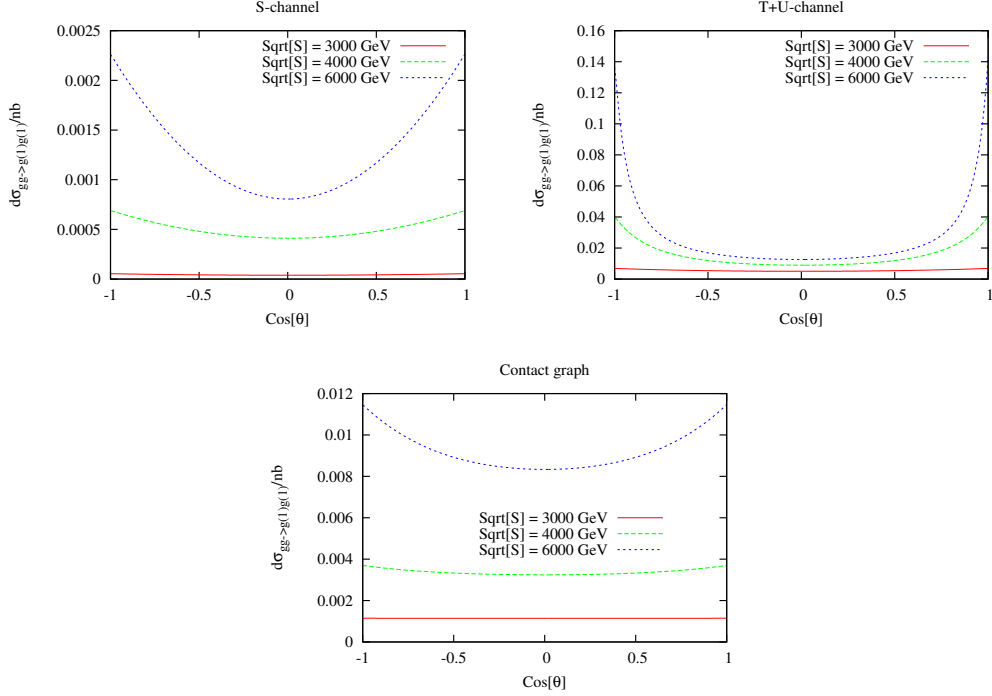


Figure 6.5: S channel, $T + U$ channel and contact graph for the cross section of two massless gluons in the initial state and two heavy gluons in the final state.

state we obtain

$$\begin{aligned}
 |\mathcal{M}_{gg \rightarrow \Sigma\Sigma}|^2 = & - \frac{9g_{4C}^2}{16 S (S + (4 m_\Sigma^2 - S) \text{Cos}(\theta)^2)^2} (3 S + (-4 m_\Sigma^2 + S) \text{Cos}(\theta)^2) \\
 & \times (32 m_\Sigma^4 - 8 m_\Sigma^2 S + S^2 + (-4 m_\Sigma^2 + S)^2 (-2 \text{Cos}(\theta)^2 + \text{Cos}(\theta)^4)). \quad (6.12)
 \end{aligned}$$

Again we summed over the polarizations and the adjoint $SU(3)$ index in the final state and averaged the initial state with respect to the polarizations and the adjoint $SU(3)$ index. The dependence of $\text{Cos}(\theta)$ and \sqrt{S} is shown in Fig. 6.6 and 6.7. As in the case above we rewrite the differential cross section in units of nb and integrated out the trivial φ dependence of the phase space. The cross section is again tree level unitary (see Fig. 6.7). Up to higher energies we may ascertain a difference in the $\text{Cos}(\theta)$ dependence to the case of two heavy gluons in the final state. The differential cross section decreases for forward and backward scattering and increases for $\pi/2$ scattering. This stems from the fact that the $T + U$ -channel increases for $\pi/2$ scattering and vanishes for $\text{Cos}(\theta) = -1$ and $\text{Cos}(\theta) = 1$. Moreover up to energies higher than 4000 GeV the contact graph decreases. The dependency comes from the phase space. This explains why the whole cross section decreases for higher energies. The dependence of the S -, $T + U$ -channel and the contact graph on $\text{Cos}(\theta)$ is plotted in Fig. 6.8.

Comparing the $2 \rightarrow 2$ cross sections with two heavy gluons and two sgluinos, respectively in the final state we find that the cross section with two heavy gluons is two magnitudes larger than the cross section with two sgluinos. This will be important for the discussion in Chap. 7, where we study whether or not the heavy gluon and sgluino can be detected at the LHC.

Finally we have to calculate the decay rates of the heavy gluon and the sgluino into quarks. We have used again FeynArts and FormCalc to get the decay probability $|\mathcal{M}|^2$ and using (6.6), we obtain for the

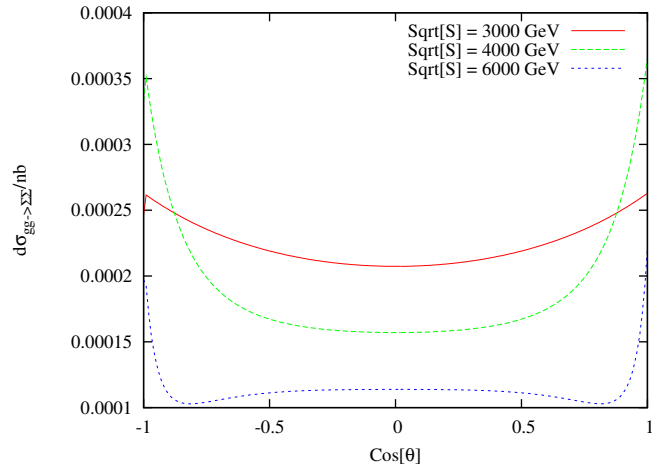


Figure 6.6: Differential cross section of two gluons in the initial state and two sgluinos in the final state depending on $\text{Cos}(\theta)$ for different values of \sqrt{S} .

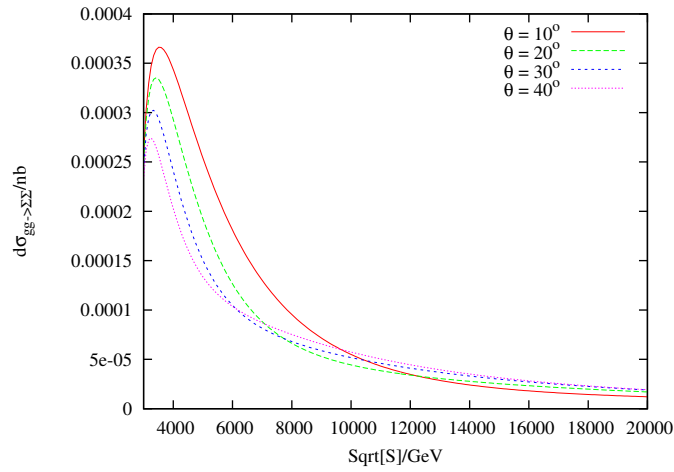


Figure 6.7: Differential cross section of two gluons in the initial state and two sgluinos in the final state depending on \sqrt{S} for different values of θ .

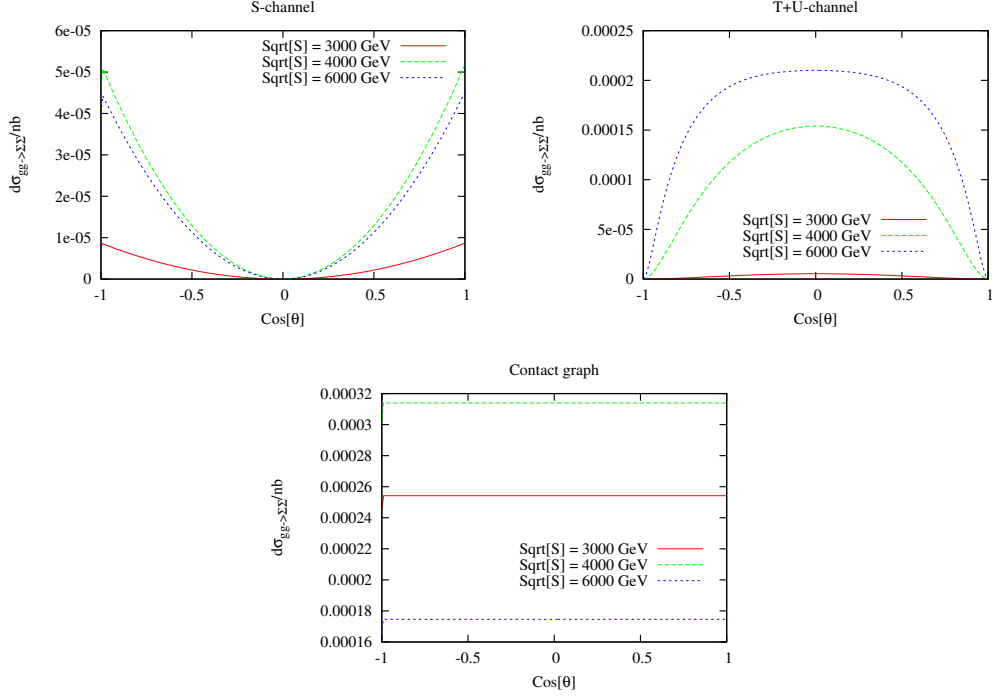


Figure 6.8: S , $T + U$ channel and contact vertex for the cross section of two massless gluons in the initial state and two sgluinos in the final state.

decay rate of the heavy gluon

$$\Gamma_{g(1) \rightarrow f\bar{f}} = \frac{1}{24\pi} \sqrt{1 - \frac{4m_f^2}{m_{g(1)}^2}} \left(6 g_{g(1)f_L\bar{f}_L} g_{g(1)f_R\bar{f}_R} m_f^2 + (g_{g(1)f_L\bar{f}_L}^2 + g_{g(1)f_R\bar{f}_R}^2) (-m_f^2 + m_{g(1)}^2) \right). \quad (6.13)$$

$g_{g(1)f_L\bar{f}_L}$ and $g_{g(1)f_R\bar{f}_R}$ are the generic couplings from the quarks to the heavy gluon. They are listed in Tab. 5.5. m_f denotes the mass of the respective quark. Plugging (6.13) in (6.6) and performing the integration over the solid angle $d\Omega$, we get the decay rate in units of GeV. The values of the decay rates are listed in Tab. 6.1. We find that the heavy gluon almost exclusively decays into bottoms and tops. This stems from the fact that the couplings of the heavy gluon to the up, down, charmed and strange quarks are negligible small (see Tab. 5.5). Summing over all possible decays, we get the width of the particle. Since the mass of two squarks is larger than the mass of the heavy gluon and sgluino, the squarks add no contribution to the decay width. In the case of the heavy gluon we obtain $\Gamma_{g(1)} = 155.93$ GeV. This is around the tenth of the particle mass and for this reason the assumption for using the narrow width approximation is justified. Furthermore we find that the decay into the bottom and the top quark dominates, which becomes important for the detection of the heavy gluon at LHC. This will be discussed in the section of hadronic cross sections.

The decay rate of the sgluino into quarks reads

$$\Gamma_{\Sigma f\bar{f}} = \frac{1}{16\pi} \sqrt{1 - \frac{4m_f^2}{m_\Sigma^2}} g_{\Sigma f\bar{f}}^2 (-4m_f^2 + m_\Sigma^2). \quad (6.14)$$

Plugging again (6.14) into (6.6) and integrating over $d\Omega$ we get the decay rates listed in Tab. 6.2. As in the case of the heavy gluon the sgluino decays almost exclusively into bottom and top quarks, which corresponds to the couplings of the sgluino to the quarks (see Tab. 5.4). It is even more dramatic, since the

$\Gamma_{g(1) \rightarrow u\bar{u}}$	0.516 GeV
$\Gamma_{g(1) \rightarrow d\bar{d}}$	0.971 GeV
$\Gamma_{g(1) \rightarrow c\bar{c}}$	0.1472 GeV
$\Gamma_{g(1) \rightarrow s\bar{s}}$	0.1472 GeV
$\Gamma_{g(1) \rightarrow t\bar{t}}$	106.32 GeV
$\Gamma_{g(1) \rightarrow b\bar{b}}$	47.827 GeV

Table 6.1: Decay rate of the heavy gluon into quarks.

$\Gamma_{\Sigma \rightarrow u\bar{u}}$	9.1×10^{-17} GeV
$\Gamma_{\Sigma \rightarrow d\bar{d}}$	0
$\Gamma_{\Sigma \rightarrow c\bar{c}}$	0
$\Gamma_{\Sigma \rightarrow s\bar{s}}$	7.1×10^{-9} GeV
$\Gamma_{\Sigma \rightarrow t\bar{t}}$	0.597 GeV
$\Gamma_{\Sigma \rightarrow b\bar{b}}$	0.0013 GeV

Table 6.2: Decay rate of the sgluino into quarks.

decay into the bottom quark is much smaller than the decay into the top quark. The width of the sgluino $\Gamma = 0.598$ GeV is very small compared to its mass. Thus we would expect that the narrow width approximation works very well in the case of the sgluino.

In the next subsection we want to check the Ward Identity for $2 \rightarrow 2$ processes. Since the couplings of the sgluinos and the gluons are gauge invariant by construction of the theory, the Ward Identity of cross sections with massless gluons in the initial state and sgluinos or heavy gluons in the final state has to be fulfilled. To ensure the correct calculation of the coupling of sgluinos and gluons we check the Ward Identity of the cross section with two gluons in the initial state and two sgluinos in the final state.

Ward Identity

Now we want to check the Ward Identity for the $2 \rightarrow 2$ process $gg \rightarrow \Sigma\Sigma$. In order to verify the validity of the Ward Identity we have to look at the single amplitudes and have to replace one of the polarization vectors of the gluons by its momentum.

$$p_{2,\nu} \mathcal{M}_1^\nu = i g^2 \epsilon_\mu(p_1) \frac{1}{(-p_1 - p_2)^2} f^{abc} f^{dec} p_{2,\nu} \times [g^{\mu\nu}(p_1 - p_2)^\rho + g^{\nu\rho}(2p_2 + p_1)^\mu + g^{\rho\mu}(-2p_1 - p_2)^\nu] (p_3 - p_4)_\rho \quad (6.15)$$

$$p_{2,\nu} \mathcal{M}_2^\nu = i g^2 \epsilon_\mu(p_1) \frac{1}{(p_1 - p_3)^2 - m_\Sigma^2} f^{dca} f^{ecb} p_{2,\nu} (2p_3 - p_1)^\mu (2p_4 - p_2)^\nu \quad (6.16)$$

$$p_{2,\nu} \mathcal{M}_3^\nu = i g^2 \epsilon_\mu(p_1) \frac{1}{(p_1 - p_4)^2 - m_\Sigma^2} f^{eca} f^{dcb} p_{2,\nu} (2p_4 - p_1)^\mu (2p_3 - p_2)^\nu \quad (6.17)$$

$$p_{2,\nu} \mathcal{M}_4^\nu = i g^2 \epsilon_\mu(p_1) p_{2,\nu} g^{\mu\nu} (f^{dac} f^{bec} + f^{eac} f^{bdc}) \quad (6.18)$$

Here we substitute $\epsilon_\nu(p_2)$ for $p_{2,\nu}$. For simplicity we calculate the Ward Identity in the center of mass frame and can then apply the relations $\vec{p}_1 = -\vec{p}_2$ and $\vec{p}_3 = -\vec{p}_4$. First of all we regard the S channel amplitude and make use of the on-shell relations $\epsilon_\mu(p_i) p_i^\mu = 0$ and $p_{i,\mu} p_i^\mu = 0$ with $i = 1, 2$. We then obtain

$$p_{2,\nu} \mathcal{M}_1^\nu = -i g^2 f^{abc} f^{dec} (p_{3,\nu} \epsilon_1^\nu - p_{4,\nu} \epsilon_1^\nu). \quad (6.19)$$

After using the relation $\vec{p}_3 = -\vec{p}_4$ we get

$$p_{2,\nu} \mathcal{M}_1^\nu = -2i g^2 f^{abc} f^{dec} p_{3,\nu} \epsilon_1^\nu. \quad (6.20)$$

We apply the same procedure to \mathcal{M}_2 and \mathcal{M}_3 by using the above relations and end up with

$$\begin{aligned} p_{2,\nu} \mathcal{M}_2^\nu &= 2i g^2 f^{dca} f^{ecb} p_{3,\nu} \epsilon_1^\nu \\ p_{2,\nu} \mathcal{M}_3^\nu &= -2i g^2 f^{eca} f^{dcb} p_{3,\nu} \epsilon_1^\nu \end{aligned} \quad (6.21)$$

$p_{2,\nu} \mathcal{M}_4^\nu$ is equal to zero because $\epsilon_{1,\mu} p_2^\mu = 0$. To see that the sum of the residual terms cancels, we have to use the properties of the structure constants [15]:

$$f^{abc} f^{dec} = \frac{2}{n} (\delta^{ad} \delta^{be} - \delta^{ae} \delta^{bd}) + (d^{adc} d^{bec} - d^{aec} d^{bdc}) \quad (6.22)$$

with

$$d^{abc} = \frac{1}{4} \text{Tr}[\{T^a, T^b\} T^c]. \quad (6.23)$$

When we apply the identities to the above results we obtain the following expressions:

$$p_{2,\nu} \mathcal{M}_1^\nu = 2i g^2 p_{3,\nu} \epsilon_1^\nu \frac{2}{n} (-\delta^{ad} \delta^{be} + \delta^{ae} \delta^{bd} - d^{adc} d^{bec} + d^{aec} d^{bdc}) \quad (6.24)$$

$$p_{2,\nu} \mathcal{M}_2^\nu = 2i g^2 p_{3,\nu} \epsilon_1^\nu \frac{2}{n} (\delta^{ab} \delta^{de} - \delta^{ae} \delta^{bd} + d^{abc} d^{dec} - d^{aec} d^{bdc}) \quad (6.25)$$

$$p_{2,\nu} \mathcal{M}_3^\nu = 2i g^2 p_{3,\nu} \epsilon_1^\nu \frac{2}{n} (-\delta^{ab} \delta^{de} + \delta^{ad} \delta^{be} - d^{abc} d^{dec} + d^{adc} d^{bec}) \quad (6.26)$$

Now it is easy to see that the sum over the three expressions is equal to zero and for this reason the Ward Identity is fulfilled.

6.2 Monte Carlo Simulation

In this section we want to perform Monte Carlo simulations for $2 \rightarrow 4$ processes with two massless gluons in the initial state and a bottom anti-bottom and a top anti-top pair in the final state. The Monte Carlo simulation allows us to calculate the $2 \rightarrow 4$ tree level cross section without using any approximations. Since we want to compare the Monte Carlo simulation with the NWA and do not want to make LHC predictions at this moment, we reduce the number of diagrams of the the full $2 \rightarrow 4$ tree level process to the number of $2 \rightarrow 4$ diagrams, which contain only $SU(3)$ contributions. Furthermore, the neglected diagrams (see Fig. 6.12 and Fig. 6.13) are single resonant diagrams and we will choose phase space cuts by which single resonant diagrams are strongly suppressed. Furthermore the neglected diagrams contain electroweak contributions. The full $2 \rightarrow 4$ tree level cross section is defined by the $2 \rightarrow 4$ cross section, which takes all possible contributions into account that are allowed by the model. By reducing the number of diagrams we have to take care about gauge invariance. We ensure gauge invariance by taking all possible $SU(3)$ contributions into account. The $SU(3)$ gauge invariant subclass of all $2 \rightarrow 4$ diagrams is shown in Fig. 6.9, 6.10 and 6.11. These diagrams are the diagrams we will concentrate on.

In the NWA we have to choose fixed final states of the $2 \rightarrow 2$ cross section. Since the heavy gluon and the sgluino have the same mass on lowest order we cannot distinguish $2 \rightarrow 4$ processes, where heavy gluons

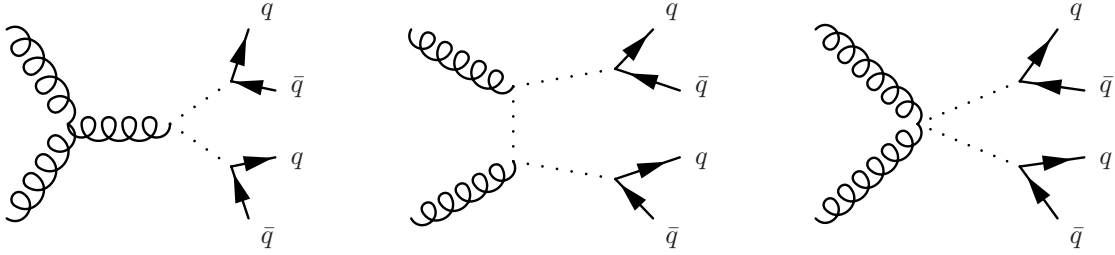


Figure 6.9: Production of two quark anti-quark pairs with two massless gluons in the initial state. These are all possible double resonant $2 \rightarrow 4$ diagrams in the $SU(3)$ sector. Note that we do not show the crossed diagrams for reasons of compactness. The dotted lines stand either for a massless gluon, a heavy gluon or a sgluino.

or sgluinos are in the intermediate state by using suitable phase space cuts. To compare the Monte Carlo simulation with the NWA, anyway we only regard cross sections where either heavy gluons or sgluinos are in the intermediate state. Note that these cross sections remain gauge invariant when taking all contributions of the massless gluon into account. Now we can examine the characteristics of the two particles separately and thus we are able to compare the results of the Monte Carlo simulation with those of the NWA. If the masses of the heavy gluon and sgluino differ on one-loop order we would have the possibility to distinguish processes with two heavy gluons or two sgluinos in the intermediate state by the choice of suitable phase space cuts. This will be discussed in Chap. 7

Since we want to study the contributions of $2 \rightarrow 4$ cross sections, where two heavy gluons or two sgluinos, respectively, are produced in the intermediate state, we have to introduce suitable phase space cuts. Therefore we restrict the invariant mass of the two quark-antiquark pairs to the mass of the decaying particles we want to measure. This will be discussed in detail when we present the results of the Monte Carlo simulation.

To perform the required Monte Carlo simulations we need several programs. To create the scattering amplitudes we use O'Mega and for the Monte Carlo generation we use Whizard. O'Mega (Optimizing Matrix Event Generator) is a tool which generates an efficient code for scattering amplitudes created by Mauro Moretti, Thorsten Ohl and Jürgen Reuter [16]. To produce a highly efficient code for calculating multiparton cross sections O'Mega uses the so called color flow decomposition. Moreover, by using this representation, it is possible to add parton showers to the multiparton cross sections. In the next section we will give a short introduction to color flow decomposition the reader needs to follow the discussion in App. D, where the implementation of the model in O'Mega is presented. Afterwards we study the Ward Identities in this color scheme to get a check for the correct calculation of the sgluino-gluon coupling in the color flow representation. Next we examine the correct implementation in O'Mega on the basis of the $2 \rightarrow 2$ processes shown in Fig. 6.1 and 6.2. In the end we will display the results of the $2 \rightarrow 4$ Monte Carlo simulation.

6.2.1 Color Flow

In this section we give a short introduction to the topic of color flow decomposition of multiparton amplitudes. This whole part is based on the paper of F. Maltoni, K. Stelzer and S. Willenbrock [17]. For calculating amplitudes, which involve many colored particles, the calculation of the color structure has to be done. In the past techniques have been developed to do this work very efficiently and the systematic organization of the $SU(N)$ color algebra is one main aspect of such methods. For example we consider a n -gluon amplitude where the gluons have the adjoint $SU(N)$ indices a_1, a_2, \dots, a_n with $n = N^2 - 1$. At tree level, such an amplitude can be decomposed as

$$\mathcal{M}(ng) = \sum_{P(2, \dots, n)} \text{Tr}(\lambda^{a_1} \lambda^{a_2} \dots \lambda^{a_n}) A(1, 2, \dots, n) \quad (6.27)$$

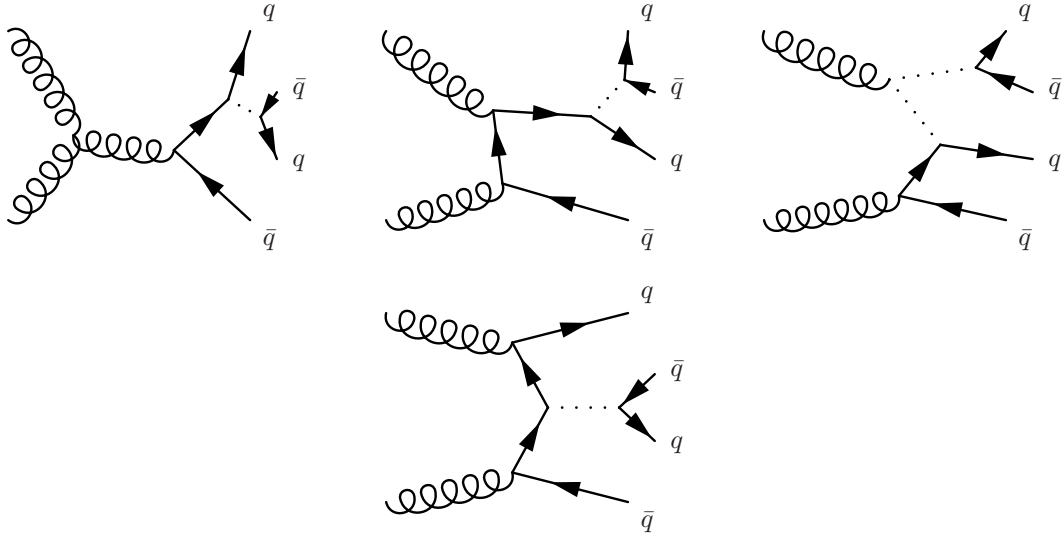


Figure 6.10: Production of two quark anti-quark pairs with two massless gluons in the initial state. These are all possible single resonant $2 \rightarrow 4$ diagrams in the $SU(3)$ sector. Note that we do not show the crossed diagrams for reasons of compactness. The dotted lines stand either for a massless gluon, a heavy gluon or a sgluino.

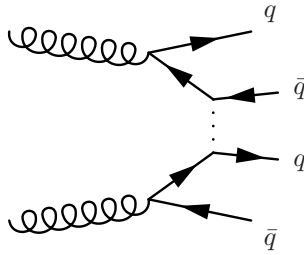


Figure 6.11: Production of two quark anti-quark pairs with two massless gluons in the initial state. These are all possible non-resonant $2 \rightarrow 4$ diagrams in the $SU(3)$ sector. Note that we do not show the crossed diagrams for reasons of compactness. The dotted lines stand either for a massless gluon, a heavy gluon or a sgluino.

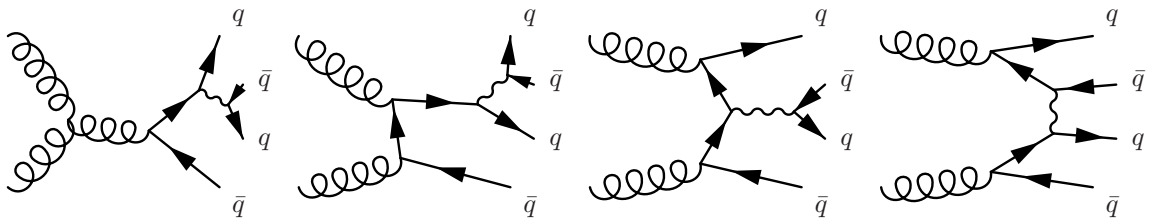


Figure 6.12: W^- , Z^- , and γ contributions of the production of two quark anti-quark pairs with two massless gluons in the initial state. Note that we do not show the crossed diagrams for reasons of compactness. The wiggly lines stand either for a W -Boson, a Z -Boson or a photon.

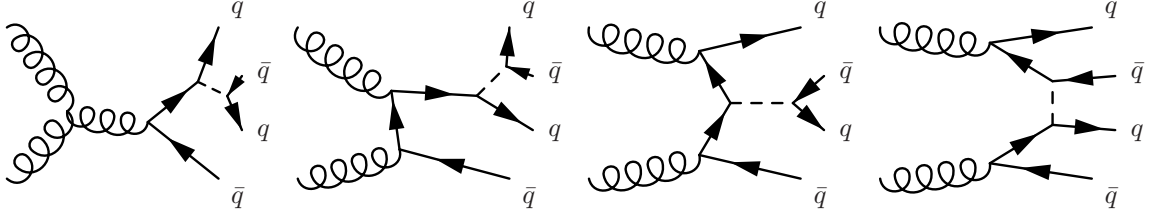


Figure 6.13: Schargino and sneutralino contributions of the production of two quark anti-quark pairs with two massless gluons in the initial state. Note that we do not show the crossed diagrams for reasons of compactness. The dashed line stands either for a schargino or a sneutralino.

where λ^a are the generators of the $SU(N)$ gauge group in the fundamental representation and the sum is over all $(n-1)!$ permutations of $(2, \dots, n)$. The partial amplitude A depends only on the four momenta p_i and the polarization vectors ϵ_i of the n gluons with $i = 1, \dots, n$.

Aside from the above decomposition there exists another one, based on the adjoint representation of $SU(N)$. The n -gluon amplitude can then be written as

$$\mathcal{M}(ng) = \sum_{P(2, \dots, n-1)} \text{Tr} (F^{a_2} F^{a_3} \dots F^{a_{n-1}})_{a_n}^{a_1} A(1, 2, \dots, n), \quad (6.28)$$

where $(F^a)_c^b = -if^{abc}$ are the adjoint-representation matrices of $SU(N)$. The sum is over all $(n-2)!$ permutations of $(2, \dots, n-1)$. The partial amplitudes A are the same as in the above decomposition. In opposite to the first decomposition scheme the second one exists only for a multigluon amplitude.

The third decomposition method is the so called color flow decomposition. For this method the gluon field is represented as a $N \times N$ matrix $(A_\mu)_j^i$ ($i, j = 1, \dots, N$) instead of the adjoint representation A_μ^a ($a = 1, \dots, N^2 - 1$), which is represented as a vector in the adjoint index. The n -gluon amplitude can then be written as

$$\mathcal{M}(ng) = \sum_{P(2, \dots, n)} \delta_{j_2}^{i_1} \delta_{j_3}^{i_2} \dots \delta_{j_1}^{i_n} A(1, 2, \dots, n), \quad (6.29)$$

where the sum is over all $(n-1)!$ permutations of $(2, \dots, n)$. Like the first decomposition this one can be used for multiparton amplitudes. The color flow decomposition describes the *flow of color* and has for this reason a very descriptive physical interpretation. This property is also useful for merging the hard-scattering cross section with shower Monte Carlo programs. Moreover this kind of decomposition allows a very fast and efficient way to calculate multiparton amplitudes.

In the color flow decomposition the color structure of the vertices is very easy (see Fig. 6.14). For the simplicity of the color structure of the vertices we get a more complicated color structure of the gluon propagator

$$\langle (A_\mu)_{j_1}^{i_1} (A_\nu)_{j_2}^{i_2} \rangle \propto \delta_{j_2}^{i_1} \delta_{j_1}^{i_2} - \frac{1}{N} \delta_{j_1}^{i_1} \delta_{j_2}^{i_2} \quad (6.30)$$

instead of the basic structured gluon propagator in the conventional adjoint representation $\langle A_\mu^a A_\nu^b \rangle \propto \delta^{ab}$. But the more complicated color structure of the gluon propagator is not eminently tragical because due to the antisymmetry of the three- and four-gluon vertices, the second color flow in the propagator does not couple to these interactions. It only couples to the gluon interactions with quarks. For amplitudes where only particles in the adjoint representation of $SU(N)$ contribute we can forget about this additional term in the gluon propagator and calculate the cross section with the reduced propagator $\langle (A_\mu)_{j_1}^{i_1} (A_\nu)_{j_2}^{i_2} \rangle \propto \delta_{j_2}^{i_1} \delta_{j_1}^{i_2}$. Only the interaction of gluon and quarks couple to the second color flow from the propagator. Since this color flow couples as a $U(1)$ gluon to the quarks we can split the propagator into a $U(N)$ gluon propagator

The figure shows three Feynman diagrams representing gluon vertices in a color flow decomposition. Each diagram is followed by its corresponding mathematical expression.

Three-gluon vertex: A central vertex with one wavy line (gluon) pointing upwards and two straight lines (quarks) pointing downwards and outwards. The top gluon line is labeled with indices μ_1 and $j_1 i_1$. The two quark lines are labeled with indices i_3, μ_3, j_3 and i_2, μ_2, j_2 respectively.

$$= i \frac{g}{\sqrt{2}} \gamma^{\mu_1} \delta_{j_1}^{i_3} \delta_{j_3}^{i_1}$$

Four-gluon vertex (crossing): A central vertex with four wavy lines (gluons) extending outwards. The top-left gluon is labeled μ_1, j_1, i_1 ; the top-right gluon is labeled j_2, μ_2, i_2 ; the bottom-left gluon is labeled i_4, μ_4, j_4 ; and the bottom-right gluon is labeled i_3, μ_3, j_3 .

$$= i \frac{g^2}{2} \sum [g^{\mu_1 \mu_2} (p_1 - p_2)^{\mu_3} + g^{\mu_2 \mu_3} (p_2 - p_3)^{\mu_1} + g^{\mu_1 \mu_3} (p_3 - p_1)^{\mu_2}] \times \delta_{j_2}^{i_1} \delta_{j_3}^{i_2} \delta_{j_1}^{i_3}$$

$$= i \frac{g^2}{2} \sum (2g^{\mu_1 \mu_3} g^{\mu_2 \mu_4} - g^{\mu_1 \mu_2} g^{\mu_3 \mu_4} - g^{\mu_1 \mu_4} g^{\mu_2 \mu_3}) \times \delta_{j_2}^{i_1} \delta_{j_3}^{i_2} \delta_{j_4}^{i_3} \delta_{j_1}^{i_4}$$

Figure 6.14: Feynman rules in the color flow decomposition. The sum in the three gluon vertex is over the two non-cyclic permutations of (1,2,3). The sum in the four gluon vertex is over the six non-cyclic permutations of (1,2,3,4).

$$\begin{aligned}
&= gf^{abc} [g^{\mu_1\mu_2}(p_1 - p_2)^{\mu_3} + g^{\mu_2\mu_3}(p_2 - p_3)^{\mu_1} + g^{\mu_1\mu_3}(p_3 - p_1)^{\mu_2}] \\
&= -ig^2 [f^{abe} f^{cde} (g^{\mu_1\mu_4} g^{\mu_2\mu_3} - g^{\mu_1\mu_3} g^{\mu_2\mu_4}) \\
&= +f^{ace} f^{bde} (g^{\mu_1\mu_2} g^{\mu_3\mu_4} - g^{\mu_1\mu_3} g^{\mu_2\mu_4}) \\
&+ f^{ade} f^{bce} (g^{\mu_1\mu_2} g^{\mu_3\mu_4} - g^{\mu_1\mu_4} g^{\mu_2\mu_3})]
\end{aligned}$$

Figure 6.15: Three and four gluon vertex in the adjoint representation.

and a $U(1)$ propagator. The bifundamental representation of the gluon has naively $3 \times 3 = 9$ degrees of freedom. The $U(1)$ gluon is unphysical and can now be interpreted as a ghostlike particle which cancels the redundant degree of freedom of the $U(N)$ gluon. Therefore the *auxiliary* gluon has to be implemented in programs which are based on the color flow representation. This we have done in App. D where we discuss the implementation.

For a better understanding of the relation between the adjoint and the color flow decomposition we want to do the explicit transformation from the adjoint to the color flow representation of the three- and four-gluon vertex. Therefore we start with the interaction vertices in the adjoint representation. First we want to transform the three-gluon vertex Fig. 6.15.

When we perform the sum of the three-gluon vertex shown in Fig. 6.14 we get a vertex with the same kinematical and Lorentz structure like in the three-gluon vertex in the adjoint representation multiplied by a color prefactor $(\delta_{j_2}^{i_1} \delta_{j_3}^{i_2} \delta_{j_1}^{i_3} - \delta_{j_3}^{i_1} \delta_{j_2}^{i_3} \delta_{j_1}^{i_2})$. To show the equivalence of the both representations we have to check the validity of

$$-f^{abc} (T^a)_{j_1}^{i_1} (T^b)_{j_2}^{i_2} (T^c)_{j_3}^{i_3} = i \frac{1}{\sqrt{2}} (\delta_{j_2}^{i_1} \delta_{j_3}^{i_2} \delta_{j_1}^{i_3} - \delta_{j_3}^{i_1} \delta_{j_2}^{i_3} \delta_{j_1}^{i_2}). \quad (6.31)$$

Therefore we have to use first that the structure constants, which can be written as $f^{abc} = -i \text{Tr}(T^a [T^b, T^c])$. We get

$$-f^{abc} = i \text{Tr}[T^a T^b T^c - T^a T^c T^b] = i(T_{k_1 k_2}^a T_{k_2 k_3}^b T_{k_3 k_1}^c - T_{k_1 k_2}^a T_{k_2 k_3}^c T_{k_3 k_1}^b) \quad (6.32)$$

Thereafter we multiply the whole expression with $(T^a)_{j_1}^{i_1} (T^b)_{j_2}^{i_2} (T^c)_{j_3}^{i_3}$ to saturate the adjoint indices. To perform the saturation we have to use the relation

$$(T^a)_j^i (T^a)_l^k = \delta_l^i \delta_j^k - 1/N \delta_j^i \delta_l^k \quad (6.33)$$

After the whole calculation the final expression for the structure constant is

$$-f^{abc} (T^a)_{j_1}^{i_1} (T^b)_{j_2}^{i_2} (T^c)_{j_3}^{i_3} = i(\delta_{j_2}^{i_1} \delta_{j_3}^{i_2} \delta_{j_1}^{i_3} - \delta_{j_3}^{i_1} \delta_{j_2}^{i_3} \delta_{j_1}^{i_2}). \quad (6.34)$$

The factor $1/\sqrt{2}$ in the three gluon vertex of the color flow decomposition comes from the fact that the $N \times N$ matrix field $(A_\mu)_j^i$ is canonically normalized $((A_\mu)_j^i \equiv \sqrt{2}(A_\mu)_j^i)$. Because of this normalization

$$= -ig^2 g^{\mu_1 \mu_2} (f^{abe} f^{cde} + f^{bde} f^{ace})$$

Figure 6.16: Quartic coupling of the lightest sgluino to two massless gluons in the adjoint representation.

the coupling constant is $g/\sqrt{2}$ rather than g .

Next we want to show the equivalence for the four gluon vertex. Therefore we have to use again the relation $f^{abc} = -i\text{Tr}(T^a[T^b, T^c])$ and get the following expressions for the color structure of the four gluon vertex in the adjoint representation

$$f^{abe} f^{cde} = \text{Tr}[T^a T^b T^c T^d] + \text{Tr}[T^b T^a T^d T^c] - \text{Tr}[T^a T^b T^d T^c] - \text{Tr}[T^b T^a T^c T^d] \quad (6.35)$$

where we also exploit (6.33). Now we multiply the obtained expression by $(T^a)_{j_1}^{i_1} (T^b)_{j_2}^{i_2} (T^c)_{j_3}^{i_3} (T^d)_{j_4}^{i_4}$, apply (6.33) once more and get

$$\begin{aligned} f^{abe} f^{cde} (T^a)_{j_1}^{i_1} (T^b)_{j_2}^{i_2} (T^c)_{j_3}^{i_3} (T^d)_{j_4}^{i_4} &= \delta_{j_2}^{i_1} \delta_{j_3}^{i_2} \delta_{j_4}^{i_3} \delta_{j_1}^{i_4} + \delta_{j_4}^{i_1} \delta_{j_1}^{i_2} \delta_{j_2}^{i_3} \delta_{j_3}^{i_4} - \delta_{j_3}^{i_1} \delta_{j_1}^{i_2} \delta_{j_4}^{i_3} \delta_{j_2}^{i_4} - \delta_{j_2}^{i_1} \delta_{j_4}^{i_2} \delta_{j_3}^{i_3} \delta_{j_1}^{i_4} \\ f^{ace} f^{bde} (T^a)_{j_1}^{i_1} (T^b)_{j_2}^{i_2} (T^c)_{j_3}^{i_3} (T^d)_{j_4}^{i_4} &= \delta_{j_4}^{i_1} \delta_{j_3}^{i_2} \delta_{j_1}^{i_3} \delta_{j_2}^{i_4} + \delta_{j_3}^{i_1} \delta_{j_4}^{i_2} \delta_{j_2}^{i_3} \delta_{j_1}^{i_4} - \delta_{j_3}^{i_1} \delta_{j_1}^{i_2} \delta_{j_4}^{i_3} \delta_{j_2}^{i_4} - \delta_{j_2}^{i_1} \delta_{j_4}^{i_2} \delta_{j_3}^{i_3} \delta_{j_1}^{i_4} \\ f^{ade} f^{bce} (T^a)_{j_1}^{i_1} (T^b)_{j_2}^{i_2} (T^c)_{j_3}^{i_3} (T^d)_{j_4}^{i_4} &= \delta_{j_4}^{i_1} \delta_{j_3}^{i_2} \delta_{j_1}^{i_3} \delta_{j_2}^{i_4} + \delta_{j_3}^{i_1} \delta_{j_4}^{i_2} \delta_{j_2}^{i_3} \delta_{j_1}^{i_4} - \delta_{j_4}^{i_1} \delta_{j_1}^{i_2} \delta_{j_2}^{i_3} \delta_{j_3}^{i_4} - \delta_{j_2}^{i_1} \delta_{j_3}^{i_2} \delta_{j_4}^{i_3} \delta_{j_1}^{i_4} \end{aligned} \quad (6.36)$$

We obtain six different color structures, which are exactly the six non-cyclic permutations of the four-gluon vertex shown in Fig. 6.14. When we now replace the structure constants in the four-gluon vertex in the adjoint representation by the expressions from Eq. (6.36) and rearrange the vertex in order to the six non-cyclic permutations of $\delta_{j_2}^{i_1} \delta_{j_3}^{i_2} \delta_{j_4}^{i_3} \delta_{j_1}^{i_4}$ the four gluon vertex reads

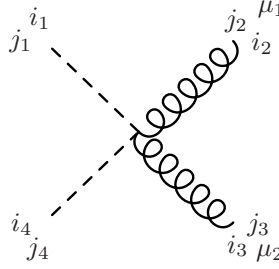
$$ig^2 \sum \delta_{j_2}^{i_1} \delta_{j_3}^{i_2} \delta_{j_4}^{i_3} \delta_{j_1}^{i_4} (2g^{\mu_1 \mu_3} g^{\mu_2 \mu_4} - g^{\mu_1 \mu_2} g^{\mu_3 \mu_4} - g^{\mu_1 \mu_4} g^{\mu_2 \mu_3}) \quad (6.37)$$

and is except for a factor 1/2 equal to the four gluon vertex of the color flow decomposition. The factor 1/2 comes again from the canonical normalization of the $N \times N$ matrix field $(A_\mu)_j^i$. The vertex of the gluon to a quark anti-quark pair can be transformed in the same way as the three- and four-gluon vertex. The 4D gluon vertices in the color flow decomposition are easily extended to the 5D one with heavy gluons, since the color structure do not change.

Lastly we want to examine the couplings of the sgluinos to the gluons and fermions in the color flow decomposition, since we need them in this representation for the implementation in O'Mega. The trilinear couplings of the sgluino to the fermions and gluons only differ in the Lorentz structure and coupling constants from the trilinear gluon couplings. Thus the color flow structure of the vertices is the same as shown in Fig. 6.14 and we only have to exchange the Lorentz structure and coupling constants. In the case of the quartic coupling of the sgluinos to the gluons we only regard the coupling of the lightest sgluino to two massless gluons for simplicity. The extension to the full theory is as easy as in the case of the gluon couplings discussed above. The vertex in the adjoint representation is shown in Fig. 6.16. To get the color flow representation of the vertex we use formula (6.36) and obtain after a short calculation the vertex shown in Fig. 6.17. The factor 1/2 comes again from the canonical normalization.

Ward Identity and Color Flows

The Ward Identity has to be fulfilled for every given setup of quantum numbers for the in- and out-states. Hence the Ward Identity has to be valid for every color flow. We want to show this item explicitly for



$$\begin{aligned}
& -i \frac{g^2}{2} g^{\mu_1 \mu_2} \left(\delta_{j_2}^{i_1} \delta_{j_3}^{i_2} \delta_{j_4}^{i_3} \delta_{j_1}^{i_4} + \delta_{j_4}^{i_1} \delta_{j_1}^{i_2} \delta_{j_2}^{i_3} \delta_{j_3}^{i_4} \right) \\
& = + \delta_{j_4}^{i_1} \delta_{j_3}^{i_2} \delta_{j_1}^{i_3} \delta_{j_2}^{i_4} + \delta_{j_3}^{i_1} \delta_{j_4}^{i_2} \delta_{j_2}^{i_3} \delta_{j_1}^{i_4} \\
& \quad - 2 \delta_{j_4}^{i_1} \delta_{j_1}^{i_2} \delta_{j_2}^{i_3} \delta_{j_3}^{i_4} - 2 \delta_{j_4}^{i_1} \delta_{j_1}^{i_2} \delta_{j_2}^{i_3} \delta_{j_3}^{i_4}
\end{aligned}$$

Figure 6.17: Quartic coupling of the lightest sgluino to two massless gluons in the color flow representation.

the process $gg \rightarrow \Sigma\Sigma$. Most of the work has been done in section 6.1.2, because we can already use the simplified expressions for the amplitudes \mathcal{M}_1^ν , \mathcal{M}_2^ν and \mathcal{M}_3^ν from (6.20) and (6.21).

$$\begin{aligned}
p_{2,\nu} \mathcal{M}_1^\nu &= -2 i g^2 f^{abc} f^{dec} p_{3,\nu} \epsilon_1^\nu \\
p_{2,\nu} \mathcal{M}_2^\nu &= 2 i g^2 f^{dca} f^{ecb} p_{3,\nu} \epsilon_1^\nu \\
p_{2,\nu} \mathcal{M}_3^\nu &= -2 i g^2 f^{eca} f^{dcb} p_{3,\nu} \epsilon_1^\nu
\end{aligned} \tag{6.38}$$

Thus the only work that has been left is the transformation of the structure constants in the color flow representation. Therefore we use the relations of (6.36) and get

$$\begin{aligned}
& -2 i g^2 f^{abc} f^{dec} (T^a)_{j_1}^{i_1} (T^b)_{j_2}^{i_2} (T^d)_{j_3}^{i_3} (T^e)_{j_4}^{i_4} p_{3,\nu} \epsilon_1^\nu = 2 i g^2 (\epsilon_1, p_3) \\
& \quad \times \left(-\delta_{j_2}^{i_1} \delta_{j_3}^{i_2} \delta_{j_4}^{i_3} \delta_{j_1}^{i_4} - \delta_{j_4}^{i_1} \delta_{j_1}^{i_2} \delta_{j_2}^{i_3} \delta_{j_3}^{i_4} + \delta_{j_3}^{i_1} \delta_{j_1}^{i_2} \delta_{j_4}^{i_3} \delta_{j_2}^{i_4} + \delta_{j_2}^{i_1} \delta_{j_4}^{i_2} \delta_{j_3}^{i_3} \delta_{j_1}^{i_4} \right) \\
& 2 i g^2 f^{adc} f^{bec} (T^a)_{j_1}^{i_1} (T^b)_{j_2}^{i_2} (T^d)_{j_3}^{i_3} (T^e)_{j_4}^{i_4} p_{3,\nu} \epsilon_1^\nu = 2 i g^2 (\epsilon_1, p_3) \\
& \quad \times \left(+\delta_{j_4}^{i_1} \delta_{j_3}^{i_2} \delta_{j_1}^{i_3} \delta_{j_2}^{i_4} + \delta_{j_3}^{i_1} \delta_{j_4}^{i_2} \delta_{j_2}^{i_3} \delta_{j_1}^{i_4} - \delta_{j_3}^{i_1} \delta_{j_1}^{i_2} \delta_{j_4}^{i_3} \delta_{j_2}^{i_4} - \delta_{j_2}^{i_1} \delta_{j_4}^{i_2} \delta_{j_3}^{i_3} \delta_{j_1}^{i_4} \right) \\
& -2 i g^2 f^{aec} f^{bdc} (T^a)_{j_1}^{i_1} (T^b)_{j_2}^{i_2} (T^d)_{j_3}^{i_3} (T^e)_{j_4}^{i_4} p_{3,\nu} \epsilon_1^\nu = 2 i g^2 (\epsilon_1, p_3) \\
& \quad \times \left(-\delta_{j_4}^{i_1} \delta_{j_3}^{i_2} \delta_{j_1}^{i_3} \delta_{j_2}^{i_4} - \delta_{j_3}^{i_1} \delta_{j_4}^{i_2} \delta_{j_2}^{i_3} \delta_{j_1}^{i_4} + \delta_{j_4}^{i_1} \delta_{j_1}^{i_2} \delta_{j_2}^{i_3} \delta_{j_3}^{i_4} + \delta_{j_2}^{i_1} \delta_{j_3}^{i_2} \delta_{j_4}^{i_3} \delta_{j_1}^{i_4} \right)
\end{aligned} \tag{6.39}$$

The sum over the three expressions is equal to zero and therefore the Ward Identity is fulfilled for every given color flow. We do not regard the amplitude of the contact-vertex because as a result of the Lorentz structure this amplitude does not contribute to the Ward Identity, as we have seen in section 6.1.2.

6.2.2 Calculation of the $2 \rightarrow 2$ cross sections with O'Mega

To check the implementation of the model into O'Mega, we want to calculate the $2 \rightarrow 2$ cross section shown in Fig. 6.1 and 6.2 using O'Mega. On one hand we can verify the validity of the Ward Identity on the basis of $2 \rightarrow 2$ cross sections and on the other hand it allows us to compare the results of O'Mega with those of FormCalc. This is in particular helpful by checking the correct implementation of the quartic coupling of the gluons to the sgluinos, since this vertex does not contribute to the Ward Identity as shown above. Since the explicit implementation is discussed in App. D, in this section we will only explain how to calculate $2 \rightarrow 2$ cross sections with O'Mega in principle.

O'Mega produces a fortran code of the scattering amplitudes. To calculate the cross section, we need the square of the absolute value of the scattering amplitude first. Therefore we have to perform the sum over the polarizations and color flows. The sum over the polarization is performed easily, since O'Mega provides tools for this. However, the sum over color will not be done automatically. For this, we have to know which different color flows exist for a $2 \rightarrow 2$ cross section, where the incoming and outgoing particles are in the bifundamental color flow representation. The six possible color flows are shown in Fig. 6.18. The indices $i_1, j_1, \dots, i_4, j_4$ are the indices of the bifundamental representation of the particles. The subscript $k = 1, 2$ of i_k and j_k denotes the incoming particles and $k = 3, 4$ the outgoing particles. Since in

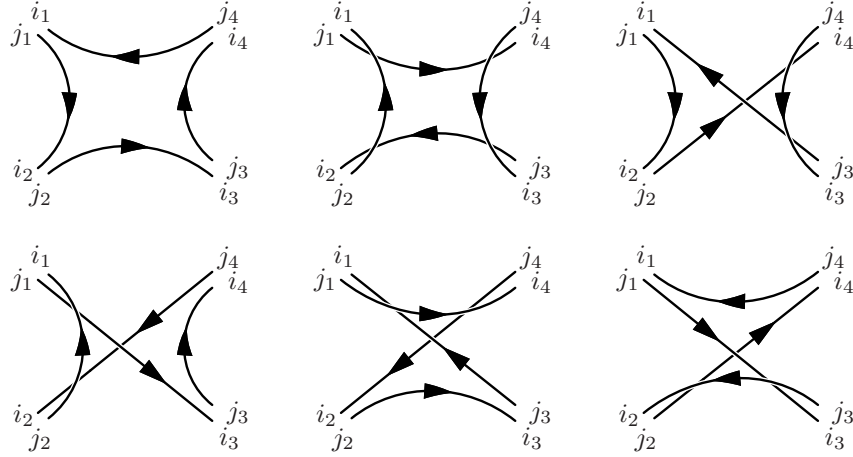


Figure 6.18: Six different color flows for a $2 \rightarrow 2$ cross section, where the initial and final particles are in the bifundamental color flow representation.

O’Mega the colored particles are not declared by the bifundamental indices of the particles but through the possible color flows $c1, c2, c3, c4, \dots$ we rewrite the bifundamental indices to the possible color flows as shown in Fig. 6.19. Note that in the case of the color flows the subscripts 1, 2, 3, 4 are no longer connected to the particles but are chosen arbitrarily. The amplitudes of the six color flows would then schematically look like

$$\begin{aligned}
 &\text{particle1}(c4, c1) \text{ particle2}(c1, c2) \rightarrow \text{particle3}(c3, c2) \text{ particle4}(c4, c3) \\
 &\text{particle1}(c1, c2) \text{ particle2}(c4, c1) \rightarrow \text{particle3}(c4, c3) \text{ particle4}(c3, c2) \\
 &\dots
 \end{aligned} \tag{6.40}$$

When squaring the whole amplitude we have to attend that the square of equal color flow amplitudes gets a symmetry factor $1/N^4$ and the square of unequal color amplitudes gets a symmetry factor $1/N^2$ [17]. N is the dimension of the fundamental representation of the $SU(N)$ gauge group. Now we are ready to calculate the square of the absolute value of the scattering amplitude, which is managed by a short fortran program.

In the scattering amplitudes, the momenta of the incoming and outgoing particles appear. To plot the differential cross section against the center of mass energy of the incoming particles and the polar angle θ we use `oplotter` a “FRIENDLY O’MEGA PLOTTING TOOL”, created by Christian Speckner [18]. From the center of mass energy, the polar and azimuthal angle it calculates the momenta of the outgoing particles in the rest frame and multiplies the square of the scattering amplitude with the phase space factor for a $2 \rightarrow 2$ process. Plotting the results we find that they agree with the results of FormCalc.

6.2.3 Results of Monte Carlo simulations

In this section we want to discuss the results of the Monte Carlo simulation. As mentioned before we only perform Monte Carlo simulations of $2 \rightarrow 4$ cross sections, where either heavy gluons or sgluinos are in the intermediate state. The diagrams we use for the Monte Carlo simulation are shown in Fig. 6.9, 6.10 and 6.11. Since we want to study the contributions of $2 \rightarrow 4$ cross sections, where two heavy gluons and two sgluinos, respectively, are produced in the intermediate state (see Fig. 6.9) we have to introduce suitable phase space cuts. Therefore we restrict the invariant mass of the two quark-antiquark pairs to the mass of the decaying particles we want to measure. The invariant mass is defined by

$$m_{q\bar{q}} = \sqrt{(p_q + p_{\bar{q}})^2} \tag{6.41}$$

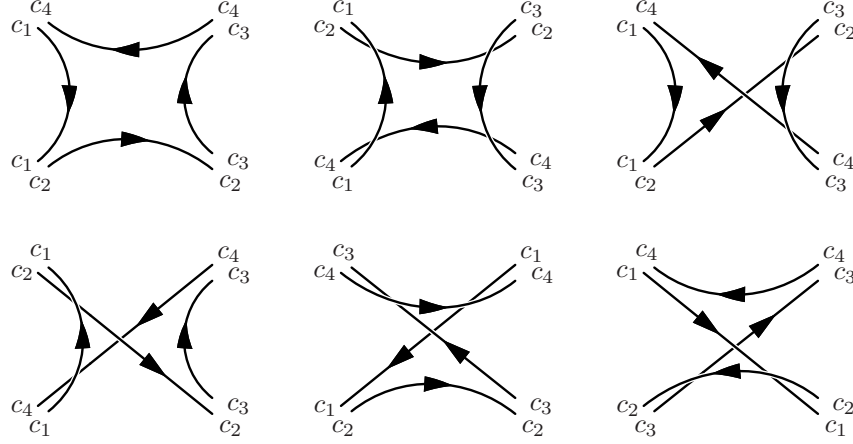


Figure 6.19: Six different color flows for a $2 \rightarrow 2$ cross section, where the bifundamental representation of the particles is denoted by their color flows.

	CUT1	CUT2
$m_{b\bar{b}} / \text{GeV}$	[1000, 2000]	[1410, 1430]
$m_{t\bar{t}} / \text{GeV}$	[1000, 2000]	[1410, 1430]

Table 6.3: Phase space cuts for the Monte Carlo simulation of the partonic $2 \rightarrow 4$ cross section with a bottom anti-bottom and a top anti-top pair in the final state.

where p_q and $p_{\bar{q}}$ are the momenta of the quark and anti-quark, respectively. Since the heavy gluon and the sgluino have a decay width, we cannot choose the invariant mass exactly to the mass of the decaying particle. Rather we have to select a sufficiently large phase space range to respect all contributions from the double resonant decay processes (see Fig. 6.9). The form of the peak in the invariant mass spectrum corresponds to a Lorentz distribution. Thus we use a phase space range which is six times the width of the decaying particle. In the case of the heavy gluon ($\Gamma = 155.93 \text{ GeV}$), we choose the invariant mass of the quark anti-quark pairs between 1000 GeV and 2000 GeV and in the case of the sgluino ($\Gamma = 0.598 \text{ GeV}$) between 1410 GeV and 1430 GeV. We will denote these phase space cuts as CUT1 and CUT2, respectively. Because the sgluino has such a tiny width, we can choose the phase space cuts much larger than six times the decay width without being at risk to take too large contributions of the single resonant processes shown in Fig. 6.10 into account. For the Monte Carlo simulation we choose the final state to a bottom anti-bottom and top anti-top pair. At this moment the choice of the final state is arbitrary, it will be important when we discuss LHC observables. To produce the plots shown in Fig. 6.20, 6.21, 6.22 and 6.23, the Monte Carlo creates 500000 events and we use a center of mass energy $\sqrt{S} = 4000 \text{ GeV}$. All the phase space cuts we use in this section are listed in Tab. 6.3.

The results of the Monte Carlo simulation for two heavy gluons in the intermediate state are shown in Fig. 6.20 and 6.21. These plots display the events depending on the invariant mass of the top anti-top pair and the absolute value of $\text{Cos}(\theta)$ of the top quark. As we would expect, we find that the peak in Fig. 6.20 is at the mass of the heavy gluon 1420.85 GeV and the width of the peak corresponds to the width of the decaying particle, which is valued 155.93 GeV. The result of the total cross section, calculated from Whizard, is

$$\sigma_{g_1 g_1}(gg \rightarrow b\bar{b}t\bar{t}) = (8816 \pm 16) \text{ fb}. \quad (6.42)$$

In the case of the two sgluinos we find the same behavior. The results of the Monte Carlo simulations are

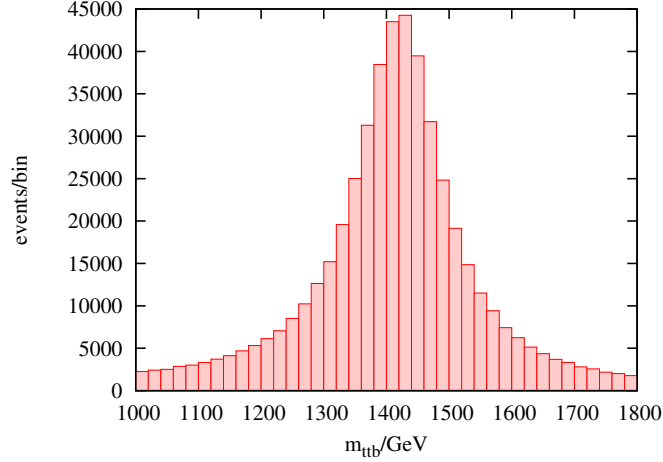


Figure 6.20: Invariant mass of a top anti-top pair with two heavy gluons in the intermediate state ($N_{\text{tot}} = 500000$ and for the phase space cut we use CUT1).

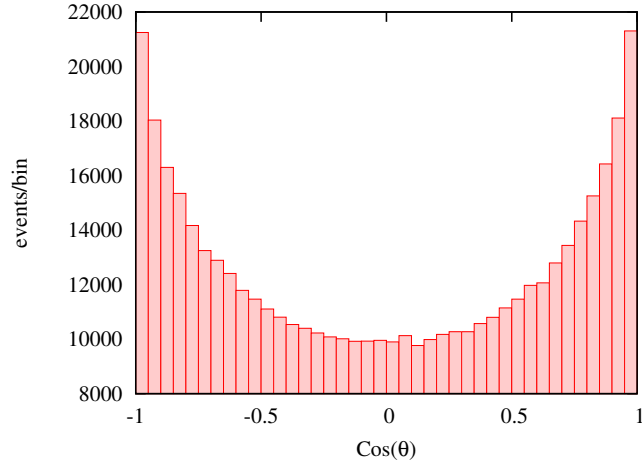


Figure 6.21: Absolute value of $\text{Cos}(\theta)$ for the top quark with two heavy gluons in the intermediate state ($N_{\text{tot}} = 500000$ and for the phase space cut we use CUT1).

shown in Fig. 6.22 and 6.23, where again the events depending on the invariant mass of the top anti-top pair and the absolute value of $\text{Cos}(\theta)$ of the top quark are shown. The peak is located at the same position as in the case of the heavy gluon, since the mass of the sgluino is equal to the mass of the heavy gluon and again the width of the peak corresponds to the width of the sgluino, which is 0.598 GeV. In this case the value of the total cross section sums up to

$$\sigma_{\Sigma\Sigma}(gg \rightarrow b\bar{b}t\bar{t}) = (1.594 \pm 0.002) \text{ fb} . \quad (6.43)$$

The huge difference of the total cross sections $\sigma_{g_1 g_1}$ and $\sigma_{\Sigma\Sigma}$ stems from the fact that on one hand the sgluinos couple considerably less to the bottoms than to the tops (see Tab. 5.4 and 5.5) and on the other hand the gluon induced $2 \rightarrow 2$ production of a sgluino pair is two orders of magnitude smaller than the $2 \rightarrow 2$ heavy gluon production (see Sec. 6.1.2).

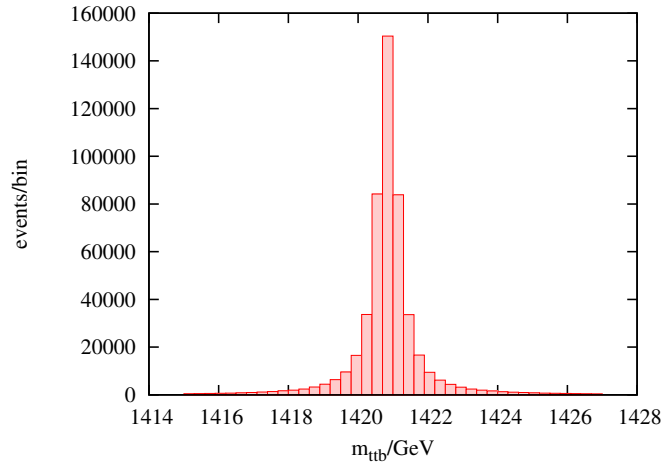


Figure 6.22: Invariant mass of a top anti-top pair with two sgluinos in the intermediate state ($N_{\text{tot}} = 500000$ and for the phase space cut we use CUT2).

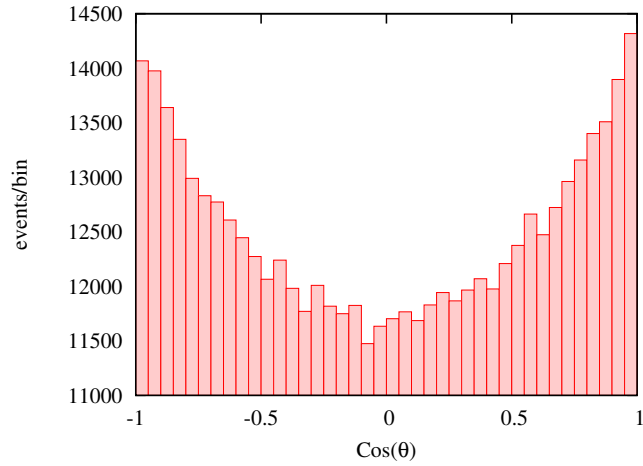


Figure 6.23: Absolute value of $\text{Cos}(\theta)$ for the top quark with two sgluinos in the intermediate state ($N_{\text{tot}} = 500000$ and for the phase space cut we use CUT2).

6.3 Narrow width vs. Monte Carlo simulation

In this section we want to compare the narrow width approximation with the results of the Monte Carlo simulation. To do this, we have to translate the events produced from the Monte Carlo simulation into the unit barn. Therefore we use the value of the total cross section, calculated by Whizard, and relate it to the contents of the histogram

$$\sigma_{\text{tot}} = \int \frac{d\sigma}{d\Phi} d\Phi \approx \sum_i \frac{\Delta\sigma_i}{\Delta\Phi_i} \Delta\Phi_i \quad (6.44)$$

The index i sums over all bins. Since all $\Delta\Phi_i$ are of the same size, we can write

$$\frac{\sigma_{\text{tot}}}{N} \sum_i N_i = \Delta\Phi \sum_i \frac{\Delta\sigma_i}{\Delta\Phi}, \quad (6.45)$$

where N is the total number of events and N_i are the events per bin. From this it follows that

$$\frac{\Delta\sigma_i}{\Delta\Phi} = \frac{\sigma_{\text{tot}}}{N\Delta\Phi} N_i. \quad (6.46)$$

For $N \rightarrow \infty$ the Monte Carlo simulation becomes the analytical calculation of the tree level $2 \rightarrow 4$ cross section.

First we want to compare the total cross sections from the NWA with the Monte Carlo simulation. The calculation of the total $2 \rightarrow 2$ cross sections for the NWA was done with `oplotter` and the values are

$$\begin{aligned} \sigma_{gg \rightarrow g_1 g_1} &= 22698 \text{ fb} \\ \sigma_{gg \rightarrow \Sigma\Sigma} &= 378.40 \text{ fb} \end{aligned} \quad (6.47)$$

As discussed in Sec. 6.1.1, we have to multiply the $2 \rightarrow 2$ cross section with the branching ratios of the decays. They are listed in Tab. 6.4. Moreover we have to multiply the $2 \rightarrow 2$ cross sections with a factor 2, which originates from the identical particles in the intermediate state. The total $2 \rightarrow 4$ cross sections for two heavy gluons then is

$$\sigma_{\text{NWA}, g_1 g_1}(gg \rightarrow b\bar{b}t\bar{t}) = 2 \text{BR}(g_1 \rightarrow b\bar{b}) \text{BR}(g_1 \rightarrow t\bar{t}) \sigma_{gg \rightarrow g_1 g_1} = 9569 \text{ fb} \quad (6.48)$$

Comparing this result with the result of the Monte Carlo simulation (6.42), we find that the total cross section of the Monte Carlo simulation is 10% smaller than the total cross section of the narrow width approximation. This stems from destructive interferences of the single resonant diagrams (see Fig. 6.10), which we cannot totally exclude by the phase space cut CUT1.

In the case of the sgluino we get for the narrow width approximation

$$\sigma_{\text{NWA}, \Sigma\Sigma}(gg \rightarrow b\bar{b}t\bar{t}) = 2 \text{BR}(\Sigma \rightarrow b\bar{b}) \text{BR}(\Sigma \rightarrow t\bar{t}) \sigma_{gg \rightarrow \Sigma\Sigma} = 1.586 \text{ fb}. \quad (6.49)$$

Comparing this result with the result of the Monte Carlo simulation (6.43), we find that the narrow width approximation deviates only by 0.05%. As we had expected, the narrow width approximation works very well in the case of the sgluino.

Next we want to compare the angular distributions shown in Fig. 6.24 and 6.25. Fig. 6.24 and 6.25 display the $\text{Cos}(\theta)$ dependence of the top quark of the final state. Note that in the case of the narrow width approximation we assume this to be the same as the decaying particle. Thus we actually plotted the $\text{Cos}(\theta)$ dependence of the heavy gluon (6.11) and sgluino (6.12), respectively. We find that in the narrow width approximation the forward and backward scattering contributes much more than in the case of the Monte Carlo simulation and is smaller for $\pi/2$ scattering. This stems from the fact that in the narrow width approximation we only consider top quarks, which move exactly in the same direction as the decaying

$\text{BR}(g_1 \rightarrow b\bar{b})$	0.31
$\text{BR}(g_1 \rightarrow t\bar{t})$	0.68
$\text{BR}(\Sigma \rightarrow b\bar{b})$	0.0021
$\text{BR}(\Sigma \rightarrow t\bar{t})$	0.998

Table 6.4: Branching ratios for the decay of the heavy gluon and sgluino, respectively into tops and bottoms.

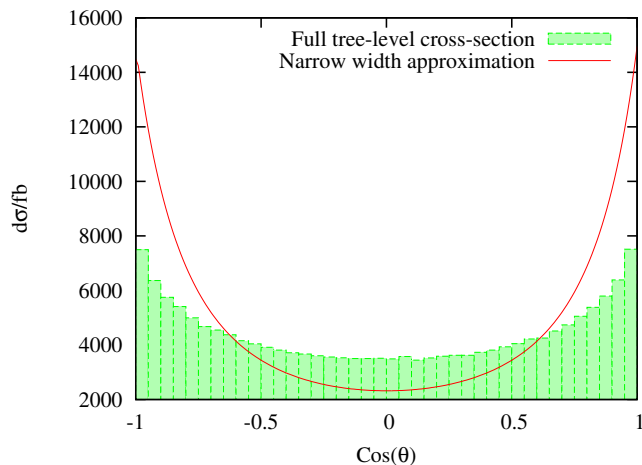


Figure 6.24: Comparison of the narrow width approximation with the full tree level cross section for the decay of two heavy gluons into two tops and two bottoms. The $\text{Cos}(\theta)$ dependence of the final state top quark is plotted, where we assume that in the case of the narrow width approximation the top quark has the same $\text{Cos}(\theta)$ dependence as the heavy gluon in the $2 \rightarrow 2$ cross section.

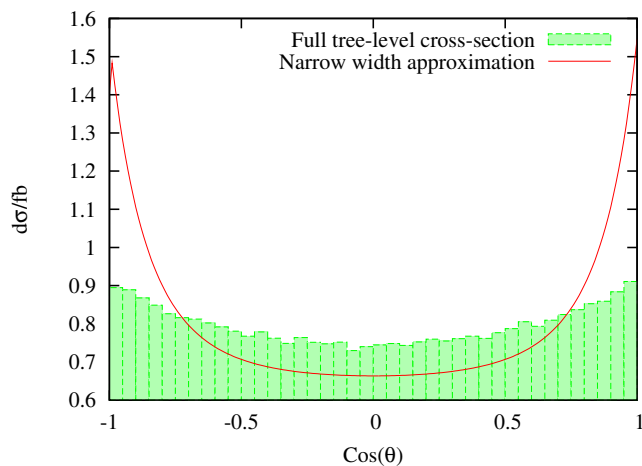


Figure 6.25: Comparison of the narrow width approximation with the full tree level cross section for the decay of two sgluinos into two tops and two bottoms. The $\text{Cos}(\theta)$ dependence of the final state top quark is plotted, where we assume that in the case of the narrow width approximation the top quark has the same $\text{Cos}(\theta)$ dependence as the sgluino of the $2 \rightarrow 2$ cross section.

particle. Thus the Lorentz factor $\beta \approx 0.7$ discussed in Sec. 6.1.1 is not sufficiently large to justify the assumption that the quarks almost exclusively decay in the direction of the heavy gluon or sgluino, respectively.

To get a better approximation we regard the decay probability f depending on θ_1 , φ_1 , θ and φ and convolve it with the $2 \rightarrow 2$ cross section (see Fig. 6.26)

$$\int d\sigma(\theta_1) f(\theta_1, \varphi_1, \theta, \varphi) \text{Sin}(\theta_1) d\theta_1 d\varphi_1. \quad (6.50)$$

θ and φ denote the coordinates of the observer and thus we can set the azimuthal angle φ to zero without loss of generality. Since the decay of the intermediate particle only depends on ϵ , it suffices to know the probability distribution depending on this parameter. Therefore we express ϵ in terms of θ_1 , φ_1 and θ

$$\text{Cos}(\epsilon) = \text{Sin}(\theta_1)\text{Cos}(\varphi_1)\text{Sin}(\theta) + \text{Cos}(\theta_1)\text{Cos}(\theta) \quad (6.51)$$

and the remaining task is the calculation of the decay probability with respect to $\text{Cos}(\epsilon)$. To get there we start with the isotropic decay probability in the rest frame and boost it to the laboratory system. Let $h(x) = \tilde{x}$ the coordinate transformation from x to be \tilde{x} . The transformed probability distribution f then reads

$$f(\tilde{x}) = \frac{dh(\tilde{x})^{-1}}{d\tilde{x}} = (h^{-1})' \quad (6.52)$$

The coordinate transformation of ϵ is given by [19]

$$\text{Cos}(\epsilon) = \frac{\text{Cos}(\epsilon') + \beta}{1 + \beta \text{Cos}(\epsilon')}, \quad (6.53)$$

where ϵ' is the coordinate in the rest frame and β is the Lorentz factor. The inverse transformation then reads

$$\text{Cos}(\epsilon') = \frac{-\text{Cos}(\epsilon) + \beta}{-1 + \beta \text{Cos}(\epsilon)} \quad (6.54)$$

and with (6.52) we obtain the following probability distribution

$$f(\text{Cos}(\epsilon)) = \frac{N}{1 + \beta \text{Cos}(\epsilon)} \left(1 + \frac{\beta(\beta - \text{Cos}(\epsilon))}{\beta \text{Cos}(\epsilon) - 1} \right) \quad (6.55)$$

N is the normalization constant, which makes sure that the probability remains conserved after the convolution. The associated normalization condition is $\int f(\epsilon) d\epsilon = 1$. When we convolve the above probability distribution with the $2 \rightarrow 2$ cross section, we get the $\text{Cos}(\theta)$ dependence shown in Fig. 6.27 and 6.28.

The convolved narrow width approximation fits the Monte Carlo simulation much better and in the case of the sgluino it is almost identical. For the coordinate transformation we used a Lorentz factor $\beta = 0.71$. For the calculation of β we make use of (6.3) and (6.5) and set the mass of the heavy gluon and sgluino $m_{g_1} = m_\Sigma = 1420.85 \text{ GeV}$.

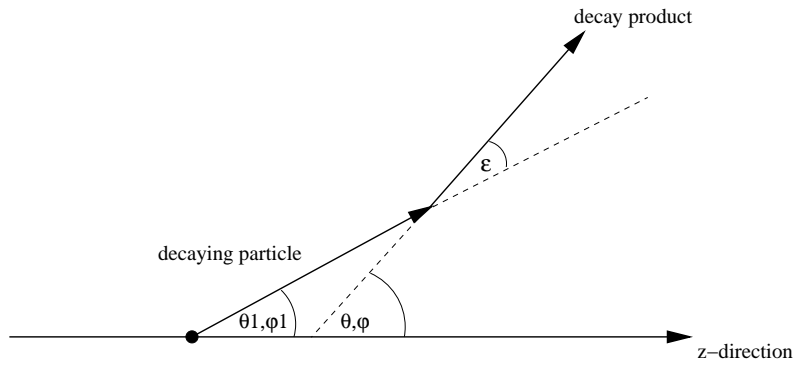


Figure 6.26: Angular dependence of the decay in the laboratory system.

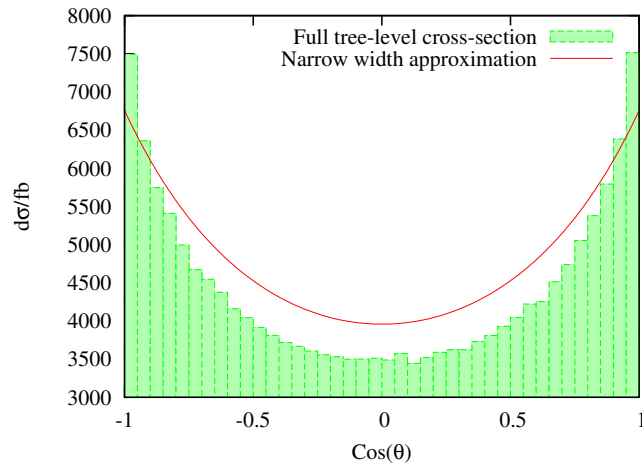


Figure 6.27: Comparison of the improved narrow width approximation with the full tree level cross section for the decay of two heavy gluons in two tops and two bottoms. Here is the $\text{Cos}(\theta)$ dependence of the top quark plotted.

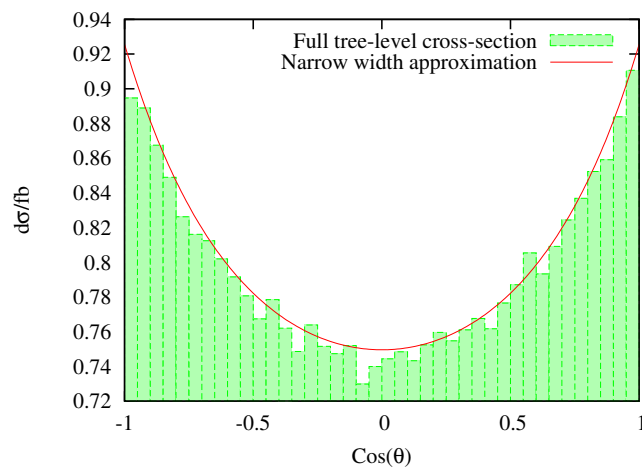


Figure 6.28: Comparison of the improved narrow width approximation with the full tree level cross section for the decay of two sgluinos in two tops and two bottoms. Here is the $\text{Cos}(\theta)$ dependence of the top quark plotted.

Chapter 7

Hadronic cross sections and LHC Distributions

In this chapter we want to derive theoretical predictions for future measurements at the LHC. In the last chapter we have calculated cross sections of the incoming gluons with fixed momenta. As a consequence of confinement, gluons and quarks cannot be observed as asymptotic particles, but only as constituents of hadrons. Observables of parton interactions can therefore not be measured directly by parton collisions, but indirectly by hadron collider experiments. To make theoretical predictions it is necessary to relate the interactions at the parton level to the interactions of the hadron level. Thus in the first part of the chapter we will give a short introduction to the parton model. In the second part we will discuss possible observables to measure sgluinos and heavy gluons at the LHC.

7.1 Factorization and the Parton Model of QCD

The parton model describes the interactions of hadrons in high energy collisions. If the energy scale of the collider experiment is sufficiently large (≥ 10 GeV), the partons can be treated as non-interacting constituents of the proton. This means that the partons of one hadron do not interact with each other within the time scale of the hadronic collision. A parton with momentum p^μ is given by

$$p^\mu = xP^\mu, \quad (7.1)$$

where P^μ is the momentum of the hadron and $x \in]0, 1[$. The probability for a parton with momentum p^μ is given by the parton distribution function (PDF), which depends on x and the factorization scale μ . The form of the parton distribution has to be measured, since it is a result of low-energy physics, where

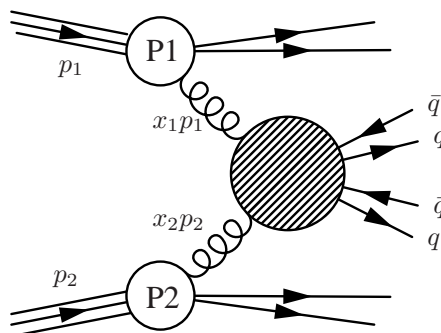


Figure 7.1: Hadronic cross section for the gluon induced production of two quark antiquark pairs.

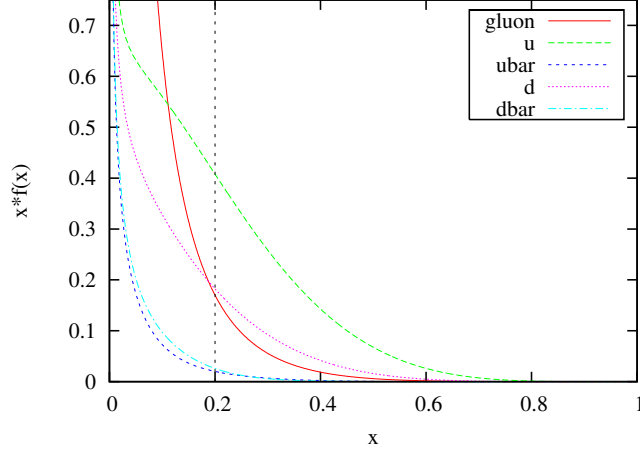


Figure 7.2: Parton distribution of the CTEQ5M series for the gluon and up and down quarks. The factorization scale is $\mu = 3000$ GeV. The black dashed line denotes a parton energy of 1400 GeV, if the proton has an energy of 7 TeV.

QCD becomes strongly interacting and perturbation theory breaks down. The factorization scale is a free parameter and should be chosen close to the energy scale of the collision. The parton distributions of the gluons, up and down quarks for $\mu = 3000$ GeV are plotted in Fig. 7.2.

The total energy at the LHC is 14 TeV, which means that each proton has an energy of 7 TeV. To produce the heavy gluon and sgluino on-shell, each of the gluons must have an energy of 1500 GeV. For a proton energy of 7 TeV this corresponds to $x \approx 0.2$ (see Fig. 7.2). We find that the probability for two gluons with an energy of 1500 GeV is sufficiently large to justify the examination of gluon induced processes. The probability for an up and an anti-up or a down and an anti-down at $x = 0.2$ is also large, but the quark induced production of heavy gluons and sgluinos is strongly suppressed, since the coupling of the up quarks to the heavy gluon and the sgluino is very small. The only quarks that couple strongly to the heavy gluon and the sgluino are the bottom and the top quark, but processes induced by them can be excluded by the parton distribution.

The proton collision with the gluon induced production of two quark-antiquark pairs is diagrammatically shown in Fig. 7.1. p_1 and p_2 are the momenta of the colliding protons. The hadronic differential cross section then reads

$$d\sigma(P_1, P_2) = \int_0^1 \int_0^1 dx_1 dx_2 f(x_1, \mu) f(x_2, \mu) d\sigma(x_1 P_1, x_2 P_2), \quad (7.2)$$

where f are the parton distribution functions.

7.2 LHC observables

Now we have to think about observables that can be measured at the LHC and which are sensitive to the physics of the sgluino and heavy gluon that are predicted by our model. Therefore we examine the full hadronic $2 \rightarrow 4$ cross section with two quark anti-quark pairs in the final state (see Fig. 7.1). We only neglect the processes that contain schargino and sneutrino contributions (see Fig. 6.13), because the implementation of the vertices in O'Mega would be extremely time-consuming but the corresponding processes only lead to small contributions, since the schargino and sneutrino weakly interact. On the

	CUT3	CUT4	CUT5
$\text{Cos}(\theta_b)$	$[-0.98, 0.98]$	$[-0.98, 0.98]$	$[-0.98, 0.98]$
$\text{Cos}(\theta_{\bar{b}})$	$[-0.98, 0.98]$	$[-0.98, 0.98]$	$[-0.98, 0.98]$
$\text{Cos}(\theta_t)$	$[-0.98, 0.98]$	$[-0.98, 0.98]$	$[-0.98, 0.98]$
$\text{Cos}(\theta_{\bar{t}})$	$[-0.98, 0.98]$	$[-0.98, 0.98]$	$[-0.98, 0.98]$
$m_{b\bar{b}} / \text{GeV}$	$[1000, 2000]$	$[1200, 1250]$	$[1600, 1650]$
$m_{t\bar{t}} / \text{GeV}$	$[1000, 2000]$	$[1200, 1250]$	$[1600, 1650]$

Table 7.1: Phase space cuts for the Monte Carlo simulation of the hadronic $2 \rightarrow 4$ cross section with a bottom anti-bottom and a top anti-top pair in the final state.

basis of the $2 \rightarrow 4$ cross sections we study the invariant mass of a quark-antiquark pair and furthermore the dependence on the polar angle of the outgoing particles. The heavy gluon and the sgluino decays almost exclusively in top anti-top pairs, but the experimental analysis of four-top final states is very complicated. This stems from the fact that the top decays directly in a bottom quark and a W -Boson, which decay further into standard model particles we can measure at the detector and neutrinos. To simplify the analysis we restrict ourselves to a bottom anti-bottom top anti-top final state. We will see that the number of events is still large enough. Moreover the lifetime of the bottoms is sufficiently long, so that its further decay is out of the collision region. This can be resolved at the detector and thus the bottom quark can be identified, which helps the analysis eminently.

To filter the processes where two heavy gluons or two sgluinos, respectively, are produced in the intermediate state we restrict the invariant mass of the top anti-top and bottom anti-bottom pair to be between 1000 GeV and 2000 GeV. Since the detector is not sensitive to forward and backward scattering, we also bound $\text{Cos}(\theta)$ of each outgoing particle to be between -0.98 and 0.98 . This phase space cut is denoted by CUT3. All the phase space cuts we use in this section are listed in Tab. 7.1. Furthermore we use a parton distribution with a dynamical factorization scale. This means that the Monte Carlo generator uses for every event the parton distribution with the factorization scale which corresponds to the center of mass energy of the event. Furthermore we use an integrated luminosity of $\int \mathcal{L} = 100 \text{ fb}^{-1}$, since this integrated luminosity will definitely be reached at the LHC. The luminosity is a value to characterize the performance of an accelerator and the integrated luminosity is the integral of the luminosity with respect to time. For a given integrated luminosity the total number of events N_{tot} can be calculated as follows

$$N_{\text{tot}} = \sigma_{\text{tot}} \times \int \mathcal{L} \quad (7.3)$$

With an integrated luminosity of 100 fb^{-1} and the phase space cuts given above, the Monte Carlo simulation calculates a total cross section of

$$\sigma_{\text{tot}} = (40.49 \pm 0.67) \text{ fb} \quad (7.4)$$

which corresponds to $N_{\text{tot}} = 4049$. If we make the same Monte Carlo simulation with the SM we obtain a total number of events which is less than 10. This is based on the fact that in the case of the SM $2 \rightarrow 4$ cross section the invariant mass of the bottom anti-bottom or top anti-top pair decreases above 20 GeV and 500 GeV, respectively, with $1/S$. Furthermore the SM contributions are strongly suppressed by the phase space cut CUT3 (see Tab. 7.1), where we restrict both invariant masses to be between 1000 GeV and 2000 GeV. Thus we can ignore standard model processes, but note that the results of our Monte Carlo simulation contain all higgsless SM contributions (see Fig. 6.12) as well. The invariant mass of the top anti-top pair and the $\text{Cos}(\theta)$ dependence are plotted in Fig. 7.3 and 7.4. As we would expect, we obtain a

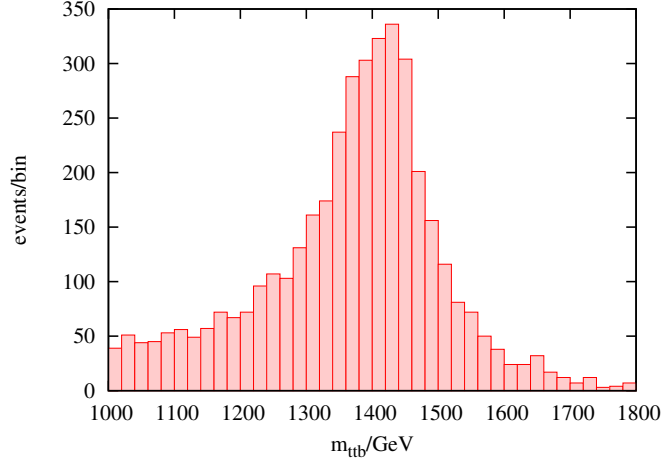


Figure 7.3: Invariant mass of a top anti-top pair for the gluon induced $2 \rightarrow 4$ cross section ($\int \mathcal{L} = 100 \text{ fb}^{-1}$). For the phase space cut we use CUT3 (see Tab. 7.1). CUT3 enhances the double resonant diagrams (see Fig. 6.9) and suppresses all single and non-resonant contributions shown in Fig. 6.10 and 6.11.

peak at the invariant mass of the heavy gluon and sgluino. The peak has a width of more than 100 GeV and thus it corresponds to the heavy gluon. Since the contribution of processes with two sgluinos in the intermediate state are considerably smaller than the processes with two heavy gluons in the intermediate state, we cannot resolve the sgluino in the invariant mass spectrum. But as mentioned in Sec. 5.2, we expect that the masses of the heavy gluon and the sgluino differ when we calculate the one-loop mass corrections. If the one-loop calculation generates a mass difference bigger than the width of the heavy gluon we would have the possibility to distinguish both particles in the invariant mass spectrum. In case that the sgluino gets a mass correction of ± 200 GeV, we perform a Monte Carlo simulation for $m_\Sigma = 1220.85$ GeV and $m_\Sigma = 1620.85$ GeV. Since the $2 \rightarrow 4$ contributions with two sgluinos in the intermediate state are very small, we take an integrated luminosity of $\int \mathcal{L} = 400 \text{ fb}^{-1}$. The results are shown in Fig. 7.5. We find that in the case of $m_\Sigma = 1220.85$ GeV we can resolve the sgluino in the invariant mass spectrum very well, but in the case of $m_\Sigma = 1620.85$ GeV this is much harder. This stems from the fact that the parton distribution of the gluons decreases with growing energy (see Fig. 7.2). For the phase space cuts we use CUT4 and CUT5 (see Tab. 7.1) for $m_\Sigma = 1220.85$ GeV and $m_\Sigma = 1620.85$ GeV, respectively. To resolve the sgluino in the invariant mass spectrum we have to study the SM and heavy gluon background. When we perform the Monte Carlo simulation for the SM contributions in the phase space range of CUT4 and CUT5 we get a total cross section, which is numerically equal to zero. The generated heavy gluon background for CUT4 and CUT5 is displayed in Fig. 7.5 by the shaded blocks. Note that the heavy gluon background contains all higgsless SM contributions as well. Furthermore the background is gauge invariant because we take all $SU(3)$ diagrams with massless gluons into account.

Finally we examine the $\text{Cos}(\theta)$ dependence of the final state top quark. As in the case of the invariant mass spectrum the $\text{Cos}(\theta)$ dependence of the top quark plotted in Fig. 7.4 arises from the decay of the heavy gluon.

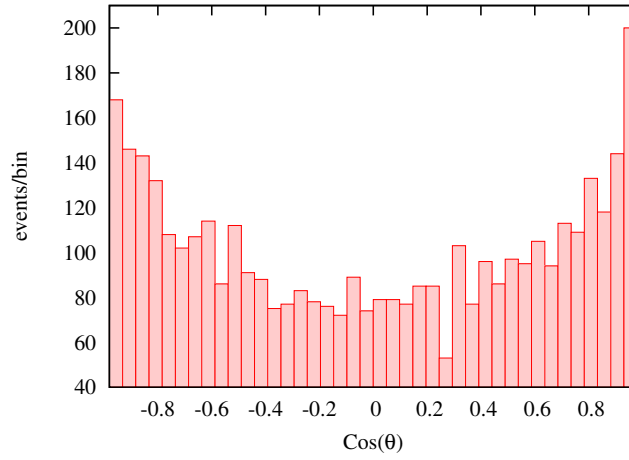


Figure 7.4: $\text{Cos}(\theta)$ dependence of the top quark for the gluon induced $2 \rightarrow 4$ cross section ($\int \mathcal{L} = 100 \text{ fb}^{-1}$). For the phase space cut we use CUT3 (see Tab. 7.1). CUT3 enhances the double resonant diagrams (see Fig. 6.9) and suppresses all single and non-resonant contributions shown in Fig. 6.10 and 6.11.

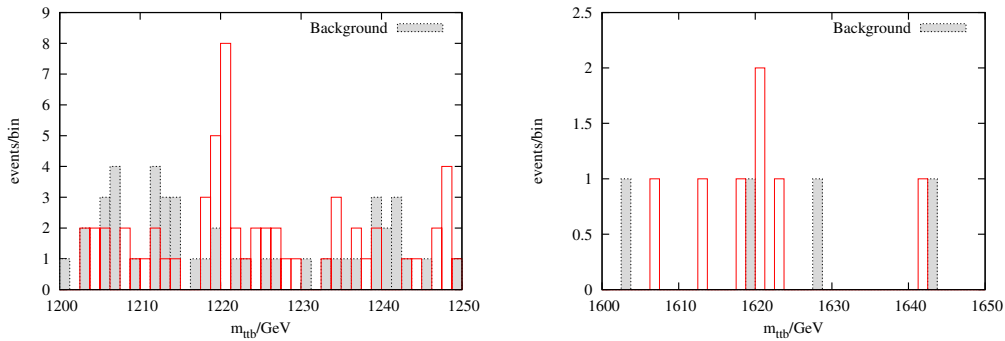


Figure 7.5: Invariant mass of a top anti-top pair for the gluon induced $2 \rightarrow 4$ cross section, where we put the mass of the sgluino to 1220 GeV or 1620 GeV, respectively ($\int \mathcal{L} = 400 \text{ fb}^{-1}$). For the phase space cuts we use CUT4 and CUT5, respectively (see Tab. 7.1). As in the case of CUT3, CUT4 and CUT5 enhance the double resonant diagrams (see Fig. 6.9) and suppress all single and non-resonant contributions shown in Fig. 6.10 and 6.11.

Chapter 8

Conclusions

In this work we have studied the LHC phenomenology of a warped higgsless supersymmetric 5D model introduced by Alexander Knochel and Thorsten Ohl [1]. Therefore we examined the characteristics of the heavy gluon and the sgluino, which are both part of the $SU(3)$ 5D SUSY gauge multiplet. For this purpose we first had to calculate the masses and the effective 4D couplings of the heavy gluon and the sgluino. We found that both particles have equal masses ($m = 1420.85$ GeV) and that they couple strongly to the bottom and in particular to the top quark. Next we have constructed the Feynman rules of the three- and four-point vertices of the gluon selfinteractions, the coupling to the quarks, and the coupling of the gluons to the sgluino.

To examine the characteristics we studied partonic $2 \rightarrow 4$ cross sections with gluons in the initial state and a bottom anti-bottom and top anti-top pair in the final state. For the calculation we first use the narrow width approximation and second a Monte Carlo simulation of the $2 \rightarrow 4$ process. Since for using the narrow width approximation we had to define fixed final states for the $2 \rightarrow 2$ cross section, we constrained the partonic $2 \rightarrow 4$ calculation to either heavy gluons or sgluinos in the intermediate state. This gave us the possibility to compare both methods. To calculate the narrow width approximation we implemented the model in FeynArts and FormCalc and for the Monte Carlo simulation we used O'Mega to create the Feynman amplitudes and Whizard to generate the Monte Carlo events. We find that the total cross sections of the narrow width approximation differ about 10% in the case of the heavy gluon and 0.05% in the case of the sgluino. The large coincidence of the Monte Carlo simulation with the narrow width approximation for sgluinos in the intermediate state stems from the fact that the sgluinos have the tiny width of $\Gamma = 0.598$ GeV. We also compared the $\text{Cos}(\theta)$ dependence of the final state top quark and we find that after the convolution of the narrow width approximation with the differential decay probability in the laboratory system both distributions fitted very well.

To make predictions for possible observables of the heavy gluon and sgluino at the LHC, we have performed Monte Carlo simulations of the hadronic $2 \rightarrow 4$ cross section. Therefore we had to convolve the $2 \rightarrow 4$ partonic cross section with the parton distribution functions of the protons. The total cross section of the $2 \rightarrow 4$ process is sufficiently large by using suitable phase space cuts, that we would detect the predicted particles in the runtime of the LHC. With an integrated luminosity of 100 fb^{-1} we would get more than 4000 events, where only about 10 are standard model induced. In the invariant mass spectrum of the top anti-top pair we find a peak at ~ 1420 GeV, which corresponds to the mass of the heavy gluon and sgluino. Since the width of the heavy gluon is 155.93 GeV and the processes with heavy gluons in the intermediate state contributes much more than the processes with sgluinos in the intermediate state, we cannot resolve the sgluino in the invariant mass spectrum. The same holds true for the $\text{Cos}(\theta)$ dependence. But we expect that the masses of the heavy gluon and the sgluino get sufficiently large one-loop corrections and this then would give us the possibility to resolve the sgluino in the invariant mass spectrum. Even when we could not resolve the sgluino, the results of the Monte Carlo simulation shows, that we would measure characteristics of the predicted model, if it proves well-founded.

Appendix A

Notation and Conventions

We use the metric convention

$$g_{MN} = \begin{pmatrix} 1 & 0 & 0 & 0 & 0 \\ 0 & -1 & 0 & 0 & 0 \\ 0 & 0 & -1 & 0 & 0 \\ 0 & 0 & 0 & -1 & 0 \\ 0 & 0 & 0 & 0 & -1 \end{pmatrix} \quad (\text{A.1})$$

and

$$\gamma^\mu = \begin{pmatrix} 0 & \sigma^\mu \\ \bar{\sigma}^\mu & 0 \end{pmatrix} \quad \gamma^5 = \begin{pmatrix} i & 0 \\ 0 & -i \end{pmatrix}, \quad (\text{A.2})$$

where $\sigma^0 = \bar{\sigma}^0 = -\mathbf{1}_2$ and $-\bar{\sigma}^i = \sigma^i$ are the Pauli matrices. For the Dirac spinors we write

$$\Psi = \begin{pmatrix} \eta_\alpha \\ \bar{\chi}^{\dot{\alpha}} \end{pmatrix}; \quad \bar{\Psi} = \Psi^\dagger \gamma^0 = \begin{pmatrix} \chi^\alpha \\ \bar{\eta}_{\dot{\alpha}} \end{pmatrix} \quad (\text{A.3})$$

The 5D Lorentz transformations of the fermions are given by

$$\Psi \rightarrow e^{-\frac{i}{4} \omega_{MN} \Lambda^{MN}} \Psi \quad (\text{A.4})$$

with the generators

$$\Lambda^{MN} = \frac{i}{2} [\gamma^M, \gamma^N] \quad (\text{A.5})$$

In theories with warped extra dimensions theories we use two coordinate systems. The *proper distance* coordinates and the *conformal* coordinates. The proper distance coordinates have $x^M = (x^\mu, y)$ with $y \in [0, \pi]$ and are related to the conformal coordinates $x^M = (x^\mu, z)$ with $z \in [1/k, 1/\Lambda_{\text{IR}}]$ through

$$z = k^{-1} e^{Rky}; \quad \Lambda_{\text{IR}} = k e^{Rk\pi} \quad (\text{A.6})$$

In proper distance coordinates the metric is

$$\hat{g}_{\mu\nu} = e^{-2Rky} g_{\mu\nu}$$

$$\begin{aligned}\hat{g}_{55} &= -R^2 g_{55} \\ \hat{g}_{\mu 5} &= 0\end{aligned}\tag{A.7}$$

and the γ -matrices then read

$$\begin{aligned}\hat{\gamma}^\mu &= -e^{Rky} \gamma^\mu \\ \hat{\gamma}^5 &= R^{-1} \gamma^5 \\ \hat{\gamma}_\mu &= \hat{g}_{\mu\nu} \hat{\gamma}^\nu \\ \hat{\gamma}_5 &= -R^2 \hat{\gamma}^5.\end{aligned}\tag{A.8}$$

In conformal coordinates the metric can be written as

$$\hat{g}_{MN} = \frac{1}{k^2 z^2} g_{MN}\tag{A.9}$$

and the γ -matrices are

$$\begin{aligned}\hat{\gamma}^M &= k z \gamma^M \\ \hat{\gamma}_M &= \hat{g}_{MN} \hat{\gamma}^N.\end{aligned}\tag{A.10}$$

For the γ -matrices we have

$$\{\hat{\gamma}^M, \hat{\gamma}^N\} = 2 \hat{g}^{MN}.\tag{A.11}$$

Appendix B

Parameters

In this appendix we list all the standard model parameters we needed for our calculations and we define all the standard model coupling constants, which were not discussed in Chap. 5. The couplings of the fermions to the photon, Z -Boson, W -Boson and massless gluon are the same as in the standard model. For the calculation we need the following parameters

$$\begin{aligned}m_W &= 80.403 \text{ GeV} \\m_Z &= 91.1876 \text{ GeV} \\G_F &= 1.16637 \text{ GeV}^{-2} \\ \alpha_S &= 0.1176\end{aligned}\tag{B.1}$$

where m_W and m_Z are the masses of the W - and Z -Boson, G_F is the Fermi coupling constant and α_S is the strong coupling constant. The Weinberg angle θ_W is given by the ratio of m_W and m_Z

$$\cos\theta_W = \frac{m_W}{m_Z}.\tag{B.2}$$

Now we are ready to calculate the electromagnetic coupling e , the weak coupling g_4 and the strong coupling g_{4C}

$$\begin{aligned}e &= 2 \sin\theta_W m_W \sqrt{\sqrt{2} G_F} \\g_4 &= \frac{e}{\sin\theta_W} \\g_{4C} &= \sqrt{4 \pi \alpha_S}\end{aligned}\tag{B.3}$$

We add the subscript 4 to the couplings, to illustrate that they are effective 4D couplings. The coupling of the up-type and down-type quarks to the photon then reads

$$\begin{aligned}g_{a,\text{up}} &= -\frac{2}{3}e \\g_{a,\text{down}} &= -\frac{1}{3}e\end{aligned}\tag{B.4}$$

and the W -Boson coupling is

$$g_{wq\bar{q}} = -\frac{g_4}{2}\tag{B.5}$$

The Z -Boson couples different to the left- and right-handed quarks

$$g_{z,\text{up}_L} = -\frac{g_4}{2\cos\theta_W}\left(1 - \frac{8}{3}\sin^2\theta_W\right)$$

$$\begin{aligned}
g_{z,\text{down}_L} &= -\frac{g_4}{2\cos\theta_W}\left(-1 + \frac{4}{3}\sin^2\theta_W\right) \\
g_{z,\text{up}_R} &= -\frac{g_4}{2\cos\theta_W} \\
g_{z,\text{down}_R} &= \frac{g_4}{2\cos\theta_W}
\end{aligned}
\tag{B.6}$$

Appendix C

Implementation of the Model in FeynArts

In order to calculate the narrow width approximation with FeynArts and FormCalc we have to create a file which includes all the particles and couplings of the model. Since we want to treat the massive gauge bosons in the unitarity gauge we define a new massive vector particle VV in `Lorentz.gen` with the following propagator

$$-\frac{i}{p^2 - m^2} \left(g^{\mu\nu} - \frac{p^\mu p^\nu}{m^2} \right). \quad (\text{C.1})$$

We implemented the entire model including all particles and couplings in FeynArts. But for vertices we would not need for the calculation of the narrow width approximation, we introduced dummy coupling constants instead of the explicit structure of the vertex. Thus we show only the part of the model file, which contains the full implementation. The model file is then given by

```
IndexRange[Index[Generation]] = Range[3];
IndexRange[Index[Colour]]      = NoUnfold[Range[3]];
IndexRange[Index[Gluon]]      = NoUnfold[Range[8]];
IndexRange[Index[KaluzaG]]    = Range[1]

M$ClassesDescription = {

(*-----
  FERMIONS
  -----*)

  (* Quarks (u): I_3 = +1/2, Q = +2/3 *)
  F[3] == {
    SelfConjugate -> False,
    Indices -> {Index[Generation], Index[Colour]},
    Mass -> MassQU,
    PropagatorLabel -> ComposedChar["u", Index[Generation]],
    PropagatorType -> Straight,
    PropagatorArrow -> Forward },

  (* Quarks (d): I_3 = -1/2, Q = -1/3 *)
  F[4] == {
    SelfConjugate -> False,
```

```

Indices -> {Index[Generation], Index[Colour]},
Mass -> MassQD,
PropagatorLabel -> ComposedChar["d", Index[Generation]],
PropagatorType -> Straight,
PropagatorArrow -> Forward },

(*-----
VECTORBOSONS
-----*)

(* Gluons: Q = 0 *)
V[5] == {
  SelfConjugate -> True,
  Indices -> {Index[Gluon]},
  Mass -> 0,
  PropagatorLabel -> ComposedChar["g"],
  PropagatorType -> Cycles,
  PropagatorArrow -> None },

VV[1] == {
  SelfConjugate -> True,
  Indices -> {Index[Gluon], Index[KaluzaG]},
  Mass -> MGluon,
  PropagatorLabel -> ComposedChar["g", "kk"Index[KaluzaG]],
  PropagatorType -> Cycles,
  PropagatorArrow -> None },

(*-----
SCALARS
-----*)

(* sGluino: Q = 0 *)
S[19] == {
  SelfConjugate -> True,
  Indices -> {Index[Gluon]},
  Mass -> MSGluino,
  PropagatorLabel ->
    ComposedChar["\\Sigma", " ", "SU(3)"],
  PropagatorType -> ScalarDash,
  PropagatorArrow -> None }
}

(* ----- Masses ----- *)

MassQU[1] = MassU;
MassQU[2] = MassC;
MassQU[3] = MassT;
MassQD[1] = MassD;
MassQD[2] = MassS;
MassQD[3] = MassB;
MassQU[gen_, _] = MassQU[gen];
MassQD[gen_, _] = MassQD[gen]

```


MSGluino[adjoint_] = MSGluino

M\$CouplingMatrices = {

(*-----
Couplings from the GAUGE SUPERFIELDS
-----*)

(* (1) SIGMA SIGMA GLUON *)
C[S[19,{ad1}],S[19,{ad2}],V[5,{ad3}]] ==
SUNF[ad1,ad2,ad3] g0EE {{1}},
C[S[19,{ad1}],S[19,{ad2}],VV[1,{ad3,k1}]] ==
SUNF[ad1,ad2,ad3] GluKEE[k1] {{1}},

(* (8) SIGMA SIGMA GLUON GLUON *)
C[S[19,{ad1}],S[19,{ad2}],V[5,{ad3}],V[5,{ad4}]] ==
- I g00EE (SUNF[ad1,ad3,ad4,ad2] + SUNF[ad2,ad3,ad4,ad1]) {{1}},
C[S[19,{ad1}],S[19,{ad2}],V[5,{ad3}],VV[1,{ad4,k1}]] ==
- I Glu2KEE[k1] (SUNF[ad1,ad3,ad4,ad2] + SUNF[ad2,ad3,ad4,ad1]) {{1}},
C[S[19,{ad1}],S[19,{ad2}],VV[1,{ad3,k1}],VV[1,{ad4,k2}]] ==
- I Glu2KKEE[k1,k2] (SUNF[ad1,ad3,ad4,ad2] + SUNF[ad2,ad3,ad4,ad1]) {{1}},

(*-----
Couplings from the INTERACTION WITH MATTER
-----*)

(* (12) FERMION FERMION GLUON *)
C[F[3,{g1,c1}],-F[3,{g2,c2}],V[5,{ad1}]] ==
I gUUG IndexDelta[g1,g2] SUNT[ad1,c1,c2] {{1},{1}},
C[F[3,{g1,c1}],-F[3,{g2,c2}],VV[1,{ad1,k1}]] ==
I IndexDelta[g1,g2] SUNT[ad1,c1,c2] {{UUGKKL[g1]},{UUGKKR[g1]}},
C[F[4,{g1,c1}],-F[4,{g2,c2}],V[5,{ad1}]] ==
I gDDG IndexDelta[g1,g2] SUNT[ad1,c1,c2] {{1},{1}},
C[F[4,{g1,c1}],-F[4,{g2,c2}],VV[1,{ad1,k1}]] ==
I IndexDelta[g1,g2] SUNT[ad1,c1,c2] {{DDGKKL[g1]},{DDGKKR[g1]}},

(* (14) FERMION FERMION SIGMA *)
C[F[3,{g1,c1}],-F[3,{g2,c2}],S[19,{ad1}]] ==
I IndexDelta[g1,g2] UUE[g2] SUNT[ad1,c1,c2] {{1},{1}},
C[F[4,{g1,c1}],-F[4,{g2,c2}],S[19,{ad1}]] ==
I IndexDelta[g1,g2] DDE[g2] SUNT[ad1,c1,c2] {{1},{1}},

(*-----
Couplings from the W_{\alpha} W_{\alpha} TERM
-----*)

(* (26) GLUON GLUON GLUON GLUON *)
C[V[5,{ad1}],V[5,{ad2}],V[5,{ad3}],V[5,{ad4}]] ==
- I g0000 * {{SUNF[ad1,ad3,ad2,ad4] - SUNF[ad1,ad4,ad3,ad2]},
{SUNF[ad1,ad2,ad3,ad4] + SUNF[ad1,ad4,ad3,ad2]},
{-SUNF[ad1,ad2,ad3,ad4] - SUNF[ad1,ad3,ad2,ad4]}}},

```

C[V[5,{ad1}],V[5,{ad2}],VV[1,{ad3,k1}],VV[1,{ad4,k2}]] ==
- I Glu4KK[k1,k2] *
  {{SUNF[ad1,ad3,ad2,ad4] - SUNF[ad1,ad4,ad3,ad2]},
  {SUNF[ad1,ad2,ad3,ad4] + SUNF[ad1,ad4,ad3,ad2]},
  {-SUNF[ad1,ad2,ad3,ad4] - SUNF[ad1,ad3,ad2,ad4]}}},

C[V[5,{ad1}],VV[1,{ad2,k1}],VV[1,{ad3,k2}],VV[1,{ad4,k3}]] ==
- I Glu4KKK[k1,k2,k3] *
  {{SUNF[ad1,ad3,ad2,ad4] - SUNF[ad1,ad4,ad3,ad2]},
  {SUNF[ad1,ad2,ad3,ad4] + SUNF[ad1,ad4,ad3,ad2]},
  {-SUNF[ad1,ad2,ad3,ad4] - SUNF[ad1,ad3,ad2,ad4]}}},

C[VV[1,{ad1,k1}],VV[1,{ad2,k2}],VV[1,{ad3,k3}],VV[1,{ad4,k4}]] ==
- I Glu4KKKK[k1,k2,k3,k4] *
  {{SUNF[ad1,ad3,ad2,ad4] - SUNF[ad1,ad4,ad3,ad2]},
  {SUNF[ad1,ad2,ad3,ad4] + SUNF[ad1,ad4,ad3,ad2]},
  {-SUNF[ad1,ad2,ad3,ad4] - SUNF[ad1,ad3,ad2,ad4]}}},

(* (27) GLUON GLUON GLUON *)
C[V[5,{ad1}],V[5,{ad2}],V[5,{ad3}]] ==
  SUNF[ad1,ad2,ad3] g000 {{1}},
C[V[5,{ad1}],VV[1,{ad2,k1}],VV[1,{ad3,k2}]] ==
  SUNF[ad1,ad2,ad3] Glu3KK[k1,k2] {{1}},
C[VV[1,{ad1,k1}],VV[1,{ad2,k2}],VV[1,{ad3,k3}]] ==
  SUNF[ad1,ad2,ad3] Glu3KKK[k1,k2,k3] {{1}}
}

```

Appendix D

Implementation of the Model in O’Mega

The purpose of this chapter is to give schematic directions how to implement a new model in O’Mega. Thus we do not explain the explicit structure of O’Mega but give only a short overview of how it works. In the paper of Mauro Moretti, Thorsten Ohl and Jürgen Reuter more details about the structure of O’Mega [16] can be found. O’Mega consists of a set of modules written in Objective Caml (Categorical Abstract Machine Language) and some FORTRAN support libraries. Objective Caml is the most popular variant of the Caml language developed since 1985 at INRIA by the Formel and Cristal teams. Further information is available from the ocaml homepage <http://caml.inria.fr/>. Most of the modules are of general nature and therefore model independent, so that the main part of the work for implementing a new model is creating the model file. To illustrate the implementation we declare sometimes only the signature and functionality of functions, to give a better understanding of the code and not to distract with programming details. Note that we only implemented the particles and couplings we need for the $2 \rightarrow 4$ cross section discussed in this thesis. A full implementation of the model is a subject of further study and is beyond the scope of this work. On compiling O’Mega, an executable `f90_nameofthemodel.opt` is generated for every model. Executing `f90_nameofthemodel.opt` then produces fortran code of the scattering amplitude. The input line for a $2 \rightarrow 2$ process would be look like this

```
./f90_nameofthemodel.opt -scatter "particle1_in particle2_in ->
particle1_out particle2_out" > scattering_amplitude.f90
```

where `scattering_amplitude.f90` is the output file which contains the fortran code of the scattering amplitude. To produce code compliant with the FORTRAN 90 standard we have to ensure that the identifiers of the particles, couplings, masses etc. are FORTRAN 90 compliant. To achieve this we have to define several functions. This is done at the end of this chapter.

Now we want to start with the implementation of the model in O’Mega. Therefore we have to create first a file `f90_nameofthemodel.ml` which contains the following code

```
module O = Omega.Make (Fusion.Mixed23) (Targets.Fortran) (ModelsX.Nameofthemodel)
let _ = O.main ()
```

This calls of a functor which maps three modules to one and subsequently calls the main code. Since the model files of all implemented models are denoted by `modelsX.ml`, where `x` is an integer, we will adopt this convention. Second we need a file `modelsX.mli` which contains

```
module Nameofthemodel : Model.T
```

Last we have to do add in `Makefile.src` in line 109

```
PROGRAMS_unreleased += f90_nameofthemodel
```

to ensure that the implemented model will be compiled. After this modifications in O’Mega we can apply ourselves to the creation of the model file `modelsX.ml`, which will be discussed below.

First we define some code which contains general information. `rcs_file` would be filled in by Subversion (SVN), which is a version control system.

```
let rcs_file = RCS.parse "warped5DSUSY" ["Warped_5D_Higgsless_SUSY_model"]
  { RCS.revision = "$Revision: alpha$"; RCS.date = "$Date: 07.01.08$";
    RCS.author = "$Author: Laslo_Reichert$";
    RCS.source = "$Source: /home/laslo/omega/src/models5.ml$" }
```

The next two lines are the Caml syntax for starting a module.

```
module Warped5Dsusy =
  struct
```

To save the trouble of prefixing all members of the O’Mega coupling library with “*Coupling.*” we make it available with

```
  open Coupling
```

The width of all particles is chosen timelike. This means that the width only appears in *S*-channel propagators.

```
  let width _ = Timelike
  let default_width = ref Timelike
```

`options` is a command line interface for changing the width treatment.

```
  let options = Options.create [
    "constant_width", Arg.Unit (fun _ → default_width := Constant),
    "use_constant_width_(also_in_t-channel)";
    "custom_width", Arg.String (fun x → default_width := Custom x),
    "use_custom_width";
    "cancel_widths", Arg.Unit (fun _ → default_width := Vanishing),
    "use_vanishing_width"]
```

Next we declare the indices we need to specify the particles we want to implement. `generation` is the index for the three generations in the standard model, `csign` differentiates between particle and anti-particle, `isospin` denotes the up and down type fermions, `color` the color flow index and `kkmode` is the Kaluza-Klein index.

```
  type generation = Gen0 | Gen1 | Gen2
  type csign = Pos | Neg
  type isospin = Iso_up | Iso_down
  type color = Q of int
  type kkmode = Kal0 | Kal1
```

Now we are ready to define the particle content. The Fermions are separated into two main classes, the quarks and leptons. Each of them have the indices we know from the standard model. The gauge bosons are the Photon *A*, the *W*-Boson *W*, the *Z*-Boson *Z*, the Gluon and its first Kaluza-Klein excitation *GluonKK*. Note that the Gluon is defined in the color flow representation and thus has two color indices. The color indices of the gluon are not the indices in the bifundamental representation but denote color flows. As discussed in 6.2.1 we have to introduce an auxiliary field *GluonAuxiliary*. Last we have to define the sgluino denoted by *Sigma* and for the same reason as in the case of the gluon, we have to introduce its auxiliary field *SigmaAuxiliary*.

```

type fermion =
  | Lepton of (csign × generation × isospin)
  | Quark of (csign × generation × isospin × color)

type gauge_boson =
  | A
  | W of csign
  | Z
  | GluonKK of (kkmode × color × color)
  | GluonAuxiliary of kkmode

type scalar =
  | Sigma of (color × color)
  | SigmaAuxiliary

```

The type *flavor* is required by the signature of O’Mega and contains of the three flavors *Fermion*, *Gauge_Boson* and *Scalar*

```

type flavor =
  | Fermion of fermion
  | Gauge_Boson of gauge_boson
  | Scalar of scalar

```

The functions *flavor_of_f*, *flavor_of_g* and *flavor_of_s* map a particle to the corresponding flavor type.

```

let flavor_of_f x = Fermion x
let flavor_of_g x = Gauge_Boson x
let flavor_of_s x = Scalar x

```

The functions *int_of_csign*, *int_of_gen* and *int_of_kk* map the types *csign*, *generation* and *kkmode* to integers

```

let int_of_csign = function Pos → 1 | Neg → -1
let int_of_gen = function Gen0 → 1 | Gen1 → 2 | Gen2 → 3
let int_of_kk = function Kal0 → 0 | Kal1 → 1

```

int_to_kk is the inverse function to *int_of_kk*

```

let int_to_kk = function
  0 → Kal0 | 1 → Kal1 | _ → failwith "int_to_kk: _invalid_argument"

```

The functions *fun_to_6tuple* and *fun_to_8tuple* apply a function *funs* to all members of an 6- and 8-tuple, respectively.

```

let fun_to_6tuple funs = function (c1, c2, c3, c4, c5, c6) →
  (funs c1, funs c2, funs c3, funs c4, funs c5, funs c6)

let fun_to_8tuple funs = function (c1, c2, c3, c4, c5, c6, c7, c8) →
  (funs c1, funs c2, funs c3, funs c4, funs c5, funs c6, funs c7, funs c8)

```

In the next part of the implementation we define essential functions and lists for the color implementation. The number of possible color flows n_{cf} for cross sections with gluons and quarks in the initial and final state is

$$n_{cf} = n_g + \frac{1}{2}n_q + \frac{1}{2}n_{\bar{q}}, \quad (D.1)$$

where n_g is the number of external gluons and n_q and $n_{\bar{q}}$ are the number of external quarks and anti-quarks, respectively. Thus in the case of two external gluons and four external quarks it is sufficient to set the maximal number of color flows nc to

```
let nc = 4
```

The type *col3* and *col4* we need later to define functions for permuting color flow indices.

```
type col3 = Col31 | Col32 | Col33
type col4 = Col41 | Col42 | Col43 | Col44
```

The function *nc_list* maps a integer to a list which contains all integers up to the given one (e.g. *nc_list* 4 = [1; 2; 3; 4])

```
let nc_list = ThoList.range 1 nc
```

The function *choose2* maps a list to the list of all ordered 2-tuples that can be built from its members (e.g. *choose2* [1; 2; 3] = [(1, 2); (1, 3); (2, 3)])

```
let choose2 set =
  List.map (function [x; y] → (x, y) | _ → failwith "choose2")
    (Combinatorics.choose 2 set)
```

inequ_pairs is a list of all possible 2-tuples, which can be created from *nc_list*. (e.g. for *nc_list* = [1; 2; 3] *inequ_pairs* reads [(1, 2); (1, 3); (2, 3); (2, 1); (3, 1); (3, 2)])

```
let inequ_pairs =
  choose2 nc_list @ choose2 (List.rev nc_list)
```

triple_col is a list of all ordered 3-tuples, which can be created from *nc_list* (e.g. for *nc_list* = [1; 2; 3; 4] *triple_col* reads [(1, 2, 3); (1, 2, 4); (1, 3, 4); (2, 3, 4)])

```
let triple_col =
  List.map (function [x; y; z] → (x, y, z) | _ →
    failwith "triple_col") (Combinatorics.choose 3 nc_list)
```

quartic_col is a list of all ordered 4-tuples, which can be created from *nc_list* (e.g. for *nc_list* = [1; 2; 3; 4] *quartic_col* reads [(1, 2, 3, 4)])

```
let quartic_col =
  List.map (function [r; s; t; u] → (r, s, t, u) | _ →
    failwith "quartic_col") (Combinatorics.choose 4 nc_list)
```

The function *color* returns the representation of the color group under which the particle transforms.

```
let color = function
| Fermion (Quark (Pos, _, _, _)) → Color.SUN 3
| Fermion (Quark (Neg, _, _, _)) → Color.SUN (-3)
| Gauge_Boson (GluonKK (_, _, _)) → Color.AdjSUN 3
| Scalar (Sigma (_, _)) → Color.AdjSUN 3
| _ → Color.Singlet
```

The function *colsymm* is implemented for future features of O'Mega and unused at the moment.

```
let colsymm = function
| Fermion f → begin match f with
| Quark (Pos, gen, Iso_down, _) → (int_of_gen gen, true), (0, false)
| Quark (Neg, gen, Iso_down, _) → (-(int_of_gen gen), true), (0, false)
| Quark (Pos, gen, Iso_up, _) → ((int_of_gen gen) + 3, true), (0, false)
| Quark (Neg, gen, Iso_up, _) → (-(int_of_gen gen) - 3, true), (0, false)
| _ → (0, false), (0, false)
end
| Gauge_Boson f → begin match f with
| GluonKK (Kal0, _, _) → (7, true), (0, false)
```

```

| GluonKK (Kal1, -, -) → (8,true), (0,false)
| GluonAuxiliary (Kal0) → (7,true), (7,true)
| GluonAuxiliary (Kal1) → (8,true), (8,true)
| - → (0,false), (0, false)
end
| Scalar f → begin match f with
| Sigma (-, -) → (9,true), (0,false)
| SigmaAuxiliary → (9,true), (9,true)
end

```

In the next part we discuss the implementation of the vertices. To implement the correct color structure we introduce several definitions, which are especially important for the implementation of the couplings of the gluons to the sgluinos and the gluon self-interactions. The implementation of these couplings will be therefore the main part of the following discussion. All other vertices are already implemented in other models in a very similar way and thus will be not discussed here in detail. To understand why we need these definitions we have to delve deeper into the inner working of O’Mega. From the definitions of the couplings in the model file, O’Mega obtains the information about the color and Lorentz structure. The coupling contains not the whole vertex structure but the minimal architecture which O’Mega needs to rebuild it. In the case of the four gluon vertex it means, that only the first term of the sum (see Fig. 6.14)

$$i \frac{g^2}{2} (2g^{\mu_1\mu_3} g^{\mu_2\mu_4} - g^{\mu_1\mu_2} g^{\mu_3\mu_4} - g^{\mu_1\mu_4} g^{\mu_2\mu_3}) \delta_{j_2}^{i_1} \delta_{j_3}^{i_2} \delta_{j_4}^{i_3} \delta_{j_1}^{i_4} \quad (\text{D.2})$$

is implemented. As mentioned in Sec. 6.2.2 the colored particles do not carry bifundamental indices but are distinguished by the possible color flows. Thus every particle has a tupel of two color flows. When the gluons of the vertex are identical O’Mega permutes the color tuples of the four particles with respect to the correct permutation of the Lorentz structure and thereby gets the whole vertex. O’Mega only permutes the indices of identical particles. Thus in the case of non identical particles we have to declare the missing permutations explicitly. We will illustrate this for the quartic coupling of two massless and two heavy gluons. Imagine four distinguishable particles. Therefore you have $4! = 24$ possibilities to arrange them. If the four particles are two equal pairs the permutations reduce by an factor $2!2! = 4$ and you end up with 6 possible configurations of the four particles. These are the six color configurations you have to put in by hand. Note that we have to care about the Lorentz structure of the vertex and have to adapt it if necessary. In the case of the trilinear coupling of two heavy gluons to one massless gluon it remains 3 possible permutations out of 6. The discussion above also covers the cases of all other couplings of gluons and sgluinos, which we therefore won’t discuss any further.

First of all we have to ensure that the numbering of the particles concerning to the color indices is irrelevant. Therefore we define the following color lists which contains the possible permutations of the same color flow. This is illustrated in Fig. D.1 and D.2.

```

let list_col3_equal = [(Col31, Col33, Col32, Col31, Col33, Col32);
(Col31, Col32, Col33, Col31, Col32, Col33)]

let list_col4_equal = [(Col41, Col44, Col42, Col41, Col43, Col42, Col44, Col43);
(Col41, Col44, Col43, Col41, Col42, Col43, Col44, Col42);
(Col41, Col43, Col44, Col41, Col42, Col44, Col43, Col42);
(Col41, Col42, Col44, Col41, Col43, Col44, Col42, Col43);
(Col41, Col43, Col42, Col41, Col44, Col42, Col43, Col44);
(Col41, Col42, Col43, Col41, Col44, Col43, Col42, Col44)]

```

Next we define the functions to get the permutations we have to put in by hand. In the case of the trilinear coupling the 3 missing arrangements can be constructed by the 3 cyclic permutations. This will be done by the function *col3_cyclic*.

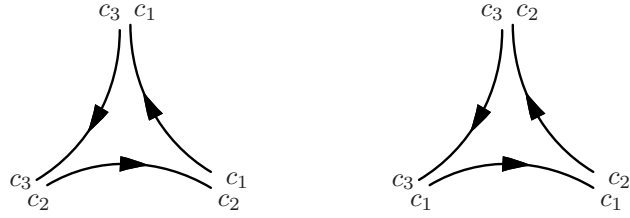


Figure D.1: All possible permutations of the same color flow for a trilinear coupling of three particles in the 3×3 color flow representation.

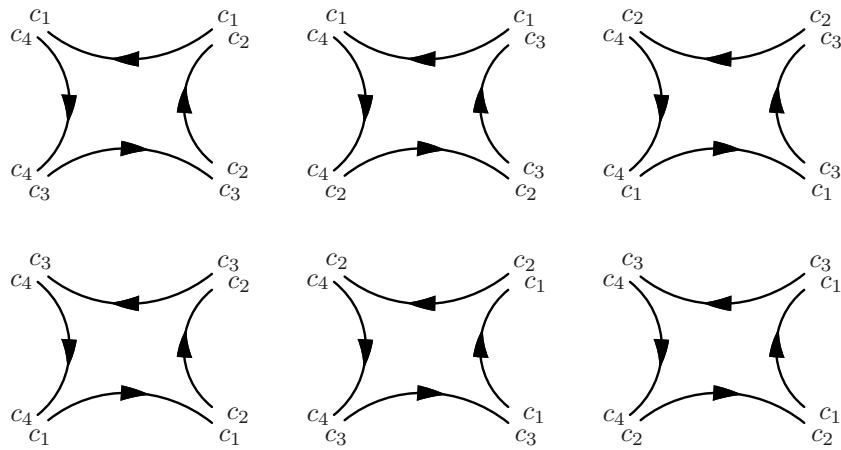


Figure D.2: All possible permutations of the same color flow for a quartic coupling of four particles in the 3×3 color flow representation.

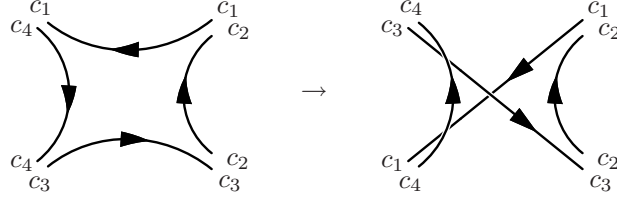


Figure D.3: Permutation of the first and the fourth color flow tuple.

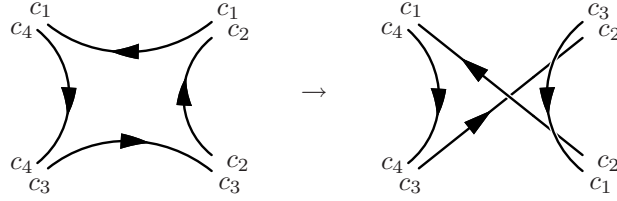


Figure D.4: Permutation of the second and the third color flow tuple.

```

let col3_cyclic =
  let col3_cyclic' = function Col31 → Col32 | Col32 → Col33 | Col33 → Col31
  in function (c1, c2, c3, c4, c5, c6) →
    (col3_cyclic' c1, col3_cyclic' c2, col3_cyclic' c3,
     col3_cyclic' c4, col3_cyclic' c5, col3_cyclic' c6)

```

In the case of the quartic coupling we have to do the 4 cyclic permutations and two anticyclic permutations. *col4_cyclic* performs the cyclic permutations. *col4_permute1* exchanges the second and the third particle and *col4_permute2* exchanges the first and the fourth particle. Cyclic permutations do not change the color flow and thus we do not have to care about adapting the Lorentz structure. But the permutations of *col4_permute1* and *col4_permute2* change the color flow shown in Fig. D.3 and D.4. This has to be taken into account by implementing these couplings.

```

let col4_cyclic =
  let col4_cyclic' = function
    Col41 → Col42 | Col42 → Col43 | Col43 → Col44 | Col44 → Col41
  in function (c1, c2, c3, c4, c5, c6, c7, c8) →
    (col4_cyclic' c1, col4_cyclic' c2, col4_cyclic' c3, col4_cyclic' c4,
     col4_cyclic' c5, col4_cyclic' c6, col4_cyclic' c7, col4_cyclic' c8)

let col4_permute1 = function (c1, c2, c3, c4, c5, c6, c7, c8) →
  (c1, c2, c5, c6, c3, c4, c7, c8)

let col4_permute2 = function (c1, c2, c3, c4, c5, c6, c7, c8) →
  (c7, c8, c3, c4, c5, c6, c1, c2)

```

Now we can construct the color lists we need for the implementation of the couplings, applying the functions, defined above to the color lists *list_col3_equal* and *list_col4_equal*.

```

let list_col3_unequal =
  let list1 = list_col3_equal
  in let list2 = List.map col3_cyclic list1
  in let list3 = List.map col3_cyclic list2
  in list1 @ list2 @ list3

```

```

let list_col4_unequal_cyc =
  let list_cyc1 = list_col4_equal
  in let list_cyc2 = List.map col4_cyclic list_cyc1
  in let list_cyc3 = List.map col4_cyclic list_cyc2
  in let list_cyc4 = List.map col4_cyclic list_cyc3
  in list_cyc1 @ list_cyc2 @ list_cyc3 @ list_cyc4

let list_col4_unequal_per =
  let list_per1 = List.map col4_permute1 list_col4_equal
  in let list_per2 = List.map col4_permute2 list_col4_equal
  in list_per1 @ list_per2

let list_col4_unequal = list_col4_unequal_cyc @ list_col4_unequal_per

```

In the next part of the implementation we define lists of tuples of Kaluza-Klein indices, which are needed for a compact definition of the couplings.

```

let kk1_list_string =
  [Kal0; Kal1]
let kk2_list_string =
  [(Kal0, Kal0); (Kal1, Kal1)]
let kk3gluonEqual_list_string =
  [(Kal0, Kal0, Kal0); (Kal1, Kal1, Kal1)]
let kk3gluonUnequal_list_string =
  [(Kal0, Kal0, Kal1); (Kal0, Kal1, Kal1)]
let kk4gluonEqual_list_string =
  [(Kal0, Kal0, Kal0, Kal0); (Kal1, Kal1, Kal1, Kal1)]
let kk4gluonUnequal1_list_string =
  [(Kal0, Kal0, Kal0, Kal1); (Kal0, Kal0, Kal1, Kal1); (Kal0, Kal1, Kal1, Kal1)]
let kk4gluonUnequal2_list_string =
  [(Kal0, Kal0, Kal1, Kal1)]

```

To loop over the particle indices we define functions mapping to the type variables *Lepton*, *Quark*, *A*, *W*, *Z*, *GluonKK*, *GluonAuxiliary* and *Sigma*.

```

let lepton cs gen iso = Lepton (cs, gen, iso)
let quark cs gen iso col = Quark (cs, gen, iso, col)
let a = A
let w cs = W cs
let z = Z
let gluonKK kk col col = GluonKK (kk, col, col)
let gluonAuxKK kk = GluonAuxiliary kk
let sigma col col = Sigma (col, col)

```

The *loop*-functions will be used later to loop over the particle indices.

```

let revmap funs v = List.map (fun x → x v) funs
let revmap2 funs values = ThoList.flatmap (revmap funs) values

let loop_cs flist = revmap2 flist [Pos; Neg]
let loop_gen flist = revmap2 flist [Gen0; Gen1; Gen2]
let loop_iso flist = revmap2 flist [Iso_up; Iso_down]
let loop_kk flist = revmap2 flist [Kal0; Kal1]

```

The type *gauge* is required by signature and is in our case chosen to the dummy variable *unit*. The gauge is implemented manifest in the unitarity gauge ($\xi \rightarrow \infty$), through the definitions of the propagators.

```

type gauge = unit

```

```
let gauge_symbol () = failwith "Models.warped5DSUSY.gauge_symbol: _internal_error"
```

Since we have chosen the unitary gauge there are no goldstone bosons

```
let goldstone x = None
```

The *pdg* function assigns every particle its *pdg* number. The function *lorentz* returns the Lorentz structure and *propagator* the propagator of the particle. *conjugate* maps the particle to its complex conjugate. *fermion* returns 1 for fermions -1 for antifermions and 0 for bosons. The assignments are shown in Tab. D.1 and D.2.

```
let pdg =
  var → int

let lorentz =
  var → var

let propagator =
  var → var

let conjugate =
  var → var

let fermion =
  var → int
```

Next we define the coupling constants.

```
type constant =
  | G_3gluonKK of (kkmode × kkmode × kkmode)
  | G_4gluonKK of (kkmode × kkmode × kkmode × kkmode)
  | G_2sigma_gluonKK of kkmode
  | G_2sigma_2gluonKK_cyc of (kkmode × kkmode)
  | G_2sigma_2gluonKK_per of (kkmode × kkmode)
  | G_sigma_2quark of (generation × isospin)
  | G_sigmaAux_2quark of (generation × isospin)
  | G_a_2quark of isospin
  | G_w_2quark
  | G_z_2quark of (generation × isospin)
  | G_gluonKK_2quark of (generation × isospin × kkmode)
  | G_gluonAux_2quark of (generation × isospin × kkmode)
```

Afterwards we rewrite the coupling constants as functions

```
let g_3gluonKK (kk1, kk2, kk3) = G_3gluonKK (kk1, kk2, kk3)
let g_4gluonKK (kk1, kk2, kk3, kk4) = G_4gluonKK (kk1, kk2, kk3, kk4)
let g_2sigma_gluonKK kk = G_2sigma_gluonKK kk
let g_2sigma_2gluonKK_cyc (kk1, kk2) = G_2sigma_2gluonKK_cyc (kk1, kk2)
let g_2sigma_2gluonKK_per (kk1, kk2) = G_2sigma_2gluonKK_per (kk1, kk2)
let g_sigma_2quark gen iso = G_sigma_2quark (gen, iso)
let g_sigmaAux_2quark gen iso = G_sigmaAux_2quark (gen, iso)
let g_a_2quark iso = G_a_2quark iso
let g_w_2quark = G_w_2quark
let g_z_2quark gen iso = G_z_2quark (gen, iso)
let g_gluonKK_2quark gen iso kk = G_gluonKK_2quark (gen, iso, kk)
let g_gluonAux_2quark gen iso kk = G_gluonKK_2quark (gen, iso, kk)
```

to construct *list_couplings* which is a list of all coupling constants.

	<i>pdg</i>	<i>lorentz</i>	<i>propagator</i>	<i>conjugate</i>
e^-	12	<i>Spinor</i>	<i>Prop_Spinor</i>	e^+
e^+	-12	<i>ConjSpinor</i>	<i>Prop_ConjSpinor</i>	e^-
ν_e	11	<i>Spinor</i>	<i>Prop_Spinor</i>	$\bar{\nu}_e$
$\bar{\nu}_e$	-11	<i>ConjSpinor</i>	<i>Prop_ConjSpinor</i>	ν_e
μ^-	14	<i>Spinor</i>	<i>Prop_Spinor</i>	μ^+
μ^+	-14	<i>ConjSpinor</i>	<i>Prop_ConjSpinor</i>	μ^-
ν_μ	13	<i>Spinor</i>	<i>Prop_Spinor</i>	$\bar{\nu}_\mu$
$\bar{\nu}_\mu$	-13	<i>ConjSpinor</i>	<i>Prop_ConjSpinor</i>	ν_μ
τ^-	16	<i>Spinor</i>	<i>Prop_Spinor</i>	τ^+
τ^+	-16	<i>ConjSpinor</i>	<i>Prop_ConjSpinor</i>	τ^-
ν_τ	15	<i>Spinor</i>	<i>Prop_Spinor</i>	$\bar{\nu}_\tau$
$\bar{\nu}_\tau$	-15	<i>ConjSpinor</i>	<i>Prop_ConjSpinor</i>	ν_τ
u	2	<i>Spinor</i>	<i>Prop_Spinor</i>	\bar{u}
\bar{u}	-2	<i>ConjSpinor</i>	<i>Prop_ConjSpinor</i>	u
d	1	<i>Spinor</i>	<i>Prop_Spinor</i>	\bar{d}
\bar{d}	-1	<i>ConjSpinor</i>	<i>Prop_ConjSpinor</i>	d
c	4	<i>Spinor</i>	<i>Prop_Spinor</i>	\bar{c}
\bar{c}	-4	<i>ConjSpinor</i>	<i>Prop_ConjSpinor</i>	c
s	3	<i>Spinor</i>	<i>Prop_Spinor</i>	\bar{s}
\bar{s}	-3	<i>ConjSpinor</i>	<i>Prop_ConjSpinor</i>	s
t	6	<i>Spinor</i>	<i>Prop_Spinor</i>	\bar{t}
\bar{t}	-6	<i>ConjSpinor</i>	<i>Prop_ConjSpinor</i>	t
b	5	<i>Spinor</i>	<i>Prop_Spinor</i>	\bar{b}
\bar{b}	-5	<i>ConjSpinor</i>	<i>Prop_ConjSpinor</i>	b

Table D.1: Functionality of the functions *pdg*, *lorentz*, *propagator* and *conjugate* for fermions.

	<i>pdg</i>	<i>lorentz</i>	<i>propagator</i>	<i>conjugate</i>
<i>A</i>	22	<i>Vector</i>	<i>Prop_Feynman</i>	<i>A</i>
<i>Z</i>	23	<i>MassiveVector</i>	<i>Prop_Unitarity</i>	<i>Z</i>
<i>W</i> ⁺	24	<i>MassiveVector</i>	<i>Prop_Unitarity</i>	<i>W</i> ⁻
<i>W</i> ⁻	-24	<i>MassiveVector</i>	<i>Prop_Unitarity</i>	<i>W</i> ⁺
<i>g</i> (<i>c</i> 1, <i>c</i> 2)	21	<i>Vector</i>	<i>Prop_Feynman</i>	<i>g</i> (- <i>c</i> 1, - <i>c</i> 2)
<i>g</i> _{aux}	21	<i>Vector</i>	<i>Prop_Col_Feynman</i>	<i>g</i> _{aux}
<i>g</i> ₁ (<i>c</i> 1, <i>c</i> 2)	9925	<i>MassiveVector</i>	<i>Prop_Unitarity</i>	<i>g</i> ₁ (- <i>c</i> 1, - <i>c</i> 2)
<i>g</i> _{1,aux}	9925	<i>MassiveVector</i>	<i>Prop_Col_Unitarity</i>	<i>g</i> _{1,aux}
Σ (<i>c</i> 1, <i>c</i> 2)	9931	<i>Scalar</i>	<i>Prop_Scalar</i>	Σ (- <i>c</i> 1, - <i>c</i> 2)
Σ _{aux}	9931	<i>Scalar</i>	<i>Prop_Col_Scalar</i>	Σ _{aux}

Table D.2: Functionality of the functions *pdg*, *lorentz*, *propagator* and *conjugate* for bosons. *c*1 and *c*2 denote the color indices of the gluons and sgluinos.

```

let list_couplings = (List.map g_3gluonKK kk3_list_string) @
  (List.map g_4gluonKK kk4_list_string) @
  (List.map g_2sigma_gluonKK kk1_list_string) @
  (List.map g_2sigma_2gluonKK_cyc kk2_list_string) @
  (List.map g_2sigma_2gluonKK_per kk2_list_string) @
  (loop_iso (loop_gen [g_sigma_2quark])) @
  (loop_iso (loop_gen [g_sigmaAux_2quark])) @
  (loop_iso [g_a_2quark]) @
  [g_w_2quark] @
  (loop_iso (loop_gen [g_z_2quark])) @
  (revmap2 (loop_iso (loop_gen [g_gluonKK_2quark])) kk1_list_string) @
  (revmap2 (loop_iso (loop_gen [g_gluonAux_2quark])) kk1_list_string)

```

max_degree is the maximal degree of the vertices.

```
let max_degree () = 4
```

In the next part of the implementation we will define the vertices.

```

let gauge4 = Vector4 [(2, C_13_42); (-1, C_12_34); (-1, C_14_23)]
let gauge4_per = Vector4 [(2, C_12_34); (-1, C_14_23); (-1, C_13_42)]

```

gauge4 is an abbreviation for the following Lorentz structure

$$2 g^{\mu_1 \mu_3} g^{\mu_4 \mu_2} - g^{\mu_1 \mu_2} g^{\mu_3 \mu_4} - g^{\mu_1 \mu_4} g^{\mu_2 \mu_3} \quad (\text{D.3})$$

and *gauge4_per* is equal to

$$2 g^{\mu_1 \mu_2} g^{\mu_3 \mu_4} - g^{\mu_1 \mu_3} g^{\mu_2 \mu_4} - g^{\mu_1 \mu_4} g^{\mu_2 \mu_3} \quad (\text{D.4})$$

They will be used for the definition of the four gluon vertex. We will illustrate the explicit implementation of the vertices on the basis of the three gluon vertex. The remaining vertices are implemented in the

same way and thus will be only shown without further explanation. First we define an auxiliary function $h_3gluonKK$ to write the proper vertex function more compact. To avoid the explicit definition of all possible trilinear gluon interactions we define the vertex as a function of Kaluza-Klein and color variables. This function is denoted by $v_3gluonKK'$ and looks like

$$v_3gluonKK' (c1a, c1b, c2a, c2b, c3a, c3b) (kk1, kk2, kk3) = \\ [(((Gauge_Boson (GluonKK kk1, Q c1a, Q (-c1b)), \\ (Gauge_Boson (GluonKK kk2, Q c2a, Q (-c2b)), \\ (Gauge_Boson (GluonKK kk3, Q c3a, Q (-c3b))), \\ Gauge_Gauge_Gauge 1, G_3gluonKK (kk1, kk2, kk3)))]$$

Note that we already execute the auxiliary function $h_3gluonKK$. $v_3gluonKK'$ is a list which contains a 5-tuple of the three particles the Lorentz structure and coupling constant. Now we have to saturate the Kaluza Klein and color variables to all possible values and write each saturation in a separate 5-tuple of the list. This is done by mapping $v_3gluonKK'$ to the lists $list_col3_equal'$, $kk3gluonEqual_list_string'$, $list_col3_equal'$ and $triple_col$. The vertex list then reads

$$vertex_3gluonKK_equal' = \\ [(((Gauge_Boson (GluonKK Kal0, Q 1, Q (-3)), \\ (Gauge_Boson (GluonKK Kal0, Q 2, Q (-1)), \\ (Gauge_Boson (GluonKK Kal0, Q 3, Q (-2))), \\ Gauge_Gauge_Gauge 1, G_3gluonKK (0, 0, 0)))] \\ [(((Gauge_Boson (GluonKK Kal1, Q 1, Q (-3)), \\ (Gauge_Boson (GluonKK Kal1, Q 2, Q (-1)), \\ (Gauge_Boson (GluonKK Kal1, Q 3, Q (-2))), \\ Gauge_Gauge_Gauge 1, G_3gluonKK (1, 1, 1)), ...)]$$

Note that we separated the vertices with the same Kaluza-Klein index and those with different one. We will see later that in the case of the quartic coupling of the gluons to the sgluinos and the quartic gluon self-interaction we need this separation to pass different Lorentz structures and coupling constants, for reasons we already discussed some pages before. The full implementation of the three gluon vertex is

$$\text{let } h_3gluonKK ((g1, g2, g3), t, c) = \\ ((Gauge_Boson (GluonKK g1), Gauge_Boson (GluonKK g2), \\ Gauge_Boson (GluonKK g3)), t, c) \\ \text{let } v_3gluonKK_equal (c1, c2, c3) = \\ \text{let } substitute = \text{function} \\ Col31 \rightarrow c1 \mid Col32 \rightarrow c2 \mid Col33 \rightarrow c3 \\ \text{in let } list_col3_equal' = \\ List.map (fun_to_6tuple substitute) list_col3_equal \\ \text{in let } v_3gluonKK' (c1a, c1b, c2a, c2b, c3a, c3b) (kk1, kk2, kk3) = \\ List.map h_3gluonKK \\ [(((kk1, Q c1a, Q (-c1b)), (kk2, Q c2a, Q (-c2b)), (kk3, Q c3a, Q (-c3b))), \\ Gauge_Gauge_Gauge 1, G_3gluonKK (kk1, kk2, kk3))] \\ \text{in let } v_3gluonKK'' = List.map v_3gluonKK' list_col3_equal' \\ \text{in revmap2 } v_3gluonKK'' kk3gluonEqual_list_string \\ \text{let } v_3gluonKK_unequal (c1, c2, c3) = \\ \text{let } substitute = \text{function} \\ Col31 \rightarrow c1 \mid Col32 \rightarrow c2 \mid Col33 \rightarrow c3 \\ \text{in let } list_col3_unequal' = \\ List.map (fun_to_6tuple substitute) list_col3_unequal \\ \text{in let } v_3gluonKK' (c1a, c1b, c2a, c2b, c3a, c3b) (kk1, kk2, kk3) = \\ List.map h_3gluonKK \\ [(((kk1, Q c1a, Q (-c1b)), (kk2, Q c2a, Q (-c2b)), (kk3, Q c3a, Q (-c3b))), \\ Gauge_Gauge_Gauge 1, G_3gluonKK (kk1, kk2, kk3))]$$

```

in let v_3gluonKK'' = List.map v_3gluonKK' list_col3_unequal'
in revmap2 v_3gluonKK'' kk3gluonUnequal_list_string

let vertex_3gluonKK_unequal =
  List.flatten (ThoList.flatmap v_3gluonKK_unequal triple_col)
let vertex_3gluonKK_equal =
  List.flatten (ThoList.flatmap v_3gluonKK_equal triple_col)

```

Next we discuss the implementation of the coupling of four gluons ($g_k g_k g_k g_k$). The coupling is separated into three parts $v_{4gluonKK_equal}$, $v_{4gluonKK_unequal_cyc}$ and $v_{4gluonKK_unequal_per}$. The first part is for four identical Kaluza-Klein gluons and can therefore be matched with the Lorentz structure $gauge_4$. As discussed above we have to implement six additional color flows in the case of two massless gluons and two heavy gluons and four additional color flows in the case of three heavy gluons and one massless gluon or one heavy gluon and three massless gluons. In the case of three identical Kaluza-Klein gluons the additional colorflows are the four cyclic permutations of the four color flow tuples and therefore have the Lorentz structure $gauge_4$. The four cyclic permutations of the coupling with two identical Kaluza Klein gluons, respectively have also the Lorentz structure $gauge_4$. The cyclic permutations are realized in the vertex function $v_{4gluonKK_unequal_cyc}$. In the case of the two non-cyclic permutations we have to adapt the Lorentz structure by $v_{4gluonKK_unequal_per}$.

```

let h_4gluonKK ((g1, g2, g3, g4), t, c) =
  ((Gauge_Boson (GluonKK g1), Gauge_Boson (GluonKK g2),
    Gauge_Boson (GluonKK g3), Gauge_Boson (GluonKK g4)), t, c)

let v_4gluonKK_equal (c1, c2, c3, c4) =
  let substitute = function
    Col41 → c1 | Col42 → c2 | Col43 → c3 | Col44 → c4
  in let list_col4_equal' =
    List.map (fun_to_stupel substitute) list_col4_equal
  in let v_4gluonKK'
    (c1a, c1b, c2a, c2b, c3a, c3b, c4a, c4b) (kk1, kk2, kk3, kk4) =
    List.map h_4gluonKK
    [(((kk1, Q c1a, Q (-c1b)), (kk2, Q c2a, Q (-c2b)), (kk3, Q c3a, Q (-c3b)),
      (kk4, Q c4a, Q (-c4b))), gauge4, G_4gluonKK (kk1, kk2, kk3, kk4))]
  in let v_4gluonKK'' = List.map v_4gluonKK' list_col4_equal'
  in revmap2 v_4gluonKK'' kk4gluonEqual_list_string

let v_4gluonKK_unequal_cyc (c1, c2, c3, c4) =
  let substitute = function
    Col41 → c1 | Col42 → c2 | Col43 → c3 | Col44 → c4
  in let list_col4_unequal_cyc' =
    List.map (fun_to_stupel substitute) list_col4_unequal_cyc
  in let v_4gluonKK'
    (c1a, c1b, c2a, c2b, c3a, c3b, c4a, c4b) (kk1, kk2, kk3, kk4) =
    List.map h_4gluonKK
    [(((kk1, Q c1a, Q (-c1b)), (kk2, Q c2a, Q (-c2b)), (kk3, Q c3a, Q (-c3b)),
      (kk4, Q c4a, Q (-c4b))), gauge4, G_4gluonKK (kk1, kk2, kk3, kk4))]
  in let v_4gluonKK'' = List.map v_4gluonKK' list_col4_unequal_cyc'
  in revmap2 v_4gluonKK'' kk4gluonUnequal1_list_string

let v_4gluonKK_unequal_per (c1, c2, c3, c4) =
  let substitute = function
    Col41 → c1 | Col42 → c2 | Col43 → c3 | Col44 → c4
  in let list_col4_unequal_per' =
    List.map (fun_to_stupel substitute) list_col4_unequal_per
  in let v_4gluonKK'
    (c1a, c1b, c2a, c2b, c3a, c3b, c4a, c4b) (kk1, kk2, kk3, kk4) =

```

```

List.map h_4gluonKK
  [(((kk1, Q c1a, Q (-c1b)), (kk2, Q c2a, Q (-c2b)), (kk3, Q c3a, Q (-c3b)),
    (kk4, Q c4a, Q (-c4b))), gauge4_per, G_4gluonKK (kk1, kk2, kk3, kk4))]
in let v_4gluonKK'' = List.map v_4gluonKK' list_col4_unequal_per'
in revmap2 v_4gluonKK'' kk4gluonUnequal2_list_string

let vertex_4gluonKK_equal =
  List.flatten (ThoList.flatmap v_4gluonKK_equal quartic_col)
let vertex_4gluonKK_unequal_cyc =
  List.flatten (ThoList.flatmap v_4gluonKK_unequal_cyc quartic_col)
let vertex_4gluonKK_unequal_per =
  List.flatten (ThoList.flatmap v_4gluonKK_unequal_per quartic_col)

```

Coupling of two sgluinos to the gluon ($\Sigma\Sigma g_k$)

```

let h_2sigma_gluonKK ((g1, g2, g3), t, c) =
  ((Gauge_Boson (GluonKK g1), Scalar (Sigma g2), Scalar (Sigma g3)), t, c)
let v_2sigma_gluonKK (c1, c2, c3) =
  let substitute = function
    Col31 → c1 | Col32 → c2 | Col33 → c3
  in let list_col3_unequal' =
    List.map (fun_to_6tuple substitute) list_col3_unequal
  in let v_2sigma_gluonKK' (c1a, c1b, c2a, c2b, c3a, c3b) kk1 =
    List.map h_2sigma_gluonKK
      [(((kk1, Q c1a, Q (-c1b)), (Q c2a, Q (-c2b)), (Q c3a, Q (-c3b)),
        Vector_Scalar_Scalar 1, G_2sigma_gluonKK kk1)]
  in let v_2sigma_gluonKK'' = List.map v_2sigma_gluonKK' list_col3_unequal'
  in revmap2 v_2sigma_gluonKK'' kk1_list_string

let vertex_2sigma_gluonKK =
  List.flatten (ThoList.flatmap v_2sigma_gluonKK triple_col)

```

Coupling of two sgluinos to two gluons ($\Sigma\Sigma g_k g_k$). The vertex structure of the coupling of two sgluinos to two gluons is (see Sec. 6.2.1)

$$\begin{aligned}
& -i \frac{g^2}{2} g^{\mu_1 \mu_2} \left(\delta_{j_2}^{i_1} \delta_{j_3}^{i_2} \delta_{j_4}^{i_3} \delta_{j_1}^{i_4} + \delta_{j_4}^{i_1} \delta_{j_1}^{i_2} \delta_{j_2}^{i_3} \delta_{j_3}^{i_4} + \delta_{j_4}^{i_1} \delta_{j_3}^{i_2} \delta_{j_1}^{i_3} \delta_{j_2}^{i_4} + \delta_{j_3}^{i_1} \delta_{j_4}^{i_2} \delta_{j_2}^{i_3} \delta_{j_1}^{i_4} \right. \\
& \quad \left. - 2 \delta_{j_4}^{i_1} \delta_{j_1}^{i_2} \delta_{j_2}^{i_3} \delta_{j_3}^{i_4} - 2 \delta_{j_4}^{i_1} \delta_{j_1}^{i_2} \delta_{j_2}^{i_3} \delta_{j_3}^{i_4} \right) \quad (D.5)
\end{aligned}$$

We find that the two non-cyclic permutations of the color flow get an additional factor -2 . Therefore we split the coupling into two parts $v_2sigma_2gluonKK_cyc$ and $v_2sigma_2gluonKK_per$ and introduce for each vertex function a separate coupling constant $G_2sigma_2gluonKK_cyc$ and $G_2sigma_2gluonKK_per$. The Lorentz structure of the vertex is symmetric under the exchange of the gluons and therefore we do not have to take care of it. Note that we only implement the coupling of either two massive or two massless gluons to two sgluinos.

```

let h_2sigma_2gluonKK ((g1, g2, g3, g4), t, c) =
  ((Gauge_Boson (GluonKK g1), Gauge_Boson (GluonKK g2),
    Scalar (Sigma g3), Scalar (Sigma g4)), t, c)
let v_2sigma_2gluonKK_cyc (c1, c2, c3, c4) =
  let substitute = function
    Col41 → c1 | Col42 → c2 | Col43 → c3 | Col44 → c4
  in let list_col4_unequal_cyc' =
    List.map (fun_to_8tuple substitute) list_col4_unequal_cyc
  in let v_2sigma_2gluonKK'
    (c1a, c1b, c2a, c2b, c3a, c3b, c4a, c4b) (kk1, kk2) =

```



```

    List.map h_2sigma_2gluonKK
    [ (((kk1, Q c1a, Q (-c1b)), (kk2, Q c2a, Q (-c2b)),
      (Q c3a, Q (-c3b)), (Q c4a, Q (-c4b))),
      Scalar2_Vector2 1, G_2sigma_2gluonKK_cyc (kk1, kk2)) ]
  in let v_2sigma_2gluonKK'' =
      List.map v_2sigma_2gluonKK' list_col4_unequal_cyc
  in revmap2 v_2sigma_2gluonKK'' kk2_list_string

let v_2sigma_2gluonKK_per (c1, c2, c3, c4) =
  let substitute = function
      Col41 → c1 | Col42 → c2 | Col43 → c3 | Col44 → c4
  in let list_col4_unequal_per' =
      List.map (fun_to_stupel substitute) list_col4_unequal_per
  in let v_2sigma_2gluonKK'
      (c1a, c1b, c2a, c2b, c3a, c3b, c4a, c4b) (kk1, kk2) =
          List.map h_2sigma_2gluonKK
          [ (((kk1, Q c1a, Q (-c1b)), (kk2, Q c2a, Q (-c2b)),
            (Q c3a, Q (-c3b)), (Q c4a, Q (-c4b))),
            Scalar2_Vector2 1, G_2sigma_2gluonKK_per (kk1, kk2)) ]
  in let v_2sigma_2gluonKK'' =
      List.map v_2sigma_2gluonKK' list_col4_unequal_per'
  in revmap2 v_2sigma_2gluonKK'' kk2_list_string

let vertex_2sigma_2gluonKK_cyc =
  List.flatten (ThoList.flatmap v_2sigma_2gluonKK_cyc quartic_col)
let vertex_2sigma_2gluonKK_per =
  List.flatten (ThoList.flatmap v_2sigma_2gluonKK_per quartic_col)

```

Coupling of the quarks to the sgluino ($\Sigma q\bar{q}$)

```

let h_sigma_2quark ((g1, g2, g3), t, c) =
  ((Fermion (Quark g1), Scalar (Sigma g2), Fermion (Quark g3)), t, c)
let v_sigma_2quark (c1, c2) =
  let v_sigma_2quark' gen iso =
      List.map h_sigma_2quark
      [ (((Neg, gen, iso, Q (-c2)), (Q c2, Q (-c1)), (Pos, gen, iso, Q c1)),
        FBF ((-1), Psibar, S, Psi), G_sigma_2quark (gen, iso)) ]
  in loop_iso (loop_gen [v_sigma_2quark'])
let vertex_sigma_2quark =
  List.flatten (ThoList.flatmap v_sigma_2quark inequ_pairs)

```

Coupling of the auxiliary field of the sgluino to the quarks ($\Sigma_{aux} q\bar{q}$)

```

let h_sigmaAux_2quark ((g1, g2, g3), t, c) =
  ((Fermion (Quark g1), Scalar g2, Fermion (Quark g3)), t, c)
let v_sigmaAux_2quark c1 =
  let v_sigmaAux_2quark' gen iso =
      List.map h_sigmaAux_2quark
      [ (((Neg, gen, iso, Q (-c1)), SigmaAuxiliary, (Pos, gen, iso, Q c1)),
        FBF ((-1), Psibar, S, Psi), G_sigmaAux_2quark (gen, iso)) ]
  in loop_iso (loop_gen [v_sigmaAux_2quark'])
let vertex_sigmaAux_2quark =
  List.flatten (ThoList.flatmap v_sigmaAux_2quark nc_list)

```

Coupling of the gluon to the quarks ($g_\kappa q\bar{q}$). When we implement left- right-couplings in O'Mega we have to multiply the couplings by 1/2 since the projectors $P_{L/R}$ are defined as $P_{L/R} = (1 \mp \gamma_5)$.

```

let h_gluonKK_2quark ((g1, g2, g3), t, c) =
  ((Fermion (Quark g1), Gauge_Boson (GluonKK g2), Fermion (Quark g3)), t, c)
let v_gluonKK_2quark (c1, c2) =
  let v_gluonKK_2quark' gen iso kk =
    List.map h_gluonKK_2quark
      [(((Neg, gen, iso, Q (-c2)), (kk, Q c2, Q (-c1)), (Pos, gen, iso, Q c1)),
        FBF ((-1), Psibar, VLR, Psi), G_gluonKK_2quark (gen, iso, kk))]
    in revmap2 (loop_iso (loop_gen [v_gluonKK_2quark'])) kk1_list_string
let vertex_gluonKK_2quark =
  List.flatten (ThoList.flatmap v_gluonKK_2quark inequ_pairs)

```

Coupling of auxiliary field of the gluon to the quarks ($g_{k,\text{aux}q\bar{q}}$)

```

let h_gluonAux_2quark ((g1, g2, g3), t, c) =
  ((Fermion (Quark g1), Gauge_Boson g2, Fermion (Quark g3)), t, c)
let v_gluonAux_2quark c1 =
  let v_gluonAux_2quark' gen iso kk =
    List.map h_gluonAux_2quark
      [(((Neg, gen, iso, Q (-c1)), GluonAuxiliary kk, (Pos, gen, iso, Q c1)),
        FBF ((-1), Psibar, VLR, Psi), G_gluonAux_2quark (gen, iso, kk))]
    in revmap2 (loop_iso (loop_gen [v_gluonAux_2quark'])) kk1_list_string
let vertex_gluonAux_2quark =
  List.flatten (ThoList.flatmap v_gluonAux_2quark nc_list)

```

Coupling of the photon to the quarks ($Aq\bar{q}$)

```

let h_a_2quark ((g1, g2, g3), t, c) =
  ((Fermion (Quark g1), Gauge_Boson g2, Fermion (Quark g3)), t, c)
let v_a_2quark c1 =
  let v_a_2quark' gen iso =
    List.map h_a_2quark
      [(((Neg, gen, iso, Q (-c1)), A, (Pos, gen, iso, Q c1)),
        FBF (1, Psibar, VL, Psi), G_a_2quark iso)]
    in (loop_iso (loop_gen [v_a_2quark']))
let vertex_a_2quark = List.flatten (ThoList.flatmap v_a_2quark nc_list)

```

Coupling of the W -Boson to the quarks ($Wq\bar{q}$)

```

let h_w_2quark ((g1, g2, g3), t, c) =
  ((Fermion (Quark g1), Gauge_Boson g2, Fermion (Quark g3)), t, c)
let v_w_2quark c1 =
  let v_w_2quark' gen =
    List.map h_w_2quark
      [(((Neg, gen, Iso_down, Q (-c1)), W Neg, (Pos, gen, Iso_up, Q c1)),
        FBF (1, Psibar, VL, Psi), G_w_2quark);
        (((Neg, gen, Iso_up, Q (-c1)), W Pos, (Pos, gen, Iso_down, Q c1)),
        FBF (1, Psibar, VL, Psi), G_w_2quark)]
    in (loop_gen [v_w_2quark'])
let vertex_w_2quark = List.flatten (ThoList.flatmap v_w_2quark nc_list)

```

Coupling of the Z -Boson to the quarks ($Zq\bar{q}$)

```

let h_z_2quark ((g1, g2, g3), t, c) =
  ((Fermion (Quark g1), Gauge_Boson g2, Fermion (Quark g3)), t, c)

let v_z_2quark c1 =
  let v_z_2quark' gen iso =
    List.map h_w_2quark
      [(((Neg, gen, iso, Q (-c1)), Z, (Pos, gen, iso, Q c1)),
        FBF (1, Psibar, VA, Psi), G_z_2quark (gen, iso))]
    in loop_iso (loop_gen [v_z_2quark'])

let vertex_z_2quark = List.flatten (ThoList.flatmap v_z_2quark nc_list)

module F = Models.Fusions (struct
  type f = flavor
  type c = constant
  let compare = compare
  let conjugate = conjugate
end)

```

vertices is a list of all vertices.

```

let vertices () =
  (vertex_3gluonKK_equal @ vertex_3gluonKK_unequal @
   vertex_2sigma_gluonKK @ vertex_sigma_2quark @
   vertex_sigmaAux_2quark @ vertex_gluonKK_2quark @ vertex_gluonAux_2quark @
   vertex_a_2quark @ vertex_w_2quark @ vertex_z_2quark,
   vertex_2sigma_2gluonKK_cyc @ vertex_2sigma_2gluonKK_per @
   vertex_4gluonKK_equal @ vertex_4gluonKK_unequal_cyc @
   vertex_4gluonKK_unequal_per, [])

let table = F.of_vertices (vertices ())

let fuse2 = F.fuse2 table
let fuse3 = F.fuse3 table
let fuse = F.fuse table

let quark_sumcol c =
let quark_col iso gen c =
  [Quark (Pos, iso, gen, Q c); Quark (Neg, iso, gen, Q (-c))]
  in List.map flavor_of_f
    (List.flatten ((revmap (loop_iso (loop_gen [quark_col])) c)))

let gluonKK_sumcol x =
  let gluonKK_col kk (n, m) = [GluonKK (kk, Q n, Q (-m))]
    in List.map flavor_of_g (List.flatten (revmap (loop_kk [gluonKK_col]) x))

let scalar_sumcol (n, m) = [Scalar (Sigma (Q n, Q (-m)))]

let external_flavors () =
  [
    "leptons", List.map flavor_of_f (loop_iso (loop_gen (loop_cs [lepton])));
    "quarks", ThoList.flatmap quark_sumcol nc_list;
    "a", [Gauge_Boson A];
    "w", [Gauge_Boson (W Pos); Gauge_Boson (W Neg)];
    "z", [Gauge_Boson Z];
    "gluonKK", (ThoList.flatmap gluonKK_sumcol inequ_pairs) @
      (List.map flavor_of_g (loop_kk [gluonAuxKK]));
    "sigma", (ThoList.flatmap scalar_sumcol inequ_pairs) @ [Scalar SigmaAuxiliary];
  ]

```

```

let flavors () = ThoList.flatmap snd (external_flavors ())
let parameters () = {input = List.map (fun x → (x, 0.)) list_couplings;
  derived = []; derived_arrays = []}

```

The following functions maps the flavor of a particle to a string. *flavor_to_string* makes the connection between the the model file and the user interface. *bcdi_of_flavor* and *flavor_symbol* renders the model parameters from the model file as FORTRAN compatible code. The assignments are tabled in Tab. D.3 and D.5.

```

let flavor_to_string =
  var → string
let bcdi_of_flavor =
  var → string
let flavor_symbol =
  var → string

```

flavor_of_string is the inverse function of *flavor_to_string*. It is copied from models3.ml.

```

let flavor_of_string x =
  let dict = List.map (fun x → (x, flavor_to_string x)) (flavors ())
  in let get_ident = function (x, _) → x
  in try
    get_ident (List.find (fun (_, y) → (x = y)) dict)
  with
    Not_found → invalid_arg "Warped5DSUSY.flavor_of_string"

```

mass_symbol maps every particle to a FORTRAN 90 compatible mass-string and *width_symbol* maps every particle a FORTRAN 90 compatible width-string. Both functions are required by signature.

```

let mass_symbol = function
  | Gauge_Boson A → "0._omega_prec"
  | Gauge_Boson (GluonKK (Kal0, -, -)) → "0._omega_prec"
  | Gauge_Boson (GluonAuxiliary (Kal0)) → "0._omega_prec"
  | x → "mass_array(" ^ (bcdi_of_flavor x) ^ ")"
let width_symbol = function
  | Gauge_Boson A → "0._omega_prec"
  | Gauge_Boson (GluonKK (Kal0, -, -)) → "0._omega_prec"
  | Gauge_Boson (GluonAuxiliary (Kal0)) → "0._omega_prec"
  | x → "width_array(" ^ (bcdi_of_flavor x) ^ ")"
let rcs = RCS.rename rcs_file "Models5.Warped5Dsusy" (["The_Warped_5D_Susy_Model"])
end

```

	<i>flavor_to_string</i>	<i>bcdi_of_flavor</i>	<i>flavor_symbol</i>
e^-	e-	e_bcd	l1
e^+	e+	e_bcd	lb1
ν_e	nue-	nue_bcd	n1
$\bar{\nu}_e$	nue+	nue_bcd	nb1
μ^-	mu-	mu_bcd	l2
μ^+	mu+	mu_bcd	lb2
ν_μ	numu-	numu_bcd	n2
$\bar{\nu}_\mu$	numu+	numu_bcd	nb2
τ^-	tau-	tau_bcd	l3
τ^+	tau+	tau_bcd	lb3
ν_τ	nutau-	nutau_bcd	n3
$\bar{\nu}_\tau$	nutau+	nutau_bcd	nb3
$u(n)$	u/n	u_bcd	u1_ n
$\bar{u}(n)$	ubar/n	u_bcd	u1b_ n
$d(n)$	d/n	d_bcd	d1_ n
$\bar{d}(n)$	dbar/n	d_bcd	d1b_ n
$c(n)$	c/n	c_bcd	u2_ n
$\bar{c}(n)$	cbar/n	c_bcd	u2b_ n
$s(n)$	s/n	s_bcd	d2_ n
$\bar{s}(n)$	sbar/n	s_bcd	d2b_ n
$t(n)$	t/n	t_bcd	u3_ n
$\bar{t}(n)$	tbar/n	t_bcd	u3b_ n
$b(n)$	b/n	b_bcd	d3_ n
$\bar{b}(n)$	bbar/n	b_bcd	d3b_ n

Table D.3: Functionality of the functions *flavor_to_string*, *bcdi_of_flavor* and *flavor_symbol* for fermions. n is the integer of the color index and |n| denotes the absolute value of n.

	<i>flavor_to_string</i>	<i>bcdi_of_flavor</i>	<i>flavor_symbol</i>
A	a		a
Z	z	z_bcd	z
W^+	w+	w_bcd	w
W^-	w-	w_bcd	w
$g(n, m)$	gluon/n(-m)		glu_n(-m)
g_{aux}	gluon0		gluAux
$g_1(n, m)$	gluonKK1/n(-m)	gluonKK1_bcd	gluKK1_n(-m)
$g_{1,aux}$	gluon0KK1	gluonAuxKK1_bcd	gluAuxKK1
$\Sigma(n, m)$	sigma/n(-m)	sigma_bcd	sig_n(-m)
Σ_{aux}	sigma0	sigmaAux_bcd	sigAux

Table D.4: Functionality of the functions *flavor_to_string*, *bcdi_of_flavor* and *flavor_symbol* for fermions. n and m denote the integer of the color index.

	<i>constant_symbol</i>
$G_{3gluonKK}(k1, k2, k3)$	g_3gluonKK_k1k2k3
$G_{4gluonKK}(k1, k2, k3, k4)$	g_4gluonKK_k1k2k3k4
$G_{2sigma_gluonKK} k1$	g_2sigma_gluonKK_00k1
$G_{2sigma_2gluonKK_cyc}(k1, k2)$	g_2sigma_2gluonKK_cyc_00k1k2
$G_{2sigma_2gluonKK_per}(k1, k2)$	g_2sigma_2gluonKK_per_00k1k2
G_{sigma_2quark}	g_sigma_qqbar
$G_{sigmaAux_2quark}$	g_sigmaAux_qqbar
$G_{a_2quark}(Iso_up)$	g_a_2uptypequark
$G_{a_2quark}(Iso_down)$	g_a_2downtypequark
G_{w_2quark}	g_w_2quark
G_{z_2quark}	g_z_qqbar
$G_{gluonKK_2quark} k1$	g_gluonKK_qqbar_k100
$G_{gluonAux_2quark} k1$	g_gluonAux_qqbar_k100

Table D.5: Functionality of the function *constant_symbol*. $k1$, $k2$, $k3$ and $k4$ denote the integer of the Kaluza-Klein index.

Bibliography

- [1] A. Knochel and T. Ohl, “Supersymmetric Extensions and Dark Matter in Models of Warped Higgsless EWSB,” 0805.1379.
- [2] C. Csaki, C. Grojean, J. Hubisz, Y. Shirman, and J. Terning, “Fermions on an interval: Quark and lepton masses without a Higgs,” *Phys. Rev.* **D70** (2004) 015012, hep-ph/0310355.
- [3] N. Arkani-Hamed, T. Gregoire, and J. G. Wacker, “Higher dimensional supersymmetry in 4D superspace,” *JHEP* **03** (2002) 055, hep-th/0101233.
- [4] L. J. Hall, Y. Nomura, T. Okui, and S. J. Oliver, “Explicit supersymmetry breaking on boundaries of warped extra dimensions,” *Nucl. Phys.* **B677** (2004) 87–114, hep-th/0302192.
- [5] D. Marti and A. Pomarol, “Supersymmetric theories with compact extra dimensions in $N = 1$ superfields,” *Phys. Rev.* **D64** (2001) 105025, hep-th/0106256.
- [6] **WMAP** Collaboration, D. N. Spergel *et al.*, “Wilkinson Microwave Anisotropy Probe (WMAP) three year results: Implications for cosmology,” *Astrophys. J. Suppl.* **170** (2007) 377, astro-ph/0603449.
- [7] T. Kaluza, “On the unification problem of physics,”. HUPD-8401.
- [8] O. Klein, “Quantum theory and five-dimensional theory of relativity,” *Z. Phys.* **37** (1926) 895–906.
- [9] G. Servant and T. M. P. Tait, “Is the lightest Kaluza-Klein particle a viable dark matter candidate?,” *Nucl. Phys.* **B650** (2003) 391–419, hep-ph/0206071.
- [10] K. Kong and K. T. Matchev, “Precise calculation of the relic density of Kaluza-Klein dark matter in universal extra dimensions,” *JHEP* **01** (2006) 038, hep-ph/0509119.
- [11] J. Wess and J. Bagger, “Supersymmetry and supergravity,”. Princeton, USA: Univ. Pr. (1992) 259 p.
- [12] L. Randall and R. Sundrum, “A large mass hierarchy from a small extra dimension,” *Phys. Rev. Lett.* **83** (1999) 3370–3373, hep-ph/9905221.
- [13] M. Maggiore, *A Modern Introduction to Quantum Field Theory*. Oxford University Press Inc., New York, first ed., 2005.
- [14] A. K. Knochel, “Electroweak symmetry breaking and perturbative unitarity in higher-dimensional field theories,” Master’s thesis, State University of New York, Stony Brook, USA, August, 2005.
- [15] A. J. MacFarlane, A. Sudbery, and P. H. Weisz, “On Gell-Mann’s λ -matrices, d tensors and f tensors, octets, and parametrizations of $SU(3)$,” *Commun. Math. Phys.* **11** (1968) 77–90.
- [16] W. Kilian, T. Ohl, and J. Reuter, “WHIZARD: Simulating Multi-Particle Processes at LHC and ILC,” 0708.4233.
- [17] F. Maltoni, K. Paul, T. Stelzer, and S. Willenbrock, “Color-flow decomposition of QCD amplitudes,” *Phys. Rev.* **D67** (2003) 014026, hep-ph/0209271.

[18] <http://theorie.physik.uni-wuerzburg.de/~cnspeckn>.

[19] C. Speckner, “Die Produktion geladener Eichbosonen im nichtkommutativen Standardmodell,” Master’s thesis, Julius-Maximilians-Universitaet, Wuerzburg, Deutschland, Oktober, 2006.

Acknowledgments

I want to thank the following persons for supporting me during the university education and diploma thesis.

- PD Dr. Thorsten Ohl for the opportunity to write my thesis in his group and answering all my questions.
- Prof. Dr. Reinhold Rückl for fascinating me for quantum physics during his lectures on quantum mechanics and quantum field theory.
- Christian Speckner for answering all my questions concerning programming and physic issues in general.
- Alexander Knochel for the various discussions about extra dimensional models.
- Simone Götz, Karoline Köpp, Christian Speckner, Alexander Knochel and Alexander Schenkel for a careful reading of this work.
- Alexander Schenkel for fascinating me for quantum physics and spending endless hours with me discussing questions and problems concerning my research and beyond.
- And last but not least my parents for supporting me during my studies in any way imaginable.

Erklärung

Hiermit erkläre ich, dass ich die vorliegende Arbeit selbständig verfasst und keine anderen als die angegebenen Hilfsmittel verwendet habe.

Würzburg, den 25. Juni 2008

Laslo Reichert